THE ASTRONOMICAL JOURNAL

PUBLISHED BY THE AMERICAN INSTITUTE OF PHYSICS
FOR THE AMERICAN ASTRONOMICAL SOCIETY

VOLUME 65 | 1960 December ~ No. 1285 | NUMBER 10

# Photoelectric Photometry of Galactic and Extragalactic Star Clusters*

G. E. KRON AND N. U. MAYALL†
*Lick Observatory, University of California*
(Received September 9, 1960)

Photoelectric observations are reported for 187 star clusters, mostly globular, in the Galaxy, Magellanic Clouds and the M31 group of galaxies. All were observed in photographic and visual light, $P$ and $V$, and 117 in the infrared, $I$. Globular clusters in the Galaxy and Clouds were measured through a series of apertures up to 25′ diameter, to obtain total magnitudes and diameters containing 0.9 the total light. For comparison of integrated colors, 28 galactic open clusters were observed with apertures large enough to include most of the cluster members. Some space-reddened F- and G-type supergiants having six-color photometry were measured to obtain total/selective absorption ratios of $A_V=(2.9\pm0.2)E_{(P-V)}=(2.3\pm1.4)E_{(V-I)}$. These ratios, with color excesses estimated in two ways from spectral types, were used to compute corrected total magnitudes, distance moduli and linear diameters for the galactic globular clusters. The principal results are: (1) The galactic globular and open clusters are generally well separated in the plot of $(P-V)$ vs $(V-I)$; (2) Linear diameters with 0.9 total light range from 20 to 50 parsecs as $M_V$ ranges from $-6.8$ to $-9.6$, but the scatter is so large that the correlation is not strong; (3) Galactic globulars appear to be systematically bluer than M31 clusters, by about 0.2 mag. in $(P-V)$, notwithstanding uncertain allowance for space reddening; (4) M31 clusters well outside the main spiral structure have an intrinsic color range of 0.4 mag.; (5) Except for a few relatively blue objects apparently like some in M33, the M31 clusters seen over the spiral have colors in the range from $(P-V)=+0.50$ to $+1.94$ mag., with the reddest being faintest; (6) From eight M31 clusters that are brightest and reddest in the $V$ vs $(P-V)$ plot, it was found that $A_V/E_{(P-V)}=2.50\pm0.14$, which is not regarded as significant of different absorbing matter in M31 than in the Galaxy; (7) Comparison of magnitude-frequency histograms gave estimates of distance moduli ranging from 23.5 to 24.0 for M31 and 19 for the Magellanic Clouds, with all values uncertain by 0.5 mag.; (8) The galactic center distance was estimated in two different ways at 12.5 and 12.0 kpc, with an uncertainty of about 1.5 kpc, on the assumption that for RR Lyrae variables $M_P=0.0$.

## I. INTRODUCTION

THERE is a large literature relating to globular cluster photometric characteristics, such as magnitudes, colors, and diameters. Visual, photographic, and photoelectric methods have been used, but in sum there still is not available a comprehensive and homogeneous set of data based on modern standards and procedures. Thus, the previous most extensive programs for the measurement of total magnitudes are those carried out by W. H. Christie (1940), who measured by the schraffierkasette method the photographic magnitudes of 68 galactic globular clusters, and by Seyfert and Nassau (1945), who measured on in-focus Schmidt telescope plates the photographic magnitudes of 212 "nebulous objects" in and near the Andromeda nebula (M31). Also, the most comprehensive investigation of their colors is that by Stebbins and Whitford (1936), who measured photoelectrically 69 galactic globular clusters. Likewise, the literature (Shapley and Sayer 1935, Mowbray 1946, others in H. B. Sawyer 1947) contains numerous diameters obtained by visual inspection, microphotometer tracing, and iris photometry of photographic plates. So far as we are aware, however, no extensive series of globular cluster diameter determinations by photoelectric techniques has been published.

The present paper gives the results from photoelectric photometry of star clusters, mostly globular, in the Galaxy, Magellanic Clouds, Fornax dwarf system, and the M31 group. A total of 187 clusters was observed in two colors, 117 of these in three colors, and 77 through a series of graded apertures. For each cluster so observed, the measurements were made with an aperture size or range sufficient to yield a reasonably close approach to integrated color, total magnitude and a diameter within which 0.9 of the total light is contained. In most cases, only a small extrapolation was necessary in order to obtain the total magnitudes and the specified diameters. These were, of course, limited chiefly by the interfering light from the surrounding field and sky. The diameter results for 10 Magellanic

* *Lick Observatory Bulletin*, No. 569. A preliminary summary was presented at the NSF-sponsored symposium, "The differences among globular clusters," Am. Astron. Soc. 103rd meeting, August 31, 1959, Toronto, Canada; *Astron. J.* **64**, 428 (1959).

† Now at Kitt Peak National Observatory, Tucson, Arizona.

TABLE I. Filter and cell combinations.

| Observations | Cell | Filters (balsam-cemented) Blue | Yellow | Infrared |
|---|---|---|---|---|
| | | Small-field photometer | | |
| 3-color, with separate infrared | 1P21, i | 0.4C3060[a]+1 mm BG12 | 2 mm GG 14+glass | ... |
| | CE25A/B, e | ... | ... | W88A[b]+cover glasses |
| 3-color, simultaneous | Lallemand, II | 2 mm BG 23+1 mm BG12 +2 mm WG1 cryolite coated | 2 mm GG11+2 mm BG18 | 2 mm BG21+2 mm RG8 |
| 1-color, separate infrared, for M31 clusters | Lallemand, II | ... | ... | 2 mm RG2 commercially coated |
| | | Large-field photometer | | |
| 3-color, with separate infrared | Dumont 6291, No. 1 | 2 mm GG13+1 mm BG12 | 2 mm GG14 | ... |
| | CE23A/B, a | ... | ... | W88A+cover glasses |
| 3-color, simultaneous | Lallemand, I | 2 mm BG23+1 mm BG12 +2 mm GG13 | 2 mm GG14+2 mm BG18 not cemented | C3966+W89+cover glass |

[a] Corning Glass number, 40% standard thickness.
[b] W refers to number of Wratten gelatine filter, furnished by Eastman Kodak Company.

Cloud clusters are reported here for the first time with the kind permission of S. C. B. Gascoigne, who, with Kron (1952), had previously published colors and total magnitudes obtained with the Mt. Stromlo Observatory's Reynolds reflector and a series of four apertures. Mainly for comparison purposes, color data also are given for 28 galactic open clusters.

## II. INSTRUMENTATION

All extragalactic clusters were measured in the blue and yellow with a 1P21 multiplier, and at Mount Hamilton the Crossley reflector was used exclusively for the measurements. Clusters in the Galaxy were measured with a stellar photometer, but the larger ones were observed in addition by means of a special, large-field photometer (Kron, Greeby, and Willson 1956). In the early part of the program, 35 galactic globular clusters were measured in the blue and yellow with a 1P21 multiplier phototube and in the infrared with a CE-25 photocell on the stellar photometer, or with a DuMont 6291 multiplier phototube (blue-yellow) and a CE-23 photocell (infrared) on the large-field photometer. In December, 1955, two superior infrared-sensitive receivers were put into operation: one, a large cathode 7-stage multiplier used with the large-field photometer, and the other a 12-stage multiplier with effective cathode size restricted by means of an electronic lens, used with the stellar photometer (Kron 1958). Both of these multipliers were generously furnished by Professor A. Lallemand, who developed them in his laboratory at the Paris Observatory. The new multipliers, employed with a revised filter system, made possible the measurement of all three colors, $P$, $V$, and $I$, in one operation, which was impossible with the infrared-sensitive photocells owing to insufficient sensitivity in the blue spectral region. All photometric receivers, with the exception of the CE-23 receiver, were refrigerated with dry ice.

In accordance with the practice of Johnson and Morgan (1951), the ultraviolet transmission of all blue filters was limited by a 2-mm thick piece of Schott GG13 glass; none of our blue filters had a red or infrared leak. The photometric system was stabilized by careful matching of filters with receivers, so that it was in practice unaffected by the changes in receivers made during the program. Thus the filter and receiver combination was the important unit, rather than only the filter; Table I lists the various filter-cell combinations. The stellar photometer is equipped with focal plane apertures graded in diameter from 4″ to 5′.5. The large-field photometer has apertures ranging from 3′.7 to 24′.8; there is an overlap with the stellar photometer of two apertures. The large-field photometer is also equipped with graded occulting disk fittings, which permit transforming the circular-hole apertures into annular apertures. Photometer sensitivity was monitored with a radium-activated light source during all of the observing.

## III. THE PHOTOMETRIC SYSTEM AND STANDARDS

A large part of the published photometry of star clusters is on the International system; we therefore adopted, as our photometric system in the blue and yellow, a photoelectric approximation to International. The only measurable systematic deviations resulted from use of an ultraviolet-free blue color. Although this circumstance causes some departure from International photographic, we feel that the use of an ultraviolet-free blue color is justified for reasons given by H. L. Johnson (1952). Our standard magnitude system is based upon observations of North Polar Sequence stars, and it is a close approximation to the International photovisual

TABLE II. Photometric standards.

| Star | $V$ | $(P-V)$ | $(V-I)$ | Sp. T. |
|---|---|---|---|---|
| North Polar Sequence | | | | |
| PS 1 | 4$^m$39 | −0$^m$06 | −0$^m$21 | A2 |
| 2 | 5.26 | −0.12 | −0.30 | B9 |
| 3 | 5.61 | +0.12 | +0.06 | F0III |
| 4 | 5.83 | +0.12 | 0.00 | A3p |
| 5 | 6.47 | −0.01 | −0.17 | A5 |
| 6 | 7.13 | +0.09 | ··· | A3 |
| 7 | 7.53 | −0.11 | −0.27 | B9 |
| 8 | 8.10 | +0.29 | +0.23 | F4III |
| 10 | 9.07 | +0.16 | ··· | A9 |
| 13 | 10.32 | +0.22 | ··· | A7 |
| 16 | 11.23 | +0.42 | ··· | ··· |
| 19 | 12.21 | +0.47 | ··· | ··· |
| 2r | 6.47 | +1.46 | +2.14 | MI:III: |
| 3r | 7.54 | +1.30 | +1.32 | K2III: |
| 4r | 8.26 | +0.97 | +0.89 | G9III |
| 5r | 8.66 | +1.46 | +1.77 | K3:III |
| 6r | 9.27 | +1.21 | +1.24 | G9III |
| 7r | 9.88 | +1.08 | ··· | G8IV |
| 8r | 10.46 | +0.97 | ··· | ··· |
| 12r | 12.61 | +1.18 | ··· | ··· |
| 2s | 6.29 | +0.25 | +0.17 | F2III |
| 3s | 6.36 | +0.30 | +0.32 | F4V |
| 4s | 9.83 | +0.48 | +0.39 | F5III |
| 6s | 10.68 | +0.71 | +0.66 | ··· |
| C6 | | | | |
| A | 6.93 | −0.09 | −0.17 | A3p |
| D | 7.38 | +0.43 | +0.45 | G0V |
| F | 8.06 | +0.33 | +0.35 | F5V |
| G | 7.79 | +0.94 | +0.89 | K2III |
| K | 7.53 | +1.54 | +1.93 | M2III |
| M | 8.41 | +1.17 | +1.16 | K3III |
| C8 | | | | |
| A | 7$^m$08 | +0$^m$49 | +0$^m$49 | G0V |
| B | 7.30 | +0.10 | +0.05 | A7p |
| C | 6.98 | +0.84 | +0.82 | K0III |
| D | 6.85 | +1.20 | +1.15 | K3III |
| E | 8.21 | +0.21 | +0.21 | F0III |
| F | 7.28 | +1.07 | +1.01 | K2III |
| D10 | | | | |
| C | 7.80 | −0.07 | −0.14 | B9 |
| E | 7.71 | +0.38 | +0.40 | F5 |
| F | 8.27 | −0.08 | −0.18 | B9 |
| H | 7.12 | +1.37 | +1.41 | K0 |
| M[a] | 7.15: | +1.28 | +3.03 | Mb |
| O | 7.85 | +1.61 | +1.97 | K2 |
| C12 | | | | |
| A[a] | 6.78 | −0.10 | −0.24 | A0 |
| C | 7.42 | +0.04 | −0.04 | A3 |
| D | 6.65 | +1.15 | +1.10 | K0III |
| E | 7.17 | +0.88 | +0.88 | K0III |
| F | 8.27 | +0.22 | +0.16 | A0p |
| G | 8.36 | +0.21 | ··· | F0p |
| I | 8.13 | +1.17 | +1.11 | K3III |
| L | 9.20 | +0.40 | ··· | F5III |
| M | 8.63 | +1.24 | +1.30 | K3III |
| N | 9.74 | +0.42 | ··· | K5III |
| O | 9.21 | +0.99 | +1.05 | K0III |

[a] Mag. var: Kron, White, and Gascoigne (1953).

system as defined by Seares and Joyner (1945). The old International photovisual magnitudes are, in fact, quite good, and the use of 24 stars permitted a very satisfactory photoelectric copy of the system. The 24 NPS stars listed in Table II were chosen to include a generous assortment of bright stars easy to find, with a good range in color. In the selection an effort was made to obtain nonvariable red stars and those of intermediate color, which are rather rare but important in establishing linearity of color and magnitude transformations. In addition, these 24 stars include the nine observed by Stebbins, Whitford, and Johnson (1950), although one of the nine is NPS 2r, a red star of doubtful light constancy. We designate our photoelectric copy of International photovisual by $V$, as originally suggested by Kron and J. L. Smith (1951). With $(P-V)$ as abscissa, Fig. 1, upper panel, shows by filled circles the deviations, $pv-V$, between our magnitudes $V$ and the International magnitudes, $pv$ as given by Seares and Joyner (1945); those with crosses represent the nine NPS stars observed by Stebbins, Whitford, and Johnson. The two most discrepant points (in parentheses) correspond to NPS 2r and 12r; if these are disregarded, a horizontal straight line, indicative of no color equation, may reasonably be drawn through the remaining points. Figure 1, lower panel, shows with open symbols the differences, $\Delta V$, between our $V$ magnitudes, and those of Johnson and Morgan (circles) and of Eggen (triangles). This plot indicates that magnitudes on our system are linearly related to the other two, within the range of $(P-V)$ from about −0.4 to +1.0 mag., according to the following formulae:

$$V_{JM}=V_{KM}-0.075(P-V)-0^m027,$$

$$V_E=V_{KM}-0.115(P-V)-0^m026;$$

where $V_{KM}$ refers to the magnitudes of this paper, $V_{JM}$ to those of Johnson and Morgan, and $V_E$ to those of Eggen. There is some suggestion that redder objects may depart systematically from a linear transformation.

We designate our blue color index by $(P-V)$ but with the difference (from Kron and Smith 1951) that here the $P$ magnitude is on an ultraviolet-free basis. For the zero point and scale of $(P-V)$, we use the same approximation to the International $CI$ employed by Eggen (1955). With this definition, $(P-V)$ can be reduced to

Johnson and Morgan's $(B\text{-}V)$ system, with a precision of $\pm 0.03$ mag., simply by adding 0.10 mag. to $(P\text{-}V)$ for the range $(P\text{-}V) = -0.4$ to $+1.0$ mag. If a more exact conversion is required over this range, and if the range is extended to include redder objects, then the following two linear relationships may be used:

$$(B\text{-}V) = +0^{m}10 + 0.96(P\text{-}V), \quad \text{for } (P\text{-}V) = -0.4 \text{ to } +1.0 \text{ mag.},$$

$$(B\text{-}V) = 0^{m}00 + 1.06(P\text{-}V), \quad \text{for } (P\text{-}V) = +1.0 \text{ to } +1.5 \text{ mag.}$$

Our decision to use a third color, $I$, which gives a second color index, $(V\text{-}I)$, was based on the hope of deriving color excesses for clusters according to the method devised by W. Becker (1938). Also, the success attained with the use of this method on stars by Johnson and Morgan (1953), who used a three-color system employing the ultraviolet, at first led us to make a number of ultraviolet observations of globular clusters. As may be expected from their color indices, however, many globular clusters are too faint in the ultraviolet for satisfactory large-aperture photometry. The situation is especially bad for the interesting and greatly reddened clusters at low declinations around the galactic center. Although even the heavily reddened, high-luminosity clusters actually have enough ultraviolet light to detect, we found in practice that the amount of skylight admitted through the large apertures reduced the ultraviolet cluster-sky ratio too much for satisfactory measurement. Likewise, with the Crossley reflector, we were unable to make any measurements of acceptable precision in the ultraviolet for the clusters in M31. On the other hand, experiments with the infrared indicated that the practical advantages in measuring in this spectral region for a third color more than made up for the large loss in quantum efficiency, which resulted from abandoning the *Sb-Cs* photosurface of the 1P21 in favor of the infrared-sensitive *CsO—Ag* photosurface.

The infrared index $(V\text{-}I)$ used here is based on an infrared photometric system like the infrared part of the $R, I$ system by Kron, White, and Gascoigne (1953). Thus if infrared magnitudes $I$ are computed from the $V$ magnitudes and $(V\text{-}I)$ color indices of the present paper, they will be on the same magnitude system as the infrared magnitudes $I$ computed from $(R\text{-}I)$ color indices.

All of the photometric standards used in this work are listed in Table II, which contains more than the data for the NPS standards. The awkwardness of direct work on the North Polar Sequence, the primary standard, persuaded us to establish secondary standards in four Harvard C and D regions. It should be noted that $I$ magnitudes derived from these standards differ slightly from those obtained from the earlier ones (Kron, White, and Gascoigne 1953), because the present data in Table II include some additional observations. In establishing these working standards, many transfers were made to the pole, as well as many cross transfers among the Harvard C and D regions. The spectral types with luminosity classes for NPS stars are by Keenan (1940), types for the C region stars are by Nassau and MacRae (1955), and for D10 from the *Henry Draper Catalogue.*

In addition to establishing secondary standards based upon the North Polar Sequence, we have measured some stars for calibration of our three-color system as a means for estimating color excess. Among these are a number of stars of known spectral type and presumed small reddening, taken from the listing of Johnson and Morgan (1953). In order to evaluate the ratio of total-to-selective absorption on our three-color system for objects of intrinsic color more nearly comparable to clusters, we also observed a number of F- and G-type supergiants for which recent six-color data were available. Some of these stars had previously been found to be much reddened in six-color photometry by Kron (1958). All these data are included in Table III, which is arranged to indicate how group means were formed to define the main sequence, and the giant and dwarf branches for late-type stars. Since the observing schedule did not provide time enough to determine new $P, V, I$ data for a complete calibration, a number of colors were obtained by conversion from previous work. Thus some $(P\text{-}V)$ colors are from the $(B\text{-}V)$ colors by Johnson and Morgan (1953), or from the $(P\text{-}V)_{E}$ colors by Eggen (1955).

## IV. OBSERVATIONAL TECHNIQUE FOR CLUSTERS

Before a cluster was observed, a photograph of the object and its surroundings was examined. Representative areas for the measurement of background light

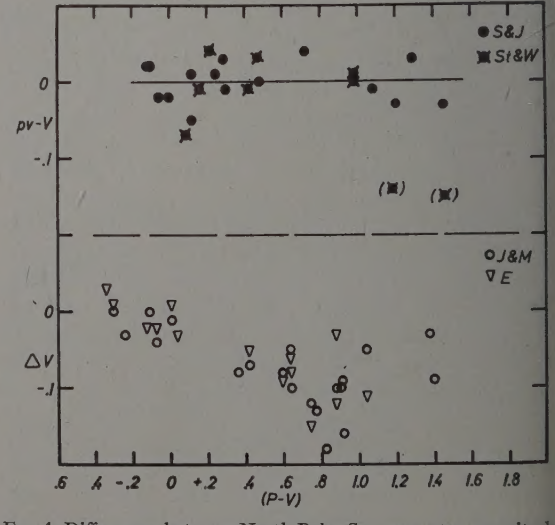


FIG. 1. Differences between North Polar Sequence star magnitudes determined by different observers.

TABLE III. Photometric data for calibration of three-color system.

| Star | Sp. T. | (*P-V*) | (*V-I*) |
|---|---|---|---|
| | Main Sequence | | |
| $\alpha$ Leo | B8 V | $-0^m24$ | $-0^m32$ |
| 134 Tau | B9 IV | $-0.18^a$ | $-0.27$ |
| $\xi^2$ Cet | B9 III | $-0.15$ | $-0.26$ |
| $\alpha$ Peg | B9 V | $-0.13$ | $-0.26$ |
| C Hya | A0 V | $-0.13^a$ | $-0.25$ |
| 109 Vir | A0 V | $-0.11$ | $-0.19$ |
| $\gamma$ Gem | A0 IV | $-0.11^a$ | $-0.16$ |
| $\gamma$ Oph | A0 V | $-0.07$ | $-0.12$ |
| $\epsilon$ Aqr | A1 V | $-0.11$ | $-0.19$ |
| HR 875 | A1 V | $-0.02^a$ | $-0.10$ |
| Means | A0 (10) | $-0.12$ | $-0.21$ |
| $\beta$ Ser | A2 IV | $-0.02^{a,b}$ | $-0.12$ |
| $\beta$ Leo | A3 V | $-0.02^{a,b}$ | $-0.08$ |
| $\lambda$ Gem | A3 V | $-0.01$ | $-0.08$ |
| $\zeta$ Lep | A3 V | $-0.00^a$ | $-0.08$ |
| $\beta$ Eri | A3 III | $+0.01$ | $-0.05$ |
| $\alpha$ Oph | A5 III | $+0.04$ | $+0.04$ |
| $\alpha$ Aql | A7 IV-V | $+0.12^{a,b}$ | $+0.08$ |
| Means | A4 (7) | $+0.02$ | $-0.04$ |
| $\zeta$ Leo | F0 III | $+0.22^b$ | $+0.23$ |
| $\gamma$ Vir | F0 V | $+0.25^b$ | $+0.26$ |
| Means | F0 (2) | $+0.24$ | $+0.24$ |
| $\alpha^1$ Lib | F5 IV | $+0.32$ | $+0.30$ |
| $\pi^3$ Ori | F6 V | $+0.36$ | $+0.35$ |
| $\gamma$ Ser | F6 V | $+0.40^{a,b}$ | $+0.37$ |
| $\iota$ Psc | F7 V | $+0.42$ | $+0.41$ |
| $\beta$ Vir | F8 V | $+0.45$ | $+0.44$ |
| Means | F6 (5) | $+0.39$ | $+0.37$ |
| $\eta$ Boo | G0 IV | $+0.50^{a,b}$ | $+0.51$ |
| $\lambda$ Ser | G0 V | $+0.52^{a,b}$ | $+0.48$ |
| Means | G0 (2) | $+0.51$ | $+0.50$ |
| $\kappa$ Cet | G5 V | $+0.59$ | $+0.55$ |
| 70 Vir | G5 V | $+0.63$ | $+0.60$ |
| $\tau$ Cet | G8 V | $+0.64$ | $+0.65$ |
| Means | G6 (3) | $+0.62$ | $+0.60$ |
| $\beta$ Aql | G8 IV | $+0.77$ | $+0.75$ |
| $o^2$ Eri A | K0 V | $+0.74^b$ | $+0.76$ |
| 107 Psc | K1 V | $+0.74$ | $+0.73$ |
| Means | K0 (3) | $+0.75$ | $+0.75$ |
| | Giants | | |
| $o$ Tau | G8 III | $+0^m82$ | $+0^m73$ |
| $\eta$ Psc | G8 III | $+0.88$ | $+0.80$ |
| Means | G8 (2) | $+0.85$ | $+0.76$ |
| $\delta$ Tau | K0 III | $+0.92$ | $+0.78$ |
| $\gamma$ Tau | K0 III | $+0.92^a$ | $+0.78$ |
| Means | K0 (2) | $+0.92$ | $+0.78$ |
| $\beta$ Oph | K2 III | $+1.04$ | $+0.96$ |
| $\alpha$ Ser | K2 III | $+1.11^{a,b}$ | $+1.01$ |
| Means | K2 (2) | $+1.08$ | $+0.98$ |
| $\beta$ Cnc | K4 III | $+1.40$ | $+1.35$ |
| $\gamma$ Dra | K5 III | $+1.44^{a,b}$ | $+1.48$ |
| $\alpha$ Tau | K5 III | $+1.44^{a,b}$ | $+1.54$ |
| Means | K5 (3) | $+1.43$ | $+1.46$ |
| | Dwarfs | | |
| $\epsilon$ Eri | K2 V | $+0.82^{a,b}$ | $+0.79$ |
| HR 753A | K3 V | $+0.91$ | $+0.91$ |
| HD 156026 | dK5 | $+1.03^b$ | $+1.13$ |
| $+2°$ 3312 | K7 V | $+1.22$ | $+1.47$ |
| $+0°$ 2989 | M0 V | $+1.31$ | $+1.66$ |
| $-3°$ 1123 | M1 V | $+1.33$ | $+2.05$ |
| $+2°$ 348 | M2 V | $+1.35$ | $+2.00$ |
| $+1°$ 4774 | M2 V | $+1.38$ | $+1.92$ |
| $+1°$ 2447 | M2 V | $+1.40$ | $+2.18$ |
| $+15°$ 4733 | M2.5 V | $+1.37$ | $+2.00$ |
| Means | M2 (5) | $+1.36$ | $+2.03$ |

F- and G-type supergiants

| HD | Sp. T. | (*P-V*) | (*V-I*) | [*V-I*] |
|---|---|---|---|---|
| 4362 | G0 Ib | $+1^m01$ | $+0^m98$ | $+0^m93$ |
| 8992 | F6 Ib | $+0.80$ | $+0.94$ | $+0.77$ |
| 9250 | G0 Ib | $+1.31$ | $+1.41$ | $+1.94$ |
| 159181 | G2 Ib | $+0.89$ | $+0.81$ | $+0.55$ |
| 165553 | F9 Ib | $+0.95$ | $+1.04$ | $+1.03$ |
| 172365 | F9 Ib | $+0.69$ | $+0.73$ | $+0.30$ |
| 174104 | G0 Ib | $+0.66$ | $+0.63$ | $+0.02$ |
| 187203 | G0 Ib | $+0.87$ | $+0.88$ | $+0.66$ |
| 204022 | G0 Ib | $+1.36$ | $+1.50$ | $+2.22$ |
| 204867 | G0 Ib | $+0.75$ | $+0.68$ | $+0.27$ |
| 209750 | G2 Ib | $+0.88$ | $+0.75$ | $+0.59$ |
| 219135 | G0 Ib | $+0.97$ | $+0.99$ | $+1.02$ |

[a] (*P-V*) from (*B-V*) determined by Johnson and Morgan (1953).
[b] (*P-V*) from (*P-V*)$_E$ determined by Eggen (1955).

were selected, and a preliminary decision on aperture sizes was made. For most clusters in the Galaxy, and for some extragalactic clusters, two or more areas were employed for measurement of background light. An inconsistency between the measures of more than one background area was always investigated, and care was taken to ensure that the photometric results were reasonably free from systematic errors due to unusually unfavorable background conditions. Because of bright stars in the field, exploratory measures on a few clusters were rejected; for some others, large-aperture photometry was not attempted. After elimination of such cases, most of the remaining globular clusters in Helen B. Sawyer's (1947) list, and north of $\delta = -38°$, were measured. Clusters in the Magellanic Clouds were observed in 1951 by Gascoigne and Kron by means of the same technique, with Harvard Region C12 as a standard (Eggen 1951).

No attempt was made to measure diameters for the clusters in the M31 group, although this may be a

good possibility with more powerful telescopic equipment. All our measurements in the M31 group were made through a focal-plane aperture of 13″.7 diameter, and the standard stars were measured through the same aperture. Measurements were not made on nights of bad seeing, as experience indicated that appreciable light was lost from these clusters when stellar images appeared to be much larger than 2″ in diameter. Good seeing was also required for reliable, visual centering of the fainter clusters in the aperture.

The photometry of M31 clusters through an aperture so large as 13″.7 required close examination of the field around each object. Stars fainter than 17.5 mag. could not always be seen reliably with the Crossley even during the very best seeing; yet, a star of 17.5 mag. in the same field of a 16.0-mag. cluster could cause the cluster measurement to be wrong by 0.25 mag. In order to minimize errors of this type, fields around the M31 clusters were inspected on enlarged prints, and on diapositives made from 100-inch reflector plates, kindly furnished by Dr. W. Baade. The comparison sky fields were selected as close as possible to the cluster, usually only about 1.5 aperture diameters away, in order to minimize errors from background brightness gradients in the spiral.

M31 is currently estimated as about 60 times more

TABLE IV. Magnitudes and related diameters of 67 galactic globular clusters.

| Aperture Diameter | | 0′.33 | 0′.49 | 0′.75<br>*8.29* | 1′.12<br>*9.95* | 1′.65<br>*11.6* | 2′.44<br>*13.4* | 3′.61<br>*16.6* | 5′.38<br>*20.0* | 6′.95<br>*24.8* | | | | | |
|---|---|---|---|---|---|---|---|---|---|---|---|---|---|---|---|
| NGC | M | *V* magnitudes[a] through above apertures[a] | | | | | | | | | $V_t$ | $n$ | $d_{0.9}$ | $n$ | Conc. Class |
| 2419 | | ... | $12^m.98$ | $12^m.26$ | $11^m.67$ | $11^m.27$ | $10^m.91$ | $10^m.65$[b] | ... | ... | $<10^m.9$ | 5 | ... | ... | ... |
| 4147 | | ... | 11.97 | 11.21 | 10.90 | 10.66 | 10.46 | 10.40 | 10.32 | ... | 10.26 | 2 | 3′.4 | 3 | (a,b) |
| 4590 | 68 | ... | ... | 10.13 | 9.42 | 9.01 | 8.81 | 8.71 | 8.46 | 8.35 | 8.31 | 3 | 6.4 | 3 | b |
| 5024 | 53 | ... | 10.53 | 9.75 | 9.19 | 8.69 | 8.33 | 8.08 | 8.00 | 7.82 | 7.76 | 2 | 8.3 | 1 | a,b |
| | | | | *7.82* | *7.80* | ... | *7.78* | ... | ... | ... | | | | | |
| 5053 | | ... | ... | ... | ... | ... | ... | ... | ... | 10.64 | 9.9 | 3 | ... | ... | ... |
| | | | | *10.36* | *10.14* | *10.05* | ... | ... | ... | ... | | | | | |
| 5272 | 3 | ... | 9.44 | 8.72 | 8.00 | 7.51 | 7.13 | 6.86 | 6.64 | 6.58 | 6.38 | 3 | 9.3 | 3 | b |
| | | | | *6.53* | *6.49* | *6.45* | *6.43* | *6.34* | ... | ... | | | | | |
| 5466 | | ... | ... | ... | ... | ... | ... | ... | 9.74 | 9.56 | 9.2 | 3 | ... | ... | ... |
| | | | ... | *9.39* | ... | ... | ... | ... | ... | ... | | | | | |
| 5634 | | ... | ... | ... | ... | ... | $9.84^b$ | ... | ... | ... | <9.8 | 2 | ... | ... | ... |
| 5694 | | 11.52 | 11.34 | 10.95 | 10.60 | 10.44 | 10.40 | 10.27 | ... | ... | 10.25 | 2 | 2.3 | 2 | a |
| 5824 | | 10.19 | 10.04 | 9.78 | 9.52 | 9.36 | 9.25 | 9.14 | 9.07 | ... | 9.04 | 4 | 3.3 | 2 | c |
| 5897 | | ... | ... | 12.30 | 11.36 | 10.61 | 10.05 | 9.40 | 8.95 | 8.80 | (8.4) | 2 | (15.7) | 2 | a |
| 5904 | 5 | ... | 9.43 | 8.55 | 7.70 | 7.26 | 6.87 | 6.59 | 6.29 | 6.17 | 5·93 | 4 | 10.7 | 3 | b |
| | | | | ... | *6.03* | ... | *5.99* | ... | *5.83* | ... | | | | | |
| 5986 | | ... | 10.47 | 9.72 | 9.16 | 8.61 | 8.25 | 8.03 | 7.77 | ... | 7.58 | 2 | 8.6 | 2 | b |
| 6093 | 80 | ... | 9.28 | 8.82 | 8.47 | 8.14 | 7.91 | 7.68 | 7.51 | 7.45 | 7.30 | 3 | 8.6 | 2 | c |
| 6121 | 4 | ... | ... | ... | 9.29 | 8.74 | 7.83 | 7.34 | 6.89 | 6.65 | 5.91 | 2 | 22.6 | 2 | a,b |
| | | | | *6.45* | *6.57* | *6.18* | *6.17* | ... | *6.08* | ... | | | | | |
| 6144 | | ... | ... | 12.53 | 11.46 | 10.70 | 9.92 | 9.62 | 9.29 | 9.51 | 9.00 | 4 | 11.1 | 2 | a |
| | | | | *9.20* | ... | ... | ... | ... | ... | ... | | | | | |
| 6171 | 107 | ... | 12.16 | 11.35 | 10.60 | 9.98 | 9.51 | 9.19 | 8.75 | 8.53 | 8.18 | 3 | 12.8 | 2 | b |
| | | | | *8.45* | *8.40* | ... | *8.31* | ... | ... | ... | | | | | |
| 6205 | 13 | ... | 10.06 | 9.20 | 8.40 | 7.69 | 7.05 | 6.58 | 6.24 | 6.10 | 5.87 | 4 | 12.9 | 3 | a |
| | | | | *6.06* | *5.99* | *5.99* | *5.96* | *5.92* | ... | ... | | | | | |
| 6218 | 12 | ... | 11.49 | 10.66 | 9.83 | 8.94 | 8.37 | 7.85 | 7.36 | 7.23 | 6.72 | 3 | 21.5 | 2 | b |
| | | | | ... | *7.03* | ... | *6.89* | ... | ... | ... | | | | | |
| 6229 | | 11.49 | 10.82 | 10.51 | 10.10 | 9.81 | 9.65 | 9.57 | 9.48 | ... | 9.44 | 2 | 3.6 | 2 | b |
| 6254 | 10 | ... | 10.98 | 9.95 | 9.20 | 8.50 | 7.97 | 7.48 | 7.22 | 7.05 | 6.64 | 3 | 16.2 | 2 | b |
| | | | | ... | *6.86* | *6.79* | *6.73* | ... | *6.70* | ... | | | | | |
| 6266 | 62 | ... | ... | ... | ... | 7.72 | 7.36 | 7.06 | 6.89 | ... | 6.66 | 3 | 8.8 | 2 | b |
| 6273 | 19 | ... | 10.15 | 9.36 | 8.67 | 8.12 | 7.64 | 7.34 | 7.13 | 7.06 | 6.88 | 4 | 9.3 | 2 | a,b |
| | | | | ... | *6.97* | ... | *6.91* | ... | ... | ... | | | | | |
| 6284 | | 10.84 | 10.53 | 10.14 | 9.81 | 9.53 | 9.39 | 9.22 | 9.05 | ... | 8.96 | 2 | 5.7 | 2 | c |
| 6287 | | ... | 11.66 | 11.25 | 10.49 | 10.17 | 9.90 | 9.74 | 9.48 | ... | 9.48 | 3 | 5.8 | 2 | b |
| 6293 | | 11.00 | 10.50 | 10.17 | 9.53 | 9.14 | 8.87 | 8.69 | 8.59 | ... | 8.43 | 2 | 6.2 | 2 | (c) |
| 6304 | | 12.10 | 11.21 | 10.34 | 9.88 | 9.46 | 9.14 | 8.88 | 8.68 | ... | 8.48 | 3 | 8.0 | 3 | b |
| 6316 | | ... | 11.62 | 10.90 | 10.53 | 10.12 | 9.64 | 9.40 | $8.90^b$ | ... | 9.11 | 3 | 7.2 | 3 | b |
| 6325 | | ... | 12.71 | 12.34 | 11.75 | 11.50 | 11.18 | 10.92 | ... | ... | 10.91 | 3 | 4.9 | 3 | b |
| 6333 | 9 | ... | 10.41 | 9.77 | 9.25 | 8.76 | 8.43 | 8.20 | 7.99 | 7.92 | 7.79 | 4 | 7.9 | 3 | b |
| 6341 | 92 | ... | 9.06 | 8.45 | 8.00 | 7.56 | 7.24 | 7.00 | 6.81 | 6.71 | 6.53 | 2 | 12.3 | 2 | b |
| | | | | | *6.64* | ... | *6.53* | ... | ... | ... | | | | | |
| 6342 | | ... | 11.92 | 11.37 | 11.04 | 10.70 | 10.43 | 10.22 | 9.86 | ... | 10.10 | 2 | 4.7 | 2 | b |
| 6355 | | ... | 12.09 | 11.39 | 10.90 | 10.62 | 10.28 | 9.98 | 9.43 | ... | 9.80 | 2 | 6.1 | 2 | b |
| 6356 | | ... | 10.84 | 10.04 | 9.52 | 9.14 | 8.87 | 8.68 | 8.50 | ... | 8.40 | 3 | 6.3 | 2 | b |
| 6401 | | ... | ... | ... | ... | ... | 9.85 | ... | ... | ... | <9.8 | 1 | ... | ... | ... |
| 6402 | 14 | ... | 11.67 | 10.68 | 9.84 | 9.08 | 8.57 | 8.16 | 7.89 | 7.78 | 7.56 | 4 | 10.8 | 2 | a |
| | | | | ... | *7.67* | ... | *7.60* | ... | ... | ... | | | | | |

TABLE IV.—*Continued.*

| Aperture Diameter | | 0′.33 | 0′.49 | 0′.75<br>*8.29* | 1′.12<br>*9.95* | 1′.65<br>*11.6* | 2′.44<br>*13.4* | 3′.61<br>*16.6* | 5′.38<br>*20.0* | 6′.95<br>*24.8* | | | | | |
|---|---|---|---|---|---|---|---|---|---|---|---|---|---|---|---|
| NGC | M | *V* magnitudes[a] through above apertures[a] | | | | | | | | | $V_t$ | $n$ | $d_{0.9}$ | $n$ | Conc. Class |
| 6426 | | ... | 14.45 | 13.90 | 13.33 | 12.71 | 11.83[b] | 11.27[b] | 10.61[b] | ... | <12.7 | 3 | ... | ... | ... |
| 6440 | | 11.47 | 10.85 | 10.30 | 10.14 | 10.01 | 9.82 | 9.61 | 9.33[b] | ... | 9.40 | 2 | 5.8 | 2 | (c) |
| 6453 | | ... | ... | ... | ... | ... | 9.94 | ... | ... | ... | <9.9 | 2 | ... | ... | ... |
| 6517 | | ... | 12.26 | 11.90 | 11.49 | 11.16 | 10.94 | 10.69 | ... | ... | 10.42 | 3 | 7.7 | 2 | c |
| 6522 | | ... | 10.24 | 9.70 | 9.32 | 9.10 | 8.89 | 8.76 | 8.53 | ... | 8.63 | 3 | 4.1 | 2 | b |
| 6528 | | ... | 10.91 | 10.42 | 9.98 | 9.78 | 9.63 | 9.55 | ... | ... | 9.54 | 3 | 3.0 | 2 | a |
| 6539 | | ... | ... | ... | ... | 11.27 | 10.83 | 10.42 | 10.15 | 9.96 | 9.67 | 5 | 13.8 | 3 | b |
| 6544 | | ... | 11.11 | 10.58 | 9.77 | 9.31 | 8.91 | 8.38[b] | 7.93[b] | ... | (8.3) | 3 | (8.4) | 2 | (b) |
| 6553 | | ... | 11.59 | 10.91 | 10.09 | 9.43 | 8.92 | 8.63 | 8.43 | ... | 8.22 | 2 | 8.2 | 2 | a |
| 6569 | | ... | 11.11 | 10.47 | 9.84 | 9.47 | 9.20 | 8.96 | 8.63[b] | ... | 8.66 | 2 | 6.6 | 1 | b |
| 6624 | | ... | ... | ... | 9.20 | 8.84 | 8.58 | 8.47 | 8.40 | ... | 8.35 | 2 | 4.2 | 2 | a |
| 6626 | 28 | ... | ... | ... | ... | 8.00 | 7.68 | 7.40 | 7.18 | 7.10 | 6.95 | 3 | 9.1 | 3 | (b) |
| 6637 | 69 | ... | 10.20 | 9.46 | 8.85 | 8.44 | 8.16 | 7.96 | 7.82 | ... | 7.67 | 2 | 6.8 | 2 | b |
| 6638 | | ... | 11.18 | 10.71 | 10.04 | 9.63 | 9.44 | 9.32 | 9.22 | ... | 9.17 | 2 | 4.3 | 2 | a |
| 6652 | | ... | 10.49 | 10.13 | 9.77 | 9.36 | 9.18 | 9.05 | 8.79[b] | ... | 8.92 | 1 | 4.2 | 1 | b |
| 6656 | 22 | ... | 10.45 | 9.56 | 8.67 | 7.84 | 7.13 | 6.50 | 6.06 | ... | 5.09 | 2 | 26.2 | 2 | b |
| | | | | *5.72* | ... | *5.53* | *5.43* | *5.32* | *5.25* | *5.22* | | | | | |
| 6681 | 70 | ... | 10.10 | 9.61 | 9.03 | 8.85 | 8.56 | 8.35 | 8.20 | ... | 8.17 | 2 | 5.1 | 2 | (b) |
| 6712 | | ... | 11.82 | 11.01 | 10.26 | 9.57 | 9.16 | 8.85 | 8.50 | 8.38 | 8.13 | 4 | 12.3 | 3 | b |
| 6715 | 54 | ... | 9.04 | 8.67 | 8.38 | 8.10 | 7.93 | 7.84 | 7.75 | ... | 7.66 | 2 | 4.8 | 2 | c |
| 6723 | | ... | 10.82 | 9.89 | 9.26 | 8.61 | 8.13 | 7.76 | 7.53 | ... | 7.21 | 2 | 11.7 | 2 | b |
| 6760 | | ... | 12.13 | 11.35 | 10.73 | 10.27 | 9.88 | 9.57 | 9.35 | ... | 9.13 | 3 | 8.9 | 2 | b |
| 6779 | 56 | ... | ... | 10.81 | 9.94 | 9.45 | 9.05 | 8.71 | 9.52 | ... | 8.21 | 3 | 10.1 | 2 | b |
| 6809 | 55 | ... | ... | 11.23 | 10.16 | 9.14 | 8.47 | 7.71 | 7.11 | ... | 6.30 | 2 | 21.1 | 2 | a |
| | | | | ... | *6.66* | *6.60* | *6.52* | ... | ... | ... | | | | | |
| 6838 | 71 | ... | 12.09 | 11.03 | 10.53 | 9.82 | 9.28 | 8.82 | 8.64 | 8.46 | 8.27 | 2 | 10.2 | 2 | (a) |
| | | | | ... | *8.39* | ... | *7.60*[b] | ... | ... | ... | | | | | |
| 6864 | 75 | ... | 9.89 | 9.65 | 9.32 | 9.06 | 8.92 | 8.78 | 8.70 | ... | 8.60 | 2 | 4.9 | 2 | c |
| 6934 | | ... | 10.74 | 10.18 | 9.73 | 9.47 | 9.28 | 9.10[b] | ... | ... | 9.12 | 3 | 3.3 | 2 | a |
| 6981 | 72 | ... | 12.22 | 11.54 | 10.79 | 10.23 | 9.86 | 9.66 | 9.50 | ... | 9.44 | 2 | 6.4 | 2 | a |
| 7006 | | ... | 11.94 | 11.53 | 11.20 | 11.04 | 10.37 | 10.76 | 10.72 | ... | 10.72 | 2 | 3.0 | 2 | b |
| 7078 | 15 | ... | 8.53 | 8.00 | 7.56 | 7.23 | 6.96 | 6.80 | 6.63 | 6.54 | 6.36 | 2 | 9.4 | 2 | c |
| | | | | *6.50* | *6.46* | ... | ... | ... | ... | ... | | | | | |
| 7089 | 2 | ... | 9.45 | 8.81 | 7.99 | 7.46 | 7.08 | 6.83 | 6.66 | 6.61 | 6.53 | 2 | 6.8 | 2 | a |
| | | | | ... | *6.57* | ... | *6.57* | ... | ... | ... | | | | | |
| 7099 | 30 | ... | 9.94 | 9.42 | 8.85 | 8.47 | 8.12 | 7.93 | 7.76 | 7.66 | 7.60 | 2 | 6.8 | 2 | b |
| | | | | *7.62* | *7.57* | ... | ... | ... | ... | ... | | | | | |

[a] *Magnitudes in italics* correspond with the *apertures in italics* at the top of the same column.
[b] One or more bright field stars in the aperture or nearby.

distant than the galactic center. Therefore, the observation of M31 clusters through an aperture of 13″.7 is equivalent to observing globular clusters near the galactic center through an aperture of approximately as many minutes. Since the diameters containing 0.9 of the light of the galactic center objects do not exceed 10′, the total magnitudes for the M31 clusters do not need to be corrected for aperture diameter before being compared with those for the galactic center globular clusters.

At an early stage in the photometry of the galactic globular clusters, measurements in each of the three colors were made through several apertures for 48 clusters. Since these data indicated that there was no appreciable dependence of diameter on integrated color, the program was completed by making color measurements through only one aperture that admitted about 75% of the total light. There was a resultant gain in accuracy because of the improved contrast with sky background, as compared with apertures that admitted a larger percentage. Finally, all the diameter measurements were repeated through a colorless filter to gain light, and through six to twelve more apertures of different sizes to gain observational weight.

Magnitude and color observations were corrected for atmospheric extinction with mean extinction coefficients determined from stellar observations with appropriate cells and filters. Clusters far south were observed close to the meridian.

## V. TOTAL MAGNITUDES AND DIAMETERS

The determination of galactic globular cluster total magnitudes and angular diameters involved the photom-

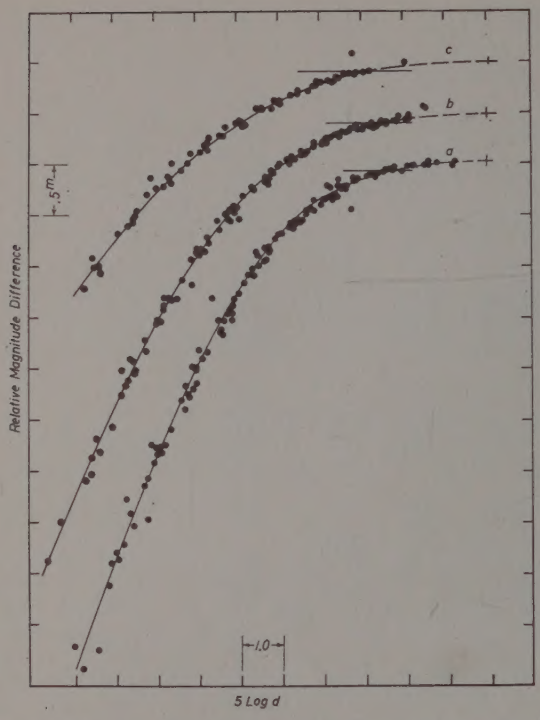


FIG. 2. Light concentration curves used to estimate total magnitudes and diameters containing 0.9 total light.

etry of surface brightnesses that decrease gradually into the field-star and sky background. Ideally, the observations should be pushed to the diameter where the photometer is unable to detect any residual cluster light in the presence of the interfering field-star and sky light. This point of diminishing or no returns depends upon such factors as night sky brightness, atmospheric extinction, and field-star density. Consequently, cluster total magnitudes and diameters are bound to be less precise than magnitudes for stars or diameters for sharply defined objects. In an attempt to allow for these factors, we have used a large range of apertures, several colors, and two photometers. The most important innovation, however, probably was the design and use of one of the photometers with apertures large enough to reach, in nearly every large object observed, the place where cluster light was almost indistinguishable from background light. In a few cases, because of brighter field stars, or of cluster low surface brightness, the observations could not be made as close to this limit as for the large majority of clusters. These cases are noted by the superscript letter b in Table IV, which gives the individual magnitudes measured through the various apertures, and the total magnitudes and diameters derived as described in the following.

For each cluster the magnitudes measured through the different apertures were plotted as ordinates against 5 log$d$ as abscissa, where $d$ is the angular diameter in minutes of arc. This procedure gave a convenient scal on which to compare the cluster "curves of shape regardless of distance. For it is clear that a plot of mag nitude for a particular cluster against the paramete 5 log$d$ will apply to all other clusters having the sam brightness distribution function, subject only to trans lation to allow for differences in linear size, distance and interstellar absorption. With the intercompariso of the cluster curves of shape thus facilitated, man superpositions of such curves on transparent pape indicated that a fair proportion, about 80%, of th observed clusters could be placed in three categories o central concentration. These categories and typical exam ples are: a (low), NGC 6205; b (medium), NGC 5272 and c (high), NGC 7078. The exceptional 20%, fo which concentration classes are not given or ar assumed (in parentheses), are very open objects (NG 5053 and 5466), too faint (NGC 6426), or too close t bright field stars (NGC 5634). Next, mean curves wer drawn through the individual curves grouped for eac category, and they were extrapolated to a horizonta tangent at their upper ends, as shown in Fig. 2. Finally the mean curves were traced on transparent paper superimposed on the individual cluster plots of $V$ against 5 log$d$, and used to estimate the total magni tudes, $V_t$, and diameters including 0.9 of the tota light, $d_{0.9}$, listed in Table IV.

As one would expect from the mean curves of Fig. 2 the derivation from their upper ends of total magnitudes did not involve serious extrapolation, because of the use of large apertures. For any particular cluster, the extrapolation actually made to obtain the total magnitude $V_t$, is given by the difference between $V_t$ and the $V$ magnitude measured through the largest aperture used without interference from bright field stars. If $V-V_t=\Delta m$, then the data in Table IV give $\langle\Delta m\rangle=0.13$ mag., with a range from 0.0 to 0.4 mag; there are only 12 clusters for which $\Delta m>0.2$ mag. The case is different, however, for the derivation of limiting diameters corresponding to the total magnitudes. Since the curves approach parallelism with the 5 log$d$ axis, a small change in the cluster magnitude is accompanied by a much larger change in 5 log$d$. Although an attempt was made to obtain limiting diameters, these proved to be so large and uncertain, with extrapolation factors for diameters averaging 4.1 and ranging up to nearly 10, that clearly some other diameter definition should be used. Some trials indicated that a fair compromise between interpolation and extrapolation could be obtained with a diameter that includes 0.9 of the total light. With this specification, the ratio $r$, between $d_{0.9}$ and the diameter of the largest aperture used without field-star interference, averages to give $\langle r\rangle=1.2$. For 27 clusters $r<1.0$, and for 33 clusters $r>1.0$; only four diameters have $r>2.0$, and of these the two largest have $r=2.3$ and 3.4 for NGC 5897 and 6544, respectively. The first value goes with the largest extrapola-

tion ($\Delta m = 0.4$ mag.) made to obtain a total magnitude, while the second is a marginal case involving field-star interference.

### VI. ERRORS IN THE PHOTOMETRY

Compared to the errors inherent in the cluster data, those in the selected stellar standards probably are inappreciable, because the point-source character and greater relative brightness practically eliminate sky background as a serious source of systematic error. On the other hand, the cluster observations may not be so free of systematic error from sky light: the galactic globulars because of their large size, and the extragalactic clusters because of their faintness. In both cluster groups, however, the internal errors of measurement seem satisfactorily small, as indicated by the average deviation, AD, from the mean of $n$ nights of observation, listed with the data in Tables VI and VII. These average deviations infrequently exceed 0.1 mag., and many are less than 0.05 mag. Nevertheless, there are several potential sources of systematic error that require discussion, separately for the galactic and extragalactic clusters because somewhat different procedures were followed in their observation.

#### Galactic Globular Clusters

For practical reasons involving photometer sensitivity, an indirect method was used initially to determine the ($V$-$I$) colors. This method was to measure the $I$ magnitudes with the infrared-sensitive photocell independently of the $V$ magnitudes, which were measured by necessity with the 1P21. This procedure was adopted only after experience had shown good agreement between ($V$-$I$) colors obtained either differentially on the same night, or by differences of $V$ and $I$ magnitudes measured on different nights. Later in the program the Lallemand multiplier phototube became available, and then all three magnitudes, $P$, $V$, and $I$ were measured successively the same night for a given cluster.

To minimize systematic errors from field stars in the large apertures, sky measurements were made for each cluster on an adjacent field that appeared visually normal in star density. When it was difficult to make a selection, two or more fields were observed, and their intensity was averaged to correct the cluster observations. In some cases, when moderately bright field stars could not be avoided, they, too, were observed and their light was subtracted from that of the cluster; but, when such stars were so bright that they outshone the cluster, observations of the latter were not attempted. We wish to emphasize that the observations for the sparsest clusters, like NGC 5053, could be considerably affected by the background sky light, but because there are no other independent measurements of similar kind, we can only hope that our data for poor clusters are of the correct order of magnitude: total

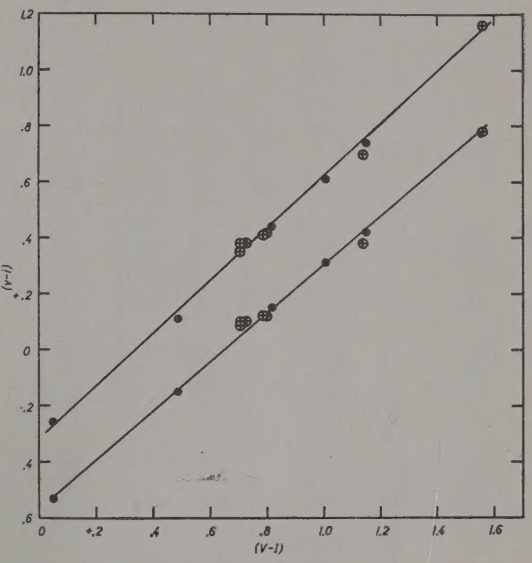


FIG. 3. Comparison of infrared color indices measured with extra-transparent red filter (above) and regular one (below).

magnitudes probably reliable to 0.5 mag., and diameters to 25%. Lastly, and for the same reason—no other comparable photoelectric data—it is impractical to evaluate in a detailed numerical manner the possible systematic errors in the diameters. For clusters of moderate-to-high surface brightness and located in uniform star fields, the night-to-night values of the diameters usually were accordant to about 5%. Since this degree of internal consistency seems satisfactory, we therefore conclude that the diameters tabulated in Table IV probably are reliable to 10% or better, except for the most open clusters, as mentioned in the foregoing.

#### Galactic Open Clusters

Compared with representative globular clusters, these clusters are of considerably larger apparent size, and of much lower mean surface brightness. In addition, they

TABLE V. Comparison of infrared filters.

| Star or Cluster | Regular Filter ($v-i$) | Light Filter ($v-i$)$-1^m.50$ | Colors Tables II, VI ($V$-$I$) |
|---|---|---|---|
| C 8 A | $-0^m.15$ | $+0^m.11$ | $+0^m.49$ |
| B | −0.53 | −0.26 | +0.05 |
| C | +0.15 | +0.44 | +0.82 |
| D | +0.42 | +0.74 | +1.15 |
| F | +0.31 | +0.61 | +1.01 |
| NGC 5024 | +0.10 | +0.35 | +0.71 |
| 5272 | +0.12 | +0.41 | +0.79 |
| 5904 | +0.12 | +0.42 | +0.80 |
| 6205 | +0.09 | +0.38 | +0.71 |
| 6254 | +0.38 | +0.70 | +1.14 |
| 6341 | +0.10 | +0.38 | +0.73 |
| 6402 | +0.78 | +1.16 | +1.56 |

TABLE VIa. Colors of star clusters in the Galaxy. Globular clusters.

| NGC | M | (*P-V*) | AD | *n* | (*V-I*) | AD | *n* | NGC | M | (*P-V*) | AD | *n* | (*V-I*) | AD | *n* |
|---|---|---|---|---|---|---|---|---|---|---|---|---|---|---|---|
| 2419[a] | | 0$^m$64 | 5 | 5 | 0$^m$92 | 7 | 4 | 6402 | 14 | 1$^m$12 | 4 | 5 | 1$^m$56 | 3 | 4 |
| 4147[a] | | 0.48 | 0 | 2 | 0.67 | 1 | 3 | 6426 | | 0.85 | 18 | 3 | 1.18 | 8 | 3 |
| 4590[a] | 68 | 0.59 | 6 | 3 | 0.81 | 2 | 3 | 6640[b] | | 1.81 | 6 | 3 | 2.51 | 0 | 2 |
| 5024[a] | 53 | 0.50 | 0 | 2 | 0.71 | 3 | 2 | 6453[b] | | 1.04: | 2 | 2 | 1.90: | 6 | 2 |
| 5053[a] | | 0.55 | 14 | 3 | 0.76 | 13 | 3 | 6517 | | 1.67 | 1 | 3 | 2.32 | 2 | 2 |
| 5272[a] | 3 | 0.56 | 4 | 3 | 0.79 | 2 | 3 | 6522[b] | | 1.02 | 8 | 3 | 1.38 | 1 | 3 |
| 5466[a] | | 0.64 | 5 | 3 | 0.67 | 2 | 3 | 6528[b] | | 1.27 | 3 | 3 | 1.56 | 3 | 3 |
| 5634[a] | | 0.56 | 2 | 2 | 0.87: | 2: | 3 | 6539 | | 1.67 | 5 | 4 | 2.23 | 8 | 3 |
| 5694[a] | | 0.61 | 0 | 2 | 0.87 | 3 | 3 | 6544[b] | | 1.27 | 6 | 3 | 1.85 | 5 | 3 |
| 5824[a] | | 0.63 | 8 | 4 | 0.94 | 7 | 3 | 6553[b] | | 1.39 | 1 | 2 | 2.17 | 4 | 2 |
| 5897[a] | | 0.62 | 0 | 2 | 0.86 | 2 | 2 | 6569[b] | | 1.11 | 6 | 2 | 1.56 | 3 | 2 |
| 5904[a] | 5 | 0.63 | 1 | 4 | 0.80 | 2 | 4 | 6624[b] | | 1.00 | 7 | 2 | 1.34 | 2 | 2 |
| 5986 | | 0.75 | 2 | 2 | 1.12 | 4 | 2 | 6626[a] | 28 | 0.97 | 2 | 3 | 1.28 | 2 | 3 |
| 6093 | 80 | 0.76 | 2 | 4 | 0.95 | 4 | 4 | 6637[b] | 69 | 0.87 | 5 | 2 | 1.18 | 6 | 2 |
| 6121 | 4 | 0.92 | 1 | 2 | 1.34 | 2 | 2 | 6638[b] | | 0.96 | 1 | 2 | 1.46 | 1 | 2 |
| 6144 | | 0.82 | 5 | 6 | 0.98 | 6 | 5 | 6652[b] | | 0.78 | ... | 1 | 1.02 | ... | 1 |
| 6171[a] | 107 | 0.97 | 6 | 5 | 1.34 | 5 | 3 | 6656 | 22 | 0.86 | 1 | 2 | 1.42 | 5 | 2 |
| 6205[a] | 13 | 0.57 | 2 | 6 | 0.71 | 3 | 4 | 6681 | 70 | 0.59 | 2 | 2 | 0.87 | 0 | 2 |
| 6218[a] | 12 | 0.77 | 1 | 5 | 1.02 | 2 | 4 | 6712 | | 1.04 | 3 | 4 | 1.59 | 7 | 4 |
| 6229[a] | | 0.64 | 1 | 2 | 0.88 | 3 | 3 | 6715 | 54 | 0.70 | 3 | 2 | 1.00 | 1 | 2 |
| 6254[a] | 10 | 0.79 | 1 | 3 | 1.14 | 1 | 2 | 6723 | | 0.61 | 1 | 2 | 0.92 | 4 | 2 |
| 6266[b] | 62 | 0.95 | 5 | 3 | 1.60 | 11 | 3 | 6760 | | 1.55 | 2 | 3 | 2.12 | 1 | 2 |
| 6273[b] | 19 | 0.90 | 3 | 4 | 1.22 | 1 | 2 | 6779 | 56 | 0.74 | 4 | 3 | 1.04 | 2 | 2 |
| 6284[b] | | 0.91 | 1 | 2 | 1.20 | 1 | 2 | 6809[b] | 55 | 0.55 | 0 | 2 | 0.83 | 5 | 2 |
| 6287[b] | | 1.13 | 2 | 3 | 1.73 | 1 | 2 | 6838 | 71 | 0.95 | 1 | 2 | 1.34 | 9 | 2 |
| 6293[b] | | 0.86 | 1 | 2 | 1.16 | 2 | 2 | 6864[a] | 75 | 0.71 | 0 | 2 | 1.09 | 4 | 2 |
| 6304[b] | | 1.22 | 2 | 3 | 1.68 | 2 | 2 | 6934[a] | | 0.62 | 1 | 3 | 0.84 | 3 | 3 |
| 6316[b] | | 1.17 | 4 | 3 | 1.81 | 1 | 2 | 6981[a] | 72 | 0.57 | 0 | 2 | 0.81 | 5 | 2 |
| 6325[b] | | 1.52 | 2 | 3 | 2.14 | 2 | 2 | 7006[a] | | 0.61 | 1 | 2 | 0.84 | 5 | 2 |
| 6333[b] | | 0.87 | 3 | 4 | 1.27 | 3 | 3 | 7078[a] | 15 | 0.59 | 1 | 2 | 0.70 | 4 | 2 |
| 6341[a] | 92 | 0.53 | 0 | 2 | 0.73 | 3 | 2 | 7089[a] | 2 | 0.57 | 1 | 2 | 0.73 | 5 | 2 |
| 6342[b] | | 1.20 | 2 | 2 | 1.42 | 2 | 2 | 7099[a] | 30 | 0.48 | 0 | 2 | 0.72 | 1 | 2 |
| 6355[b] | | 1.41 | 3 | 2 | 1.76 | 5 | 2 | | | | | | | | |
| 6356[b] | | 1.06 | 2 | 3 | 1.38 | 1 | 2 | | | | | | | | |
| 6401[b] | | 1.17: | ... | 1 | 1.89: | ... | 1 | | | | | | | | |

[a] Clusters with $|b| \geq 20°$.
[b] Galactic center group.

are usually found close to the galactic plane and in rich star fields. A single bright field star, if measured along with the cluster and not properly compensated by an equivalent object in one of the background measurements, could easily seriously affect the resultant measurement on the cluster. It must, therefore, be recognized that these photometric data for the open clusters probably are more subject to systematic error than those for the other objects observed in this program.

## Extragalactic Clusters

For these objects, too, we are convinced that the most serious source of systematic error probably is the failure of a sample of comparison sky to be accurately representative of that for a cluster, particularly in parts of systems having steep structural gradients or high-intensity levels of light. The error from intrusive field stars, however, is expected to be small for clusters 16 mag. or brighter, because a 19.5-mag. field star would produce an error of only 0.05 mag., and such a star could hardly have been overlooked in the examination of the survey plates for comparison sky fields. Nevertheless, the results for the fainter M31 clusters may in some instances have larger systematic errors. For example, the object B327 was measured as 18.9 mag. in the blue, so that a field star of photographic magnitude 21.5 in a comparison sky field could cause an error of 0.1 mag. An attempt to minimize this possibility was made by observing several sky fields and checking their agreement. Also, for clusters such as H89 in fields having a steep background-light gradient, the sky brightness was measured on several sides of the cluster, and the cluster measurement was corrected by linear interpolation. This procedure yielded results for which systematic errors from sky background are unlikely to be greater than 0.1 to 0.2 mag.

In addition to the foregoing type of error, there was a possibility that the infrared measurements of the M31 clusters could be affected by a systematic error of instrumental nature. Following some preliminary work, it was found desirable to gain more light by use

TABLE VIb. Colors of star clusters in the Galaxy. Open clusters.

| NGC, *IC* | M | (*P-V*) | AD | (*V-I*) | AD | *n* | Aper. | NGC, *IC* | M | (*P-V*) | AD | (*V-I*) | AD | *n* | Aper. |
|---|---|---|---|---|---|---|---|---|---|---|---|---|---|---|---|
| 457 | | 0m47 | 0 | 0m62 | 3 | 2 | 16′6 | 2099 | 37 | 0m45 | 2 | 0m52 | 4 | 4 | 24′8 |
| 559 | | 0.69 | 2 | 1.36 | 8 | 4 | 9.95 | 2682 | 67 | 0.68 | 8 | 0.71 | 2 | 3 | 24.8 |
| 581 | 103 | 0.30 | 3 | 0.88 | 2 | 3 | 8.29 | *4725* | 25 | 0.48 | ··· | 0.81 | ··· | 1 | 24.8 |
| 637 | | 0.25 | 4 | 0.30 | 8 | 4 | 5.38 | 6633 | | 0.20 | 1 | 0.03 | 8 | 2 | 24.8 |
| 663 | | 0.63 | 0 | 1.31 | 10 | 2 | 24.8 | 6811 | | 0.55 | 1 | 0.80 | 4 | 2 | 16.6 |
| 869 | h Per | 0.29 | 2 | 0.30 | 5 | 3 | 24.8 | 6866 | | 0.31 | 1 | 0.38 | 5 | 2 | 11.6 |
| 884 | χ Per | 0.54 | 6 | 1.22 | 5 | 3 | 24.8 | 6940 | | 0.49 | 1 | 1.20 | 4 | 2 | 24.8 |
| *1805* | | 0.43 | 10 | 0.63 | 6 | 4 | 24.8 | 7092 | 39 | −0.14 | 4 | −0.16 | 15 | 2 | 24.8 |
| Tr2 | | 0.40 | 6 | 0.82 | 12 | 4 | 24.8 | 7209 | | 0.36 | 2 | 0.79 | 8 | 2 | 24.8 |
| 1027 | | 0.41 | 6 | 0.54 | 2 | 4 | 24.8 | 7243 | | −0.15 | 3 | −0.03 | 3 | 2 | 24.8 |
| 1502 | | 0.38 | 4 | 0.50 | 2 | 4 | 16.6 | 7380 | | 0.27 | 1 | 0.44 | 1 | 2 | 11.6 |
| 1528 | | 0.25 | 3 | 0.47 | 9 | 2 | 24.8 | 7789 | | 0.86 | 1 | 1.05 | 4 | 2 | 20.0 |
| 1662 | | 0.41 | 9 | 0.62 | 10 | 3 | 20.0 | 7790 | | 0.49 | 3 | 0.64 | 14 | 2 | 20.0 |
| 1912 | 38 | 0.25 | 0 | 0.44 | 4 | 2 | 24.8 | | | | | | | | |
| 1960 | 36 | −0.02 | 4 | 0.03 | 10 | 4 | 24.8 | | | | | | | | |

of a more transparent filter, i.e., one with a broader transmission band. For this it was assumed that the reduction to the standard system was the same as that for the less transparent filter used for the brighter objects. As a preliminary test of this assumption, two different infrared filters were used, and accordant magnitudes were obtained. Since this check was necessary but not sufficient, we also used the Lal II infrared-sensitive multiplier with the stellar photometer provided with the GG 11+BG 18 yellow filter, the BG 21+RG 8 regular infrared filter used on bright objects, and finally the RG 2 extra-transparent filter with which the *I* magnitudes of the M31 clusters were obtained. We then measured a number of bright objects with the yellow filter and with both the normal and lighter infrared filters. These "natural" photoelectric colors, (*v-i*), were then compared with others on the standard (*V-I*) system, with the results given in Table V and shown in Fig. 3. The upper set of points is for the more transparent *I* filter, the lower for the regular one. From the fact that observations made with either filter give points that fall on a single straight line for both stars and clusters—as indicated in the figure—we conclude that the *I* magnitudes for the fainter M31 clusters probably have no large (*v-i*) to (*V-I*) transformation errors due to the use of a more transparent filter than that used for the brighter galactic globular clusters.

## VII. OBSERVATIONAL MATERIAL

The observations made at Mount Hamilton were begun in July, 1953, and were completed in August, 1957; those at Mount Stromlo were obtained during September through November, 1951. The principal results are collected in Table VI for the galactic objects and in Table VII for the extragalactic.

In Table VI, the column headings are self-explanatory; Table VI b contains three-color data for 28 open clusters included mainly for purposes of comparison with globular clusters. In most cases, these open clusters were observed with photometric apertures sufficiently large to give a satisfactory integrated color of a majority of the cluster members.

In Table VII, the first column contains identifying letters and numbers that mean the following: The letter H, in M31 with arabic numbers and in NGC 205 with roman numerals, designates clusters found by Hubble (1932). The letter B denotes those found by Baade, who communicated the identifications for clusters with numbers of 200 to 300 to Nassau and Seyfert (1945), and who also kindly sent us a marked chart with later discoveries, to which he assigned numbers of 300 and larger, and to which we gave numbers greater than 140 and less than 200 for unnumbered objects; M means those found by Mayall and discussed by him and Eggen (1953), except for M V, which is a later identification; the Anon. object at the end of the table of M31 objects is one of two that Hubble (1932, footnote p. 54) considered as "probable." For those in M33, we used an unpublished print marked by Hubble to show the objects we list as Ha, Hb, and Hd, while Mc is an unpublished identification by Mayall. In NGC 185, we observed two of the three reported by Baade (1944), and Ba is our designation for the object on his chart (1944, Plate IV) with coordinates 33.0 mm *E* and 37.4 mm *N* of the center of the system, and with Bc the one 12.4 mm *E* and 3.5 mm *S*. These objects in M31, some not previously charted in the literature, are marked in Figs. 4 and 5. In the Fornax dwarf system, the Anon. cluster is the one 6′.7 *E* and 1′.5 *S* of CD −35°919 (Baade and Hubble 1939). The three-color measurements are not so complete as we should like, mainly because they represent results so close to the useful limit of our infrared photometer that they could be obtained only under the very best observing conditions.

An additional group of clusters of considerable interest is that in M33. With the Crossley, these objects are faint and difficult to see, and for this reason we were able to measure only four (Fig. 6) of more than 100


FIG. 4. Outlying star clusters observed in M31.

discovered by Sandage (Bowen 1956). We shall therefore mention here only the fact that these four M33 clusters are unusually blue. The two bluest objects may be rich Population I clusters like some of those in the Large Magellanic Cloud. The nature of the other two cannot be determined from the present data, but if they are Population II objects, their stellar content must b considerably different than that of globular cluste found in the other major systems. Of the two cluste measured in NGC 205, H III seems normal, whil H VIII seems blue and faint like the clusters in M3 The clusters Ba and Bc in NGC 185 are of norma

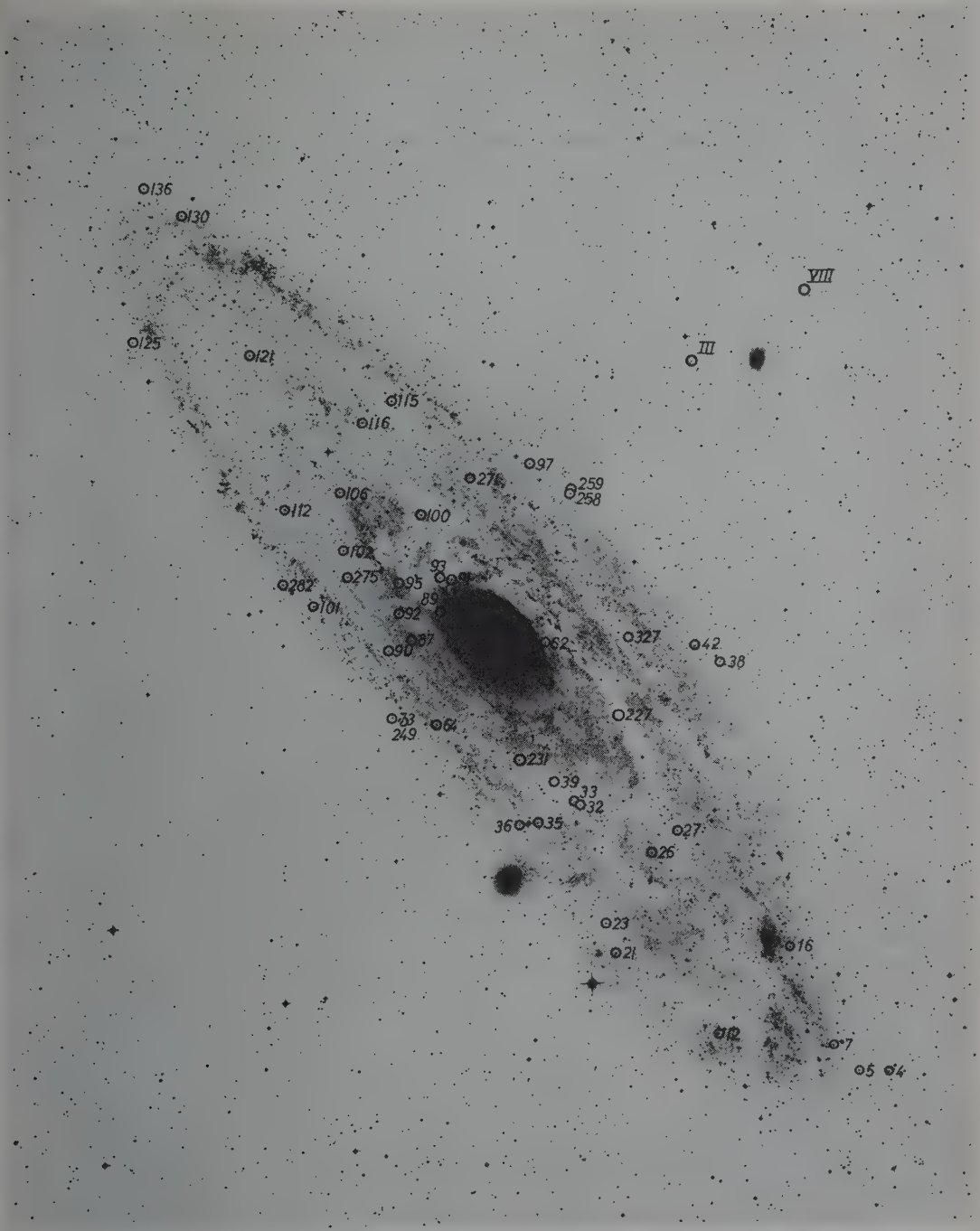


FIG. 5. Star clusters observed over or in main body of M31 and around NGC 205 (upper right).

observed color, but they are of rather low luminosity, unless NGC 185 is somewhat more distant than M31. Their lower luminosity, however, is consistent with the concept that the brightest objects in a low-luminosity parent system may be systematically fainter than those in a system of normal or high luminosity.

## VIII. DISCUSSION OF THE THREE-COLOR OBSERVATIONS

### Stars

The three-color data for the relatively unreddened stars in Table III are plotted in Fig. 7. The main

sequence, and the giant and dwarf separation for late-type stars, at about spectral type K0, may readily be seen. This plot therefore establishes rough thermal loci for relatively unreddened, probably single stars. In Fig. 8 are plotted the three-color individual observations for the 12 F- and G-type supergiants that show a large range in reddening (Kron 1958). The latter define a reddening line for objects whose intrinsic colors

TABLE VII. Photometric data for extragalactic star clusters.

| Cluster | $V$ | AD | $(P\text{-}V)$ | AD | $n$ | $(V\text{-}I)$ | AD | $n$ |
|---|---|---|---|---|---|---|---|---|
| | | | | M31 | | | | |
| H 4 | $15^m50$ | 3 | $+0^m74$ | 5 | 3 | ... | ... | ... |
| H 5 | 16.37 | 3 | +0.11 | 2 | 2 | $+0^m47$ | 4 | 3 |
| H 7 | 16.94 | 4 | +0.20 | 12 | 3 | ... | ... | ... |
| H 12 | 14.31 | 1 | +0.74 | 1 | 2 | +0.89 | 8 | 3 |
| H 16 | 15.72 | 4 | +0.92 | 3 | 3 | +1.06 | 10 | 2 |
| H 19[a] | 15.67 | 5 | +0.69 | 1 | 2 | ... | ... | ... |
| H 21 | 17.02 | 8 | +0.09 | 14 | 4 | ... | ... | ... |
| H 23 | 15.06 | 4 | +0.70 | 3 | 2 | +0.93 | 9 | 2 |
| H 26 | 15.57 | 3 | +0.71 | 3 | 3 | ... | ... | ... |
| H 27 | 15.68 | 1 | +0.71 | 4 | 3 | ... | ... | ... |
| H 32 | 16.45 | 3 | +1.32 | 15 | 4 | ... | ... | ... |
| H 33 | 16.06 | 10 | +0.67 | 8 | 3 | ... | ... | ... |
| H 35 | 15.66 | 6 | +0.73 | 4 | 2 | ... | ... | ... |
| H 36 | 16.40 | 2 | +0.59 | 4 | 2 | ... | ... | ... |
| H 38 | 16.15 | 5 | +0.93 | 3 | 3 | ... | ... | ... |
| H 39 | 15.65 | 2 | +1.48 | 1 | 2 | +1.90 | 4 | 2 |
| H 42 | 14.32 | 0 | +0.97 | 1 | 2 | +1.33 | 5 | 3 |
| H 44[a] | 14.96 | 4 | +0.83 | 4 | 2 | +1.01 | 9 | 3 |
| H 55[a] | 15.64 | 2 | +0.77 | 2 | 3 | ... | ... | ... |
| H 57[a] | 15.97 | 2 | +0.85 | 4 | 2 | ... | ... | ... |
| H 62 | 15.05 | 2 | +0.61 | 4 | 2 | ... | ... | ... |
| H 64 | 14.73 | 2 | +0.81 | 2 | 2 | +0.95 | 1 | 2 |
| H 73 | 15.41 | 2 | +0.80 | 1 | 2 | ... | ... | ... |
| H 76[a] | 15.65 | 6 | +0.50 | 4 | 2 | ... | ... | ... |
| H 87 | 15.23 | 6 | +0.81 | 6 | 3 | ... | ... | ... |
| H 89 | 16.17 | 6 | +0.73 | 6 | 3 | ... | ... | ... |
| H 90 | 15.59 | 5 | +0.79 | 6 | 3 | ... | ... | ... |
| H 91 | 15.34 | 11 | +0.80 | 1 | 3 | +0.80 | 6 | 2 |
| H 92 | 15.23 | 6 | +0.67 | 1 | 2 | ... | ... | ... |
| H 93 | 14.89 | 4 | +1.18 | 4 | 5 | +1.33 | 2 | 2 |
| H 94[a] | 15.90 | 2 | +0.85 | 2 | 2 | ... | ... | ... |
| H 95 | 15.08 | 4 | +0.62 | 2 | 3 | +0.80 | 3 | 2 |
| H 97 | 15.49 | 2 | +1.01 | 6 | 2 | ... | ... | ... |
| H 99[a] | 15.66 | 1 | +0.65 | 0 | 2 | ... | ... | ... |
| H100 | 15.13 | 1 | +0.93 | 2 | 2 | +1.29 | 2 | 2 |
| | | | | NGC 205 | | | | |
| HIII | 15.04 | 8 | +0.72 | 5 | 3 | +1.07 | 1 | 2 |
| HVIII | 16.72 | 2 | +0.44 | 5 | 2 | ... | ... | ... |
| | | | | NGC 185 | | | | |
| Ba | 16.93 | 4 | +0.73 | 6 | 3 | ... | ... | ... |
| Bc | 16.79 | ... | +0.60 | ... | 1 | ... | ... | ... |

| Cluster | $V$ | AD | $(P\text{-}V)$ | AD | $n$ | $(V\text{-}I)$ | AD | $n$ |
|---|---|---|---|---|---|---|---|---|
| | | | | M31 | | | | |
| H101 | $14^m81$ | 1 | $+0^m70$ | 0 | 2 | $+0^m83$ | 5 | 3 |
| H102 | 15.46 | 2 | +0.62 | 3 | 3 | ... | ... | ... |
| H106 | 15.05 | 3 | +0.81 | 2 | 2 | +0.81 | 8 | 2 |
| H112 | 15.47 | 4 | +0.63 | 4 | 2 | ... | ... | ... |
| H115 | 15.58 | 2 | +0.82 | 5 | 3 | ... | ... | ... |
| H116 | 15.41 | 1 | +0.86 | 5 | 3 | ... | ... | ... |
| H118[a] | 15.75 | 1 | +0.65 | 1 | 2 | ... | ... | ... |
| H121 | 15.87 | 7 | +0.75 | 4 | 3 | ... | ... | ... |
| H125 | 15.67 | 3 | +0.84 | 1 | 2 | ... | ... | ... |
| H126[a] | 15.69 | 2 | +0.65 | 2 | 2 | ... | ... | ... |
| H130 | 16.30 | 5 | +0.87 | 7 | 3 | ... | ... | ... |
| H134[a] | 16.56 | 4 | +0.82 | 4 | 3 | ... | ... | ... |
| H136 | 16.66 | 5 | +0.65 | 4 | 3 | ... | ... | ... |
| H140[a] | 15.22 | 6 | +0.59 | 2 | 2 | +0.85 | 3 | 2 |
| B191[a] | 15.67 | ... | +0.55 | ... | 1 | ... | ... | ... |
| B195[a] | 16.13 | 33 | +0.53 | 5 | 2 | ... | ... | ... |
| B196[a] | 15.21 | 3 | +0.63 | 5 | 2 | +0.67 | 0 | 2 |
| B197[a] | 15.86 | 2 | +0.72 | 2 | 2 | ... | ... | ... |
| B198[a] | 17.19 | 12 | +0.57 | 1 | 2 | ... | ... | ... |
| B199* | 16.36 | 8 | +0.55 | 4 | 3 | ... | ... | ... |
| B227 | 16.17 | 4 | +1.51 | 5 | 3 | +1.47 | 6 | 2 |
| B231 | 15.26 | 3 | +0.75 | 3 | 4 | ... | ... | ... |
| B249 | 16.13 | 4 | +0.66 | 2 | 3 | ... | ... | ... |
| B258 | 15.82 | 1 | +1.02 | 7 | 3 | ... | ... | ... |
| B259 | 16.67 | 3 | +0.94 | 5 | 3 | ... | ... | ... |
| B271 | 16.13 | 2 | +0.80 | 2 | 3 | ... | ... | ... |
| B275 | 15.79 | 2 | +0.87 | 0 | 2 | ... | ... | ... |
| B282 | 14.21 | 0 | +0.81 | 0 | 2 | +1.11 | 1 | 2 |
| B295[a] | 15.97 | 2 | +0.73 | 2 | 2 | ... | ... | ... |
| B327 | 16.97 | 18 | +1.94 | 13 | 3 | +2.71 | 2 | 2 |
| MII[a] | 13.75 | 2 | +0.73 | 3 | 3 | +0.93 | 4 | 2 |
| MIII[a] | 15.83 | 3 | +0.59 | 2 | 2 | ... | ... | ... |
| MIV[a] | 15.13 | 4 | +0.54 | 1 | 2 | +0.81 | 6 | 2 |
| MV[a] | 16.14 | 6 | +0.89 | 1 | 2 | ... | ... | ... |
| MVI[a] | 16.09 | 1 | +0.69 | 6 | 2 | ... | ... | ... |
| Anon[a] | 16.27 | 5 | +0.86 | 1 | 3 | ... | ... | ... |
| | | | | M33 | | | | |
| Ha | 16.19 | 2 | +0.37 | 2 | 2 | ... | ... | ... |
| Hb | 16.54 | ... | +0.02 | ... | 1 | ... | ... | ... |
| Mc | 15.97 | ... | +0.48 | ... | 1 | ... | ... | ... |
| Hd | 16.58 | ... | +0.02 | ... | 1 | ... | ... | ... |

Small Magellanic Cloud

| NGC | $V_t$ | $(P\text{-}V)$ | $d_{0.9}$ | 5 log $d_{0.9}$ | Conc. Class |
|---|---|---|---|---|---|
| 121 | 10.6 | +0.74 | 3'.2 | 2.5 | (b) |
| 339 | 11.8 | +0.50 | 5.8 | 3.8 | (a) |
| 416 | 11.2 | +0.65 | 2.6 | 2.1 | (b) |
| 419 | 10.0 | +0.59 | 3.2 | 2.5 | a |
| Anon[b] | 11.2 | +0.64 | ... | ... | ... |

Large Magellanic Cloud

| NGC | $V_t$ | $(P\text{-}V)$ | $d_{0.9}$ | 5 log $d_{0.9}$ | Conc. Class |
|---|---|---|---|---|---|
| 1783 | 9.9 | +0.53 | 4'.7 | 3.4 | a |
| 1806 | 10.5 | +0.64 | 4.1 | 3.0 | a |
| 1835 | 10.0 | +0.61 | 1.95 | 1.4 | b |
| 1846 | 10.3 | +0.63 | 5.2 | 3.6 | (a) |
| 1978 | 9.8 | +0.68 | 4.5 | 3.2 | a |
| 2121 | (10.9) | +0.76 | (6.3) | (4.0) | (a) |

Fornax Dwarf

| | | | | | |
|---|---|---|---|---|---|
| 1049 | 12.5 | +0.53 | 2.0 | 1.5 | (b) |

Anon[c] 13.7 +0.63 0.91 −0.2 (b)

[a] Outlying objects (Fig. 4).
[b] Object No. 81 in *Harvard Circ.* No. 276.
[c] Cluster 6'.7*E* and 1'.5*S* of CD-35°919; Baade and Hubble (1939).


FIG. 6. Star clusters observed in M33.

may be comparable with those of the globular clusters. The line is straight within the accuracy of the observations. A least-squares solution for an assumed linear relationship gave

$$(P\text{-}V) = +0.20 \pm 0.05 + (0.77 \pm 0.047)(V\text{-}I).$$

It is noteworthy that the adopted color system has good resolution within the color range represented, for even among these few supergiants the effects of space reddening are well separated from those of thermal reddening. As the figure shows, the later spectral types, G2, lie above the least-squares line, while the earlier

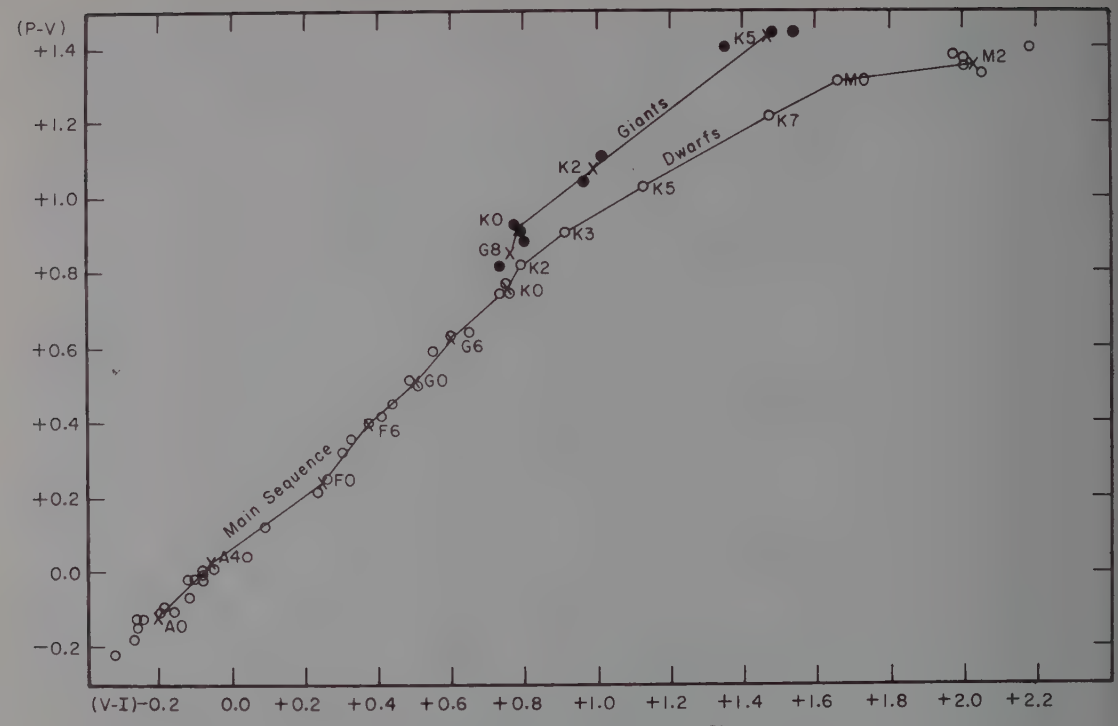


FIG. 7. Three-color (two color-index) diagram for unreddened stars observed to define main, dwarf, and giant sequences in $P$, $V$, $I$ system.

types, F6 to F9, lie below it; the unlabeled points all correspond to type G0.

## Reddening/Absorption Ratios

With the six-color $[V\text{-}I]$ data in Table III for the F- and G-type supergiants, least-squares solutions of the form $(P\text{-}V)$ and $(V\text{-}I)=a+b[V\text{-}I]$ were made, since the plots of $(P\text{-}V)$ and $(V\text{-}I)$ against $[V\text{-}I]$, Fig. 9, show satisfactorily close linear correlations. Solutions for the 12 stars tabulated, and for only the 7 G0 Ib stars, agreed so closely that only the result for all the stars is given here, with probable errors:

$$(P\text{-}V)=+0.642\pm0.017+(0.330\pm0.016)[V\text{-}I].$$

Hence

$$\Delta[V\text{-}I]=(1/0.330)\Delta(P\text{-}V),$$

or

$$E_{[V-I]}=(3.03\pm0.15)E_{(P-V)}.$$

According to Morgan, Harris, and Johnson (1953), an investigation (unpublished) by Harris and Johnson gave the following fundamental relation between total visual absorption, $A_V$, and the six-color $E_{[V-I]}$ excess: $A_V=0.96\pm0.05)E_{[V-I]}$. On this basis we find: $A_V=(2.91\pm0.22)E_{(P-V)}$, which agrees within the limits of error with the result, $A_V=(3.0\pm0.2)E_{(B-V)}$, found by Morgan, Harris, and Johnson (1953) from much more extensive material involving $(B\text{-}V)$ colors. By an exactly similar procedure, we find from the $(V\text{-}I)$ colors of the same 12 supergiants that $A_V=(2.33\pm0.14)\times E_{(V-I)}$.

## Clusters

In Fig. 10 are plotted all the three-color data that have resulted from the present study of star clusters in the Galaxy. The data are taken from Table VI. The main sequence, dwarf and giant branches from Fig. 7, and the reddening locus from Fig. 8 for the supergiants, are drawn in Fig. 10 as light lines. To obtain a reddening line for the galactic globular clusters, linear least-squares solutions for the regression lines were made for the globular cluster three-color data given in Table VI and plotted in Fig. 10, with the average result:

$$(P\text{-}V)=+0.022\pm0.025+(0.706\pm0.030)(V\text{-}I).$$

Although probably not significant, the slope happens to agree closely with that found for the F- and G-type supergiant stars. Several features are apparent.

(1) The open clusters in the Galaxy separate fairly well from the globular clusters in this three-color photometry, even in the presence of appreciable reddening.

(2) The distribution of the points for all objects is parallel to the reddening lines; this result suggests that the most important factor contributing to the elongated distribution of points in the diagram is space reddening.

(3) There is some indication that open clusters may

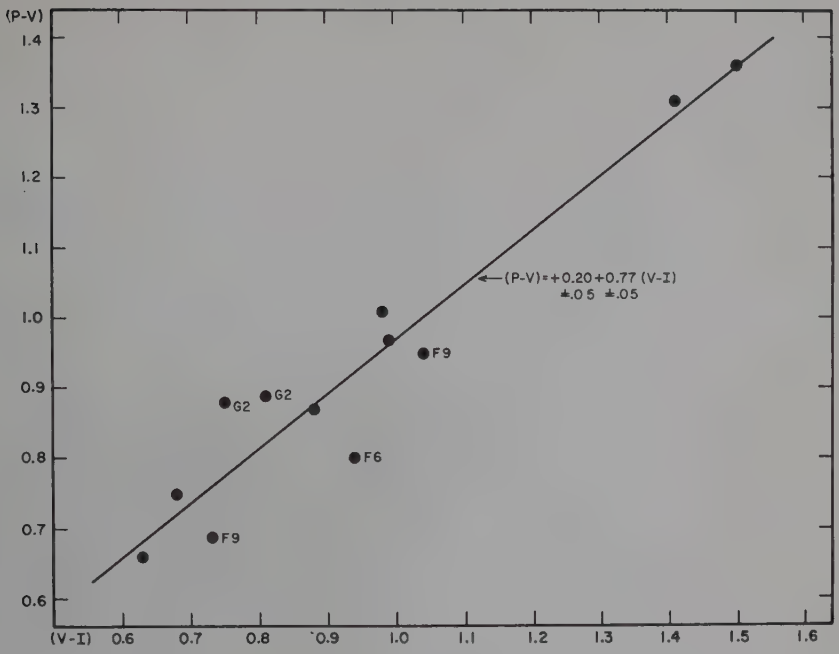


FIG. 8. Three-color (two color-index) plot and reddening line for 12 F- and G-type supergiants.

be classified according to some parameter, which may be age, from three-color photometry of their integrated light. Some older open clusters like M67 and NGC 7789, for example, plot among the globular cluster group, whereas younger open clusters like NGC 869 (h Per) plot below it.

(4) The use of an infrared color may be helpful in distinguishing clusters in which there are some bright red stars. Thus, among the galactic clusters whose $(V\text{-}I)$ colors place them systematically redward of the others, all but one, NGC 559, are known to contain high-luminosity red stars. Unfortunately, the presence of bright red stars, or the effect of high space-reddening are not easily separable.

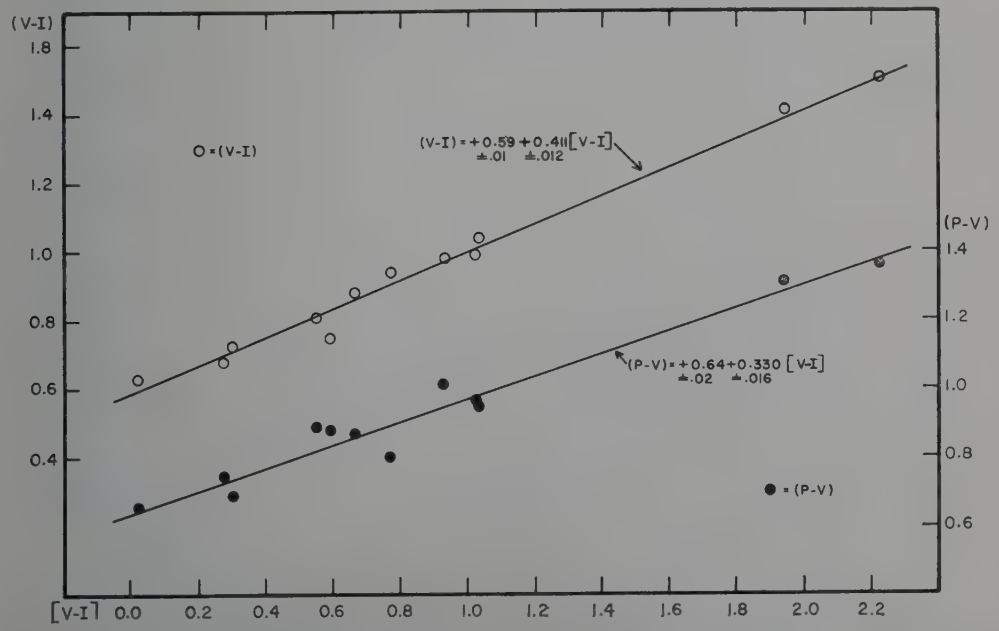


FIG. 9. Relationships between $(V\text{-}I)$ and $(P\text{-}V)$ vs six-color $[V\text{-}I]$ indices for 12 F- and G-type supergiants used to evaluate the ratio between total and selective absorption.

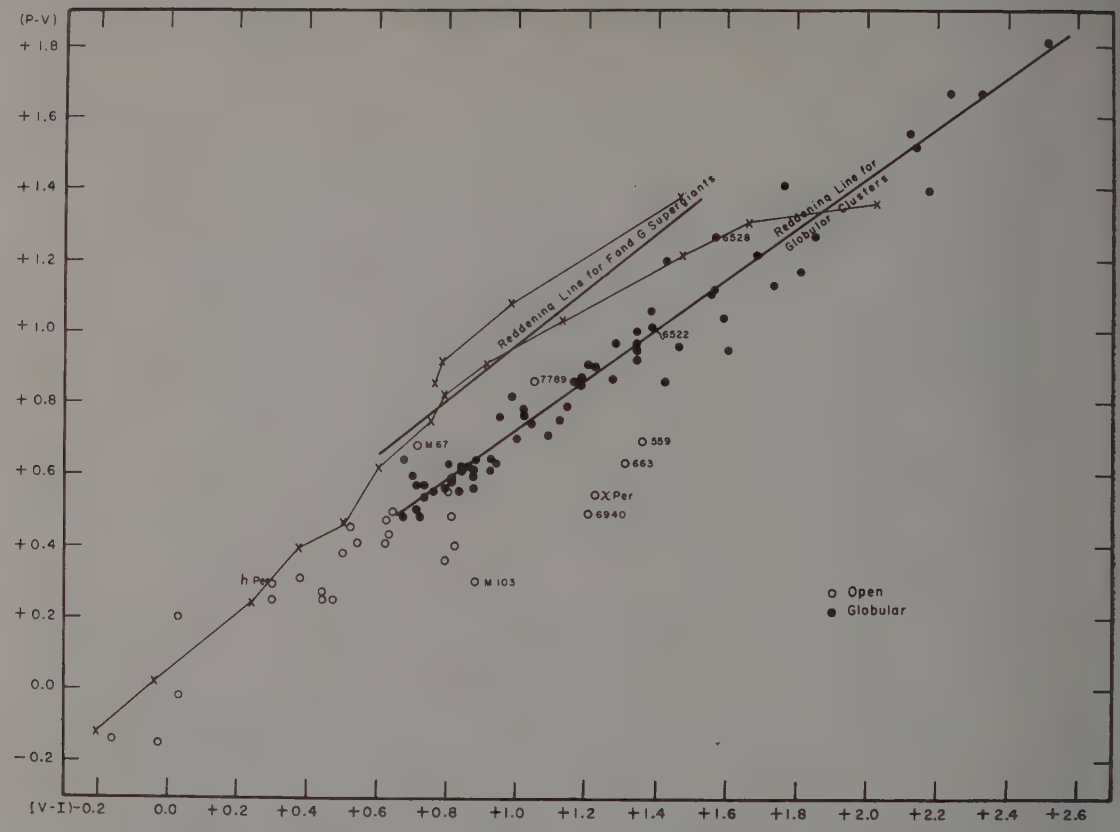


FIG. 10. Three-color (two color-index) diagram for all observed galactic open and globular clusters.

These results for galactic clusters are only of a preliminary and exploratory nature, but they suggest that further photometry of their integrated light may be worthwhile, especially if comparisons are to be made with similar objects in other galaxies.

## Spectral Types

As a preliminary step to study any possible correlation between the three-color data and spectral types of globular clusters, we next examine a group probably having little or no reddening. This group was formed by selection of the 22 observed clusters at high galactic latitudes, $|b| \geq 20°$, and for which spectral types were available. The three-color data for these objects are plotted in Fig. 11. In this figure it is clear that there is no strong correlation between these color data and spectral type, a result that is not surprising in view of the composite nature of the stellar content of globular clusters. Nevertheless, two A-type clusters are grouped together in the lower left-hand corner, whereas F-type clusters tend to lie above and to the right of them. The only high-latitude G-type cluster observed is NGC 6981, which in the figure falls among the F-type clusters. NGC 6681 and 6723 are other G-type clusters, not at high latitude but apparently little reddened, that would plot near NGC 6981. Four clusters in the upper right-hand part of the plot appear to be well separated from the main group. For one of these, NGC 6254, however, Arp (1955) found a color excess of $E_{CI}=0.4$ mag., more than enough to account for its position in the diagram. This case suggests that the other three clusters in this part of the diagram may also be there because of reddening. This possibility is strongly supported by the fact that three of these clusters, NGC 6171, 6218, and 6254, all lie rather close to each other near $l=340°$ and $b=+22°$, which is a region of low galaxy counts (Shane and Wirtanen 1954). Furthermore, by means of a method (Kron 1958) using the six-color photometry of Stebbins and Whitford (1945), we find that the K3 giant, HD 152601, which lies within 2° of NGC 6254, has a $(P\text{-}V)$ color excess of between 0.2 and 0.3 mag., even though its distance is doubtless much less than those of the globular clusters. The fourth cluster, NGC 6864, may be a similar case of appreciable reddening. It lies in the same region as the G3 Ib supergiant star HD 192876 ($\alpha^1$ Capricorni), which has a $(P\text{-}V)$ color excess of +0.18 mag. (Kron 1958).

We conclude that globular clusters, even if allowance is made for space reddening, have intrinsic properties that cause dispersion both perpendicular and parallel to a reddening line in a plot like Fig. 10. Since certain

TABLE VIII. Comparison of spectral type estimates.

| NGC | 36″—Crossley (1946) | (1956) | Δ | 82″—McD (1956) | Δ | Revised (1959) |
|---|---|---|---|---|---|---|
| 5024 | F2 | | | F4 | +2 | F4 |
| 5272 | F5 | | | F7 | +2 | F7 |
| 5904 | F6 | | | F5 | −1 | F6 |
| 6205 | F7 | | | F5 | −2 | F6 |
| 6229 | G0 | | | F7 | −3 | F8 |
| 6266 | G1 | F8 | −3 | | | G2 |
| 6273 | F2 | F5 | +3 | | | F3 |
| 6284 | G1 | F8 | −3 | | | G2 |
| 6293 | A9 | F5 | +6 | | | F0 |
| 6304 | G3 | G5 | +2 | | | G4 |
| 6333 | F1 | F2 | +1 | | | F2 |
| 6341 | A9 | | | F2 | +3 | F1 |
| 6356 | G2 | G5 | +3 | G5 | +3 | G4 |
| 6440 | G3 | G5 | +2 | G5 | +2 | G5 |
| 6441 | G4 | G2 | −2 | | | G5 |
| 6624 | G4 | G2 | −2 | | | G5 |
| 6626 | G0 | F9 | −1 | | | G1 |
| 6637 | G5 | G5 | 0 | G5 | 0 | G5 |
| 6638 | G3 | G1 | −2 | | | G4 |
| 6652 | G3 | G2 | −1 | | | G4 |
| 6712 | G4 | G1 | −3 | | | G5 |
| 6838 | G5 | G2 | −3 | | | G6 |
| 7078 | F0 | | | F3 | +3 | F2 |
| | | Means | −0.2 | | +0.9 | |

of these intrinsic properties are doubtless indicated by spectral type, we decided to try to correct for the loose correlation between color and type in estimating color excesses from these three-color data, as described in the next section.

### IX. COLOR EXCESS AND ABSORPTION

As the first step in using spectral types to estimate color excesses and absorptions for the galactic globular clusters, we compare the previously available, most extensive set of types (Mayall 1946), based on Mount Wilson standards, with those more recently determined by Morgan (1956), referred to the Yerkes MK system. For some clusters, Morgan's estimates depend on the old, low-dispersion Crossley data, while for others they come from new, higher dispersion material obtained with the Cassegrain spectrograph of the 82-inch McDonald reflector, as indicated in Table VIII. The comparison shows no appreciable systematic difference between the estimates depending on the Crossley plates, and only a tenth of a spectral class for the McDonald types. Since the latter are undoubtedly preferable, all the 1946 types were increased by one-tenth spectral class, and, where a 1956 McDonald type was available, it was averaged in with double weight. These revised types are given in the last column of Table VIII, and in the second column of Table X.

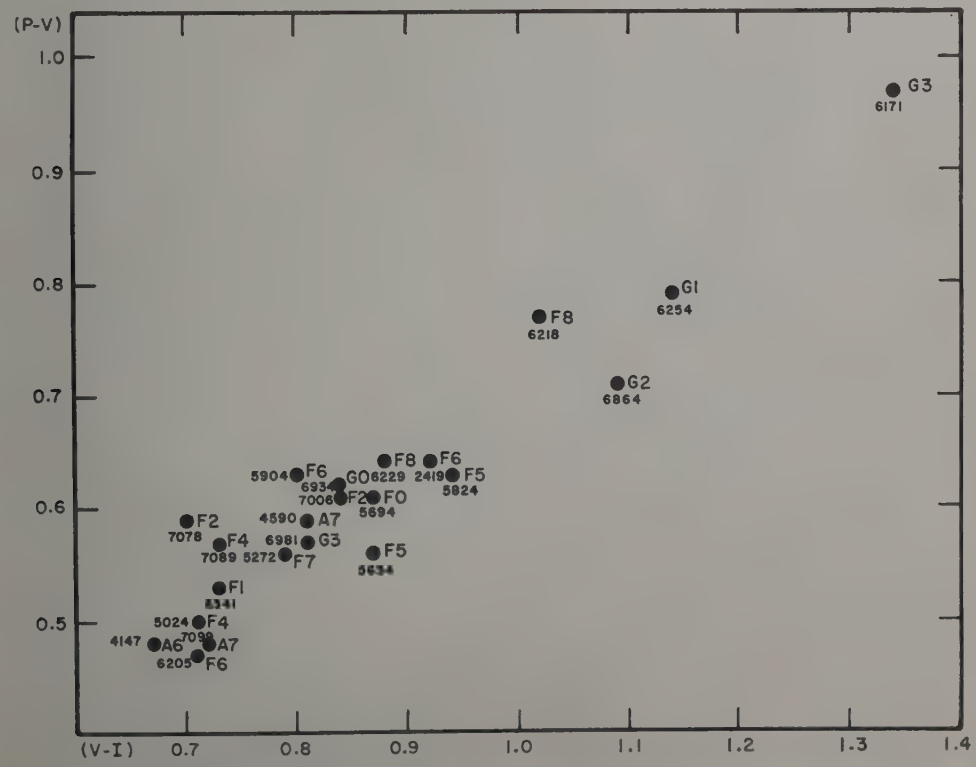


FIG. 11. Three-color, or two color-index plot for globular clusters of known spectral type and for which $|b| \geqslant 20°$.

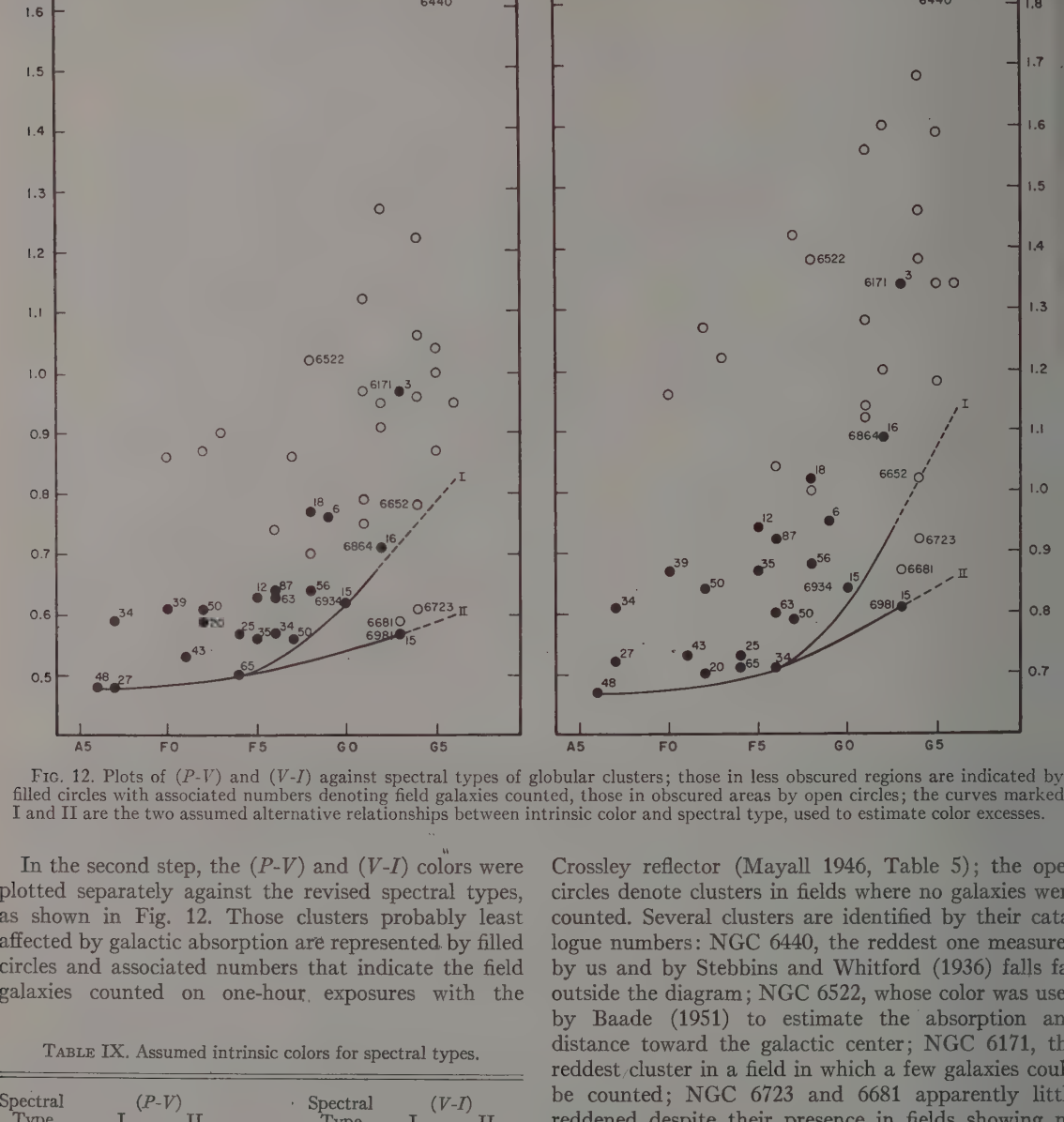


FIG. 12. Plots of $(P\text{-}V)$ and $(V\text{-}I)$ against spectral types of globular clusters; those in less obscured regions are indicated by filled circles with associated numbers denoting field galaxies counted, those in obscured areas by open circles; the curves marked I and II are the two assumed alternative relationships between intrinsic color and spectral type, used to estimate color excesses.

In the second step, the $(P\text{-}V)$ and $(V\text{-}I)$ colors were plotted separately against the revised spectral types, as shown in Fig. 12. Those clusters probably least affected by galactic absorption are represented by filled circles and associated numbers that indicate the field galaxies counted on one-hour exposures with the Crossley reflector (Mayall 1946, Table 5); the ope circles denote clusters in fields where no galaxies wer counted. Several clusters are identified by their cata logue numbers: NGC 6440, the reddest one measure by us and by Stebbins and Whitford (1936) falls fa outside the diagram; NGC 6522, whose color was use by Baade (1951) to estimate the absorption an distance toward the galactic center; NGC 6171, th reddest cluster in a field in which a few galaxies coul be counted; NGC 6723 and 6681 apparently litt reddened despite their presence in fields showing n galaxies; NGC 6981, whose estimated spectral typ seems somewhat too late for its color; and NGC 665 and 6864, which were used as limiting cases to draw th "bluest-color" bounding curve I, described in th following.

TABLE IX. Assumed intrinsic colors for spectral types.

| Spectral Type | $(P\text{-}V)$ I | $(P\text{-}V)$ II | Spectral Type | $(V\text{-}I)$ I | $(V\text{-}I)$ II |
|---|---|---|---|---|---|
| A6-F0 | $0^m.48$ | | A6-A8 | $0^m.67$ | |
| F1-F2 | 0.49 | | A9-F2 | 0.68 | |
| F3-F4 | 0.50 | | F3-F4 | 0.69 | |
| F5 | $0^m.51$ | $0^m.50$ | F5 | 0.70 | |
| F6 | 0.53 | 0.51 | F6 | 0.71 | |
| F7 | 0.55 | 0.52 | F7 | $0^m.73$ | $0^m.72$ |
| F8 | 0.57 | 0.53 | F8 | 0.75 | 0.73 |
| F9 | 0.59 | 0.53 | F9 | 0.78 | 0.75 |
| G0 | 0.62 | 0.54 | G0 | 0.81 | 0.76 |
| G1 | 0.65 | 0.55 | G1 | 0.86 | 0.78 |
| G2 | 0.69 | 0.56 | G2 | 0.92 | 0.79 |
| G3 | 0.72 | 0.57 | G3 | 0.97 | 0.81 |
| G4 | 0.75 | 0.58 | G4 | 1.02 | 0.83 |
| G5 | 0.79 | 0.59 | G5 | 1.07 | 0.84 |
| G6 | 0.82 | 0.60 | G6 | 1.14 | 0.86 |

As might be expected for composite stellar system Fig. 12 shows no close dependence of color upon spectra type. Nevertheless, there appears to be a genera tendency, among the least obscured clusters, for th later types to be redder. Unfortunately, however, ther are so few clusters of latest type in unobscured field that the picture is badly confused in the range fro G0 to G5. Thus any attempt to obtain a curve tha would relate the "unreddened," or "normal," c

TABLE X. Revised spectral types, color excesses, and absorptions.

| NGC | Sp.T.[a] | $E_{(P-V)}$ I | $E_{(P-V)}$ II | $E_{(V-I)}$ I | $E_{(V-I)}$ II | $A_V$ from (P-V) I | $A_V$ from (P-V) II | $A_V$ from (V-I) I | $A_V$ from (V-I) II | $\langle A\rangle_V$ I | $\langle A\rangle_V$ II | $\langle E\rangle_{(P-V)}$ I | $\langle E\rangle_{(P-V)}$ II |
|---|---|---|---|---|---|---|---|---|---|---|---|---|---|
| 2419 | F6 | 0.11 | 0.13 | 0.21 | | 0.3 | 0.4 | 0.5 | | 0m4 | 0m4 | 0m14 | 0m14 |
| 4147 | A6 | 0.00 | | 0.00 | | 0.0 | | 0.0 | | 0.0 | 0.0 | 0.00 | 0 00 |
| 4590 | A7 | 0.11 | | 0.14 | | 0.3 | | 0.3 | | 0.3 | 0.3 | 0.10 | 0.10 |
| 5024 | F4 | 0.10 | | 0.02 | | 0.0 | | 0.0 | | 0.0 | 0.0 | 0.00 | 0.00 |
| 5053 | (F5) | 0.04 | 0.05 | 0.06 | | 0.1 | 0.1 | 0.1 | | 0.1 | 0.1 | 0.03 | 0.03 |
| 5272 | F7 | 0.01 | 0.04 | 0.06 | 0.07 | 0.0 | 0.1 | 0.1 | 0.2 | 0.0 | 0.2 | 0.00 | 0.07 |
| 5466 | (F5) | 0.13 | 0.14 | (0) | | 0.4 | 0.4 | (0) | | 0.4 | 0.4 | 0.14 | 0.14 |
| 5634 | F5 | 0.05 | 0.06 | 0.17: | | 0.1 | 0.2 | 0.4: | | 0.1 | 0.2 | 0.03 | 0.07 |
| 5694 | F0 | 0.13 | | 0.19 | | 0.4 | | 0.4 | | 0.4 | 0.4 | 0.14 | 0.14 |
| 5824 | F5 | 0.12 | 0.13 | 0.24 | | 0.3 | 0.4 | 0.6 | | 0.4 | 0.5 | 0.14 | 0.17 |
| 5897 | (F5) | 0.11 | 0.12 | 0.16 | | 0.3 | 0.3 | 0.4 | | 0.4 | 0.4 | 0.14 | 0.14 |
| 5904 | F6 | 0.10 | 0.12 | 0.09 | | 0.3 | 0.3 | 0.2 | | 0.2 | 0.2 | 0.07 | 0.07 |
| 5986 | G1 | 0.10 | 0.20 | 0.26 | 0.34 | 0.3 | 0.6 | 0.6 | 0.8 | 0.4 | 0.7 | 0.14 | 0.24 |
| 6093 | F9 | 0.17 | 0.23 | 0.17 | 0.20 | 0.5 | 0.7 | 0.4 | 0.5 | 0.4 | 0.6 | 0.14 | 0.21 |
| 6121 | (G0) | 0.30 | 0.38 | 0.53 | 0.58 | 0.9 | 1.1 | 1.2 | 1.3 | 1.0 | 1.2 | 0.34 | 0.41 |
| 6144 | (G0) | 0.20 | 0.28 | 0.17 | 0.22 | 0.6 | 0.8 | 0.4 | 0.5 | 0.5 | 0.6 | 0.17 | 0.21 |
| 6171 | G3 | 0.25 | 0.40 | 0.37 | 0.53 | 0.7 | 1.2 | 0.9 | 1.2 | 0.8 | 1.2 | 0.28 | 0.41 |
| 6205 | F6 | 0.04 | 0.06 | 0.00 | | 0.1 | 0.2 | 0.0 | | 0.0 | 0.1 | 0.00 | 0.03 |
| 6218 | F8 | 0.20 | 0.24 | 0.27 | 0.29 | 0.6 | 0.7 | 0.6 | 0.7 | 0.6 | 0.7 | 0.21 | 0.24 |
| 6229 | F8 | 0.07 | 0.11 | 0.13 | 0.15 | 0.2 | 0.3 | 0.3 | 0.3 | 0.2 | 0.3 | 0.07 | 0.10 |
| 6254 | G1 | 0.14 | 0.24 | 0.28 | 0.36 | 0.4 | 0.7 | 0.6 | 0.8 | 0.5 | 0.8 | 0.17 | 0.28 |
| 6266 | G2 | 0.26 | 0.39 | 0.63 | 0.81 | 0.8 | 1.1 | 1.6 | 1.9 | 1.2 | 1.5 | 0.41 | 0.52 |
| 6273 | F3 | 0.40 | | 0.53 | | 1.2 | | 1.2 | | 1.2 | 1.2 | 0.41 | 0.41 |
| 6284 | G2 | 0.22 | 0.35 | 0.28 | 0.41 | 0.6 | 1.0 | 0.6 | 0.9 | 0.6 | 1.0 | 0.21 | 0.34 |
| 6287 | (G5) | 0.34 | 0.54 | 0.66 | 0.89 | 1.0 | 1.6 | 1.5 | 2.0 | 1.2 | 1.8 | 0.41 | 0.62 |
| 6293 | F0 | 0.38 | | 0.48 | | 1.1 | | 1.1 | | 1.1 | 1.1 | 0.38 | 0.38 |
| 6304 | G4 | 0.47 | 0.64 | 0.66 | 0.85 | 1.4 | 1.9 | 1.5 | 2.0 | 1.4 | 2.0 | 0.48 | 0.69 |
| 6316 | (G5) | 0.38 | 0.58 | 0.74 | 0.97 | 1.1 | 1.7 | 1.7 | 2.2 | 1.4 | 2.0 | 0.48 | 0.69 |
| 6325 | (G5) | 0.73 | 0.93 | 1.07 | 1.30 | 2.1 | 2.7 | 2.5 | 3.0 | 2.3 | 2.8 | 0.79 | 0.96 |
| 6333 | F2 | 0.38 | | 0.59 | | 1.1 | | 1.4 | | 1.2 | 1.2 | 0.41 | 0.41 |
| 6341 | F1 | 0.04 | | 0.05 | | 0.1 | | 0.1 | | 0.1 | 0.1 | 0.03 | 0.03 |
| 6342 | (G5) | 0.41 | 0.61 | 0.35 | 0.58 | 1.2 | 1.8 | 0.8 | 1.3 | 1.0 | 1.6 | 0.34 | 0.55 |
| 6355 | (G5) | 0.62 | 0.82 | 0.69 | 0.92 | 1.8 | 2.4 | 1.6 | 2.1 | 1.7 | 2.2 | 0.59 | 0.76 |
| 6356 | G4 | 0.31 | 0.48 | 0.36 | 0.55 | 0.9 | 1.4 | 0.8 | 1.3 | 0.8 | 1.4 | 0.28 | 0.48 |
| 6401 | (G5) | 0.38: | 0.58: | 0.82: | 1.05: | 1.1: | 1.7: | 1.9: | 2.4: | 1.5: | 2.0: | 0.52: | 0.69: |
| 6402 | G1 | 0.47 | 0.57 | 0.70 | 0.78 | 1.4 | 1.7 | 1.6 | 1.8 | 1.5 | 1.8 | 0.52 | 0.62 |
| 6426 | (G0) | 0.23 | 0.31 | 0.37 | 0.42 | 0.7 | 0.9 | 0.9 | 1.0 | 0.8 | 1.0 | 0.28 | 0.34 |
| 6440 | G5 | 1.02 | 1.22 | 1.44 | 1.67 | 3.0 | 3.5 | 3.3 | 3.8 | 3.2 | 3.6 | 1.10 | 1.24 |
| 6453 | (G5) | 0.25: | 0.45: | 0.83: | 1.06: | 0.7: | 1.3: | 1.9: | 2.4: | 1.3: | 1.8: | 0.45: | 0.62: |
| 6517 | (G0) | 1.05 | 1.13 | 1.51 | 1.56 | 3.0 | 3.3 | 3.5 | 3.6 | 3.2 | 3.4 | 1.10 | 1.17 |
| 6522 | F8[b] | 0.45 | 0.49 | 0.63 | 0.65 | 1.3 | 1.4 | 1.4 | 1.5 | 1.4 | 1.4 | 0.48 | 0.48 |
| 6528 | (G5) | 0.48 | 0.68 | 0.49 | 0.72 | 1.4 | 2.0 | 1.1 | 1.7 | 1.2 | 1.8 | 0.41 | 0.62 |
| 6539 | (G0) | 1.05 | 1.13 | 1.42 | 1.47 | 3.0 | 3.3 | 3.3 | 3.4 | 3.2 | 3.4 | 1.10 | 1.17 |
| 6544 | G2 | 0.58 | 0.71 | 0.93 | 1.06 | 1.7 | 2.1 | 2.1 | 2.4 | 1.9 | 2.2 | 0.65 | 0.76 |
| 6553 | (G5) | 0.60 | 0.80 | 1.10 | 1.33 | 1.7 | 2.3 | 2.5 | 3.1 | 2.1 | 2.7 | 0.72 | 0.93 |
| 6569 | (G5) | 0.32 | 0.52 | 0.49 | 0.72 | 0.9 | 1.5 | 1.1 | 1.7 | 1.0 | 1.6 | 0.34 | 0.55 |
| 6624 | G5 | 0.21 | 0.41 | 0.27 | 0.50 | 0.6 | 1.2 | 0.6 | 1.1 | 0.6 | 1.2 | 0.21 | 0.41 |
| 6626 | G1 | 0.32 | 0.42 | 0.42 | 0.50 | 0.9 | 1.2 | 1.0 | 1.1 | 1.0 | 1.2 | 0.34 | 0.41 |
| 6637 | G5 | 0.08 | 0.28 | 0.11 | 0.34 | 0.2 | 0.8 | 0.3 | 0.8 | 0.2 | 0.8 | 0.07 | 0.28 |
| 6638 | G4 | 0.21 | 0.38 | 0.44 | 0.63 | 0.6 | 1.1 | 1.0 | 1.4 | 0.8 | 1.2 | 0.28 | 0.41 |
| 6652 | G4 | 0.03 | 0.20 | 0.00 | 0.19 | 0.1 | 0.6 | 0.0 | 0.4 | 0.0 | 0.5 | 0.00 | 0.17 |
| 6656 | F7 | 0.31 | 0.34 | 0.69 | 0.70 | 0.9 | 1.0 | 1.6 | 1.6 | 1.2 | 1.3 | 0.41 | 0.45 |
| 6681 | G3 | (0) | 0.02 | (0) | 0.06 | (0) | 0.1 | (0) | 0.1 | (0) | 0.1 | (0) | 0.03 |
| 6712 | G5 | 0.25 | 0.45 | 0.52 | 0.75 | 0.7 | 1.3 | 1.2 | 1.7 | 1.0 | 1.5 | 0.34 | 0.52 |
| 6715 | F8 | 0.13 | 0.17 | 0.25 | 0.27 | 0.4 | 0.5 | 0.6 | 0.6 | 0.5 | 0.6 | 0.17 | 0.21 |
| 6723 | G4 | (0) | 0.03 | (0) | 0.09 | (0) | 0.1 | (0) | 0.2 | (0) | 0.2 | (0) | 0.07 |
| 6760 | (G0) | 0.93 | 1.01 | 1.31 | 1.36 | 2.7 | 2.9 | 3.0 | 3.1 | 2.8 | 3.0 | 0.96 | 1.03 |
| 6779 | F6 | 0.21 | 0.23 | 0.33 | | 0.6 | 0.7 | 0.8 | | 0.7 | 0.8 | 0.24 | 0.28 |
| 6809 | (F5) | 0.04 | 0.05 | 0.13 | | 0.1 | 0.1 | 0.3 | | 0.2 | 0.2 | 0.07 | 0.07 |
| 6838 | G6 | 0.13 | 0.35 | 0.20 | 0.48 | 0.4 | 1.0 | 0.5 | 1.1 | 0.4 | 1.0 | 0.14 | 0.34 |
| 6864 | G2 | 0.02 | 0.15 | 0.17 | 0.30 | 0.1 | 0.4 | 0.4 | 0.7 | 0.2 | 0.6 | 0.07 | 0.21 |
| 6934 | G0 | 0.00 | 0.08 | 0.03 | 0.08 | 0.0 | 0.2 | 0.1 | 0.2 | 0.0 | 0.2 | 0.00 | 0.07 |
| 6981 | G3 | (0) | 0.00 | (0) | 0.00 | (0) | 0.0 | (0) | 0.0 | (0) | 0.0 | (0) | 0.00 |
| 7006 | F2 | 0.12 | | 0.16 | | 0.3 | | 0.4 | | 0.4 | 0.4 | 0.14 | 0.14 |
| 7078 | F2 | 0.10 | | 0.02 | | 0.3 | | 0.4 | | 0.2 | 0.2 | 0.07 | 0.07 |
| 7089 | F4 | 0.07 | | 0.04 | | 0.2 | | 0.1 | | 0.2 | 0.2 | 0.07 | 0.07 |
| 7099 | A7 | 0.00 | | 0.05 | | 0.0 | | 0.1 | | 0.0 | 0.0 | 0.00 | 0.00 |

[a] Types in parentheses are assumed.
[b] New estimate by Morgan (1956).

"intrinsic" color of a globular cluster with its estimated spectral type is bound to involve considerable uncertainty and judgment—at least with the present material. This uncertainty, of course, enters directly into the deduced color excesses, which are obtained as the differences between the measured colors and those given by the assumed or inferred "normal color"-spectrum relationship. Compared to this source of uncertainty, the errors in the measured colors probably are of minor importance in color excess estimates.

The third and last step in deriving color excesses was to draw in Fig. 12 curves representing such "normal color"-spectrum relationships for both the $(P\text{-}V)$ and $(V\text{-}I)$ colors. Obviously, such curves could be drawn in several ways, such as an average through the presumably least reddened clusters (filled circles) which would yield a number of negative excesses, or as "bluest-color" bounding envelopes that give either zero or a small color excess for the highest latitude clusters. While for the latter some color-magnitude diagrams of individual stars have been interpreted as indicating a small amount of reddening, we have preferred to risk under- rather than over-correction. We have, therefore, drawn limiting curves through the bluest clusters, as shown in Fig. 12 by the single lines for types A6 to F5 for $(P\text{-}V)$, or to F6 for $(V\text{-}I)$. Since for later types it was difficult to know whether or not to place full faith in the estimates of spectral types for NGC 6681 and 6723, we decided to use the two alternatives represented by the branching curves labeled I and II. The first ignores the three clusters in question, while the second gives them full weight. NGC numbers identify those clusters used to define the curves, which are dashed near their extremities to show that their course is conjectural because of insufficient data. The colors corresponding to these curves are listed in Table IX, and they are given to 0.01 mag. only to facilitate further computations. Their probable errors are doubtless much larger, because of the subjectivity of the procedure. We mention as reasonably conservative, estimated probable errors of $\pm 0.05$ mag. for types A5 to about G0, and of $\pm 0.1$ mag. for G0 to G5. We also note that the ranges in the tabulated colors are: for alternative I, 0.34 mag. in $(P\text{-}V)$ and 0.47 mag. in $(V\text{-}I)$; for II, 0.12 mag. in $(P\text{-}V)$ and 0.19 mag. in $(V\text{-}I)$. Thus alternative II is not far from the assumption of the same intrinsic color for clusters of all spectral types—an assumption whose usefulness was demonstrated nearly 25 years ago by Stebbins and Whitford (1936). Alternative I, on the other hand, allows for a fairly large variation in color. Depending on which alternative is the more tenable, color excesses estimated with I may be too small, those with II too large; perhaps the truth lies somewhere between. But because we cannot be sure, we shall in the subsequent discussion carry through parallel calculations for each alternative, in order to show the range of values in such quantities as corrected colors, total magnitudes, distance moduli, and diameters.

The foregoing procedure was used to compute color excesses for all clusters of known spectral type, and the results are given in Table X under the column headings $E_{(P-V)}$ and $E_{(V-I)}$. For clusters of unknown spectral type, F5 was assumed for those with $|b| \geqslant 20°$, G0 for those with $-20° < b < +20°$, and G5 for those in the group around the galactic center direction; these assumed types are in parentheses in the table.

Table X also contains the visual absorptions, $A_V$, obtained from 2.9 $E_{(P-V)}$ and 2.3 $E_{(V-I)}$ (Sec. VIII). Since $A_V$ should be the same regardless of the spectral regions used for its estimation, we have a useful internal check on the material and procedure. If the two poor-data cases of NGC 6401 and 6453 are disregarded, the frequency distribution of the differences without regard to sign, $|\Delta A_V| = 2.3\ E_{(V-I)} - 2.9\ E_{(P-V)}$, is as follows for 65 clusters:

| $\lvert\Delta A_V\rvert$ | 0.0 | 0.1 | 0.2 | 0.3 | 0.4 | 0.5 | 0.6 | 0.7 | 0.8 |
|---|---|---|---|---|---|---|---|---|---|
| I | 14 | 17 | 11 | 11 | 5 | 3 | 1 | 1 | 2 |
| II | 15 | 21 | 10 | 11 | 3 | 2 | 1 | 0 | 2 |

Thus there is a satisfactorily high concentration of small differences, which amounts to 94% (I) and 95% (II) for $|\Delta A_V| \leqslant 0.5$ mag. The two largest differences of 0.8 mag. are for NGC 6266 and 6553; for the former the $(V\text{-}I)$ measurements have the unusually large AD of 0.11 mag.; for the latter, the spectral type is assumed as G5, but a still later type would give more consistent color excesses by this procedure. If averages of all 65 differences are taken, the mean difference without regard to sign is 0.21 mag. (I) and 0.18 mag. (II); with sign, +0.15 mag. (I) and +0.09 mag. (II). The size of the latter systematic differences suggests, as one possibility for better agreement, the use of slightly different total-to-selective absorption ratios. For example, if 3.1 for $(P\text{-}V)$ and 2.1 for $(V\text{-}I)$ were used, the systematic difference between the $V$ absorptions derived from the two color indices would be close to zero. Another possibility is, of course, to use somewhat different curves in Figure 12. Such refinements seem neither justifiable or desirable to us, however, so we have taken averages for alternatives I and II of $A_V$ obtained from $(P\text{-}V)$ and $(V\text{-}I)$; these are listed as $\langle A \rangle_V$ in the next to the last two columns of Table X. Finally, we computed from $\langle A \rangle_V / 2.9$ the values of $\langle E \rangle_{(P-V)}$ listed in the last two columns.

Since the procedure used here to derive color excesses for the galactic globular clusters is admittedly arbitrary, it is of interest to compare the present results with others recently obtained by different means. Usually the latter have involved color-magnitude diagrams determined from individual cluster stars, with the space-reddening estimated from the position of the giant branch, of the main sequence, or of the RR Lyrae variable-star "gap." Most of the modern photoelectric

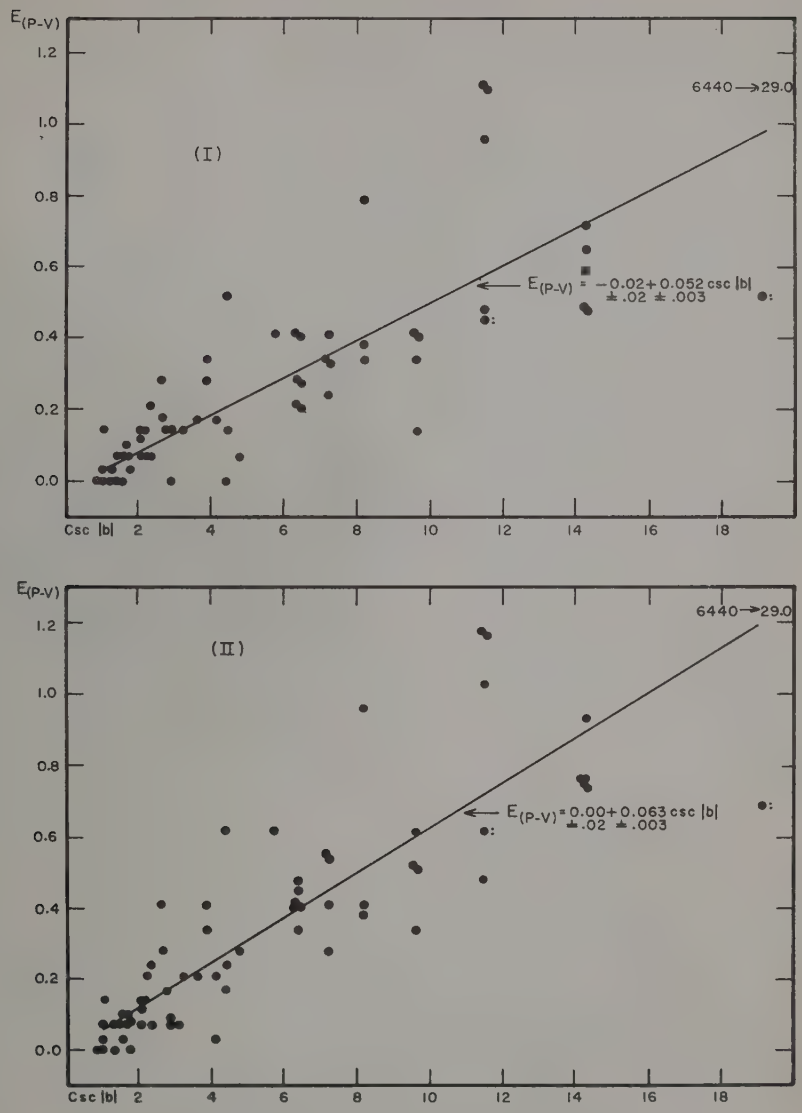


FIG. 13. Cosecant-law representations of globular cluster color excesses estimated from alternatives I and II.

material refers to the larger, brighter and little reddened high-latitude clusters, so that we cannot get a good check on the larger color excesses. If we limit the comparison to the best-observed clusters, we find the results listed in Table XI.

We consider this comparison to be generally satisfactory, probably to a precision of about 0.05 mag., except possibly for the case of NGC 6254 (M10). This cluster has no known RR Lyrae variables, and the color-magnitude diagram depends on only one 60-inch reflector plate in each color. Under these circumstances, the photometric estimate of color excess may be as uncertain as the one based on its spectral type, by ±0.1 mag.

It is also of interest to examine the correlation between galactic latitude and the color excesses derived here. We assume that the actual patchy distribution of absorbing material may be treated statistically as a thin, uniform layer centered on the galactic plane and sun. If the clusters are outside such a layer, then the reddening and absorption in magnitudes vary linearly with cosecant $b$. Figure 13 shows a plot of $E_{(P-V)}$ for alternatives I and II, with the lines resulting from the least-squares solutions, which with probable errors are (with 6440 omitted because of its dominating weight):

$$\text{I, } E_{(P-V)} = -0.018 \pm 0.022 + (0.052 \pm 0.003) \csc |b|,$$

$$\text{II, } E_{(P-V)} = +0.001 \pm 0.022 + (0.063 \pm 0.003) \csc |b|.$$

Similar results were obtained many years ago by Stebbins and Whitford (1933, 1936, 1937) and, to make a comparison, we reduce their data to the $P$, $V$ system,

as follows. Stebbins' original (1933) solution for 42 clusters gave $E_2 = (0.0237 \pm 0.0018) \csc|b|$, which was later (1936) discussed in terms of the cluster color scale $E$. Since this scale is equivalent to $E_1$ for stars, and $E_1 = 1.68\, E_2$, then $E_1 = (0.040 \pm 0.003) \csc|b|$. Also, in their first report (1937) on the colors of extragalactic nebulae, they obtained $E_1 = (0.015 \pm 0.005) \csc|b|$ as the average from two solutions of 66 nebulae and of 19 globular clusters outside Hubble's zone of avoidance. Moreover, Stebbins and Whitford (1936) found that $1.6\, E_1 = E_{CI}$, we assume that $E_{CI} = E_{(P-V)}$, and Morgan, Harris, and Johnson (1953) deduced that $A_V = 6.1\, E_1$. These relationships provide the comparison in Table XII of these photoelectric determinations of the reddening and absorption toward the galactic poles.

Considering all the assumptions and uncertainties involved, especially the difficult decision of what to use for a "normal" color of a globular cluster, we consider that both the older and newer data agree well enough to confirm Stebbins and Whitford's earlier conclusion: *on the average*, there is very little space-reddening and absorption toward the galactic poles.

We wish to emphasize that this result based on the assumed cosecant law is mainly useful in comparisons of photometries of the globular cluster system as a whole; computed cosecant law color excesses for individual objects have little significance because of the very patchy, irregular distribution of interstellar matter.

## X. LUMINOSITIES, COLORS, DISTANCES AND DIAMETERS

With the color excesses and absorptions deduced as described in the preceding section, we may obtain corrected apparent total magnitudes, integrated colors, distances and linear diameters. But first we shall derive a set of absolute total magnitudes, or luminosities, since they may be obtained independently of absorption whenever the distance moduli depend only upon apparent magnitudes of brightest stars or variables measured in the same spectral region. Such a list of apparent distance moduli, based on the assumption that $M_{pg} = 0.0$ for RR Lyrae variables, has recently been published by Dr. Helen Sawyer Hogg (1959), and we are indebted to her for sending it to us in advance of publication. These apparent moduli, $(m-M)_{pg}$, are given in the third column of Table XIII, except that the moduli for NGC 2419, 6426 and 6638 represent revisions or additions based on later work.

TABLE XI. Comparison of color excesses.

| NGC | M | $E_{(P-V)}$ I | $E_{(P-V)}$ II | $E_{CI}$ | Reference |
|---|---|---|---|---|---|
| 4147 | ... | 0m00 | 0m00 | <0m15 | Sandage and Walker (1955) |
| 4147 | ... | 0.00 | 0.00 | 0.00 | Newburn (1957) |
| 5272 | 3 | 0.00 | 0.07 | 0.00 | Arp (1955) |
| 5904 | 5 | 0.07 | 0.07 | 0.16 | Arp (1955) |
| 6205 | 13 | 0.00 | 0.03 | 0.16 | Arp (1955) |
| 6254 | 10 | 0.17 | 0.28 | 0.4 | Arp (1955) |
| 6341 | 92 | 0.03 | 0.03 | 0.00 | Arp (1955) |
| 6656 | 22 | 0.41 | 0.45 | 0.4–0.5 | Arp and Melbourne (1959) |
| 7078 | 15 | 0.07 | 0.07 | 0.00 | Arp (1955) |
| 7089 | 2 | 0.07 | 0.07 | 0.05 | Arp (1955) |

TABLE XII. Polar reddening and absorption.

| No. Cl. | Sol. | $E_{(P-V)}$ | $A_V$ |
|---|---|---|---|
| 64 | I | 0m052±0m003 | 0m15±0m01 |
| 64 | II | 0.063±0.003 | 0.18±0.01 |
| 42 | (1936) | 0.064±0.005 | 0.24±0.02 |
| 19 | (1937) | 0.024±0.008 | 0.09±0.03 |

### Luminosities

Since most of the moduli depend on photographic observations, we give in the sixth column of Table XIII the absorption-free, total absolute photographic magnitudes, $M_{Pt}$, obtained from $V_t$ in Table IV, from $(P\text{-}V)$ in Table VI, and from $(m-M)_{pg}$ in Table XIII; thus $M_{Pt} = V_t + (P\text{-}V) - (m-M)_{pg}$. Also, because much modern photometry of clusters is being done in visual light, we have derived a set of apparent, visual-light moduli, $(m-M)_V$ in the fourth and fifth columns of Table XIII, from $(m-M)_{pg} - \langle E \rangle_{(P-V)}$. To correspond with these moduli, we also computed total absolute visual magnitudes, $M_{Vt}$ in the seventh column, from $M_{Pt} - \langle P\text{-}V \rangle_c$; for this purpose the corrected colors, $(P\text{-}V)_c$ in the eighth and ninth columns, were averaged for alternatives I and II, since the maximum difference is only 0.21 mag.

The values of $M_{Vt}$, which involve measurements in both photographic and visual light, are obviously absorption-free only if the color excesses have been correctly estimated. We have a partial check, however, from the few globular clusters having modern, visual-light photometry (Table XI). Thus with $M'_{Vt}$ obtained from $V_t$ and the directly observed, visual-light apparent moduli, $(m-M)'_V$, we obtain the comparison with $M_{Vt}$ shown in Table XIV. Since the average differences with and without regard to sign are only −0.01 and 0.14 mag., with none greater than 0.3 mag., the comparison seems satisfactory for these clusters. As mentioned previously, however, this small group includes only one appreciably reddened cluster (NGC 5264), so this check on the estimated color excesses, while necessary, is hardly sufficient.

The frequencies of the total absolute photographic and visual magnitudes are given in Table XV and are shown as histograms in Fig. 14; clusters omitted are NGC 2419, 5634, 5897, 5401, 6416, 6453, and 6544 because of uncertain $V_t$, and 6838 because of uncertain $(m-M)_{pg}$. This material has also been subdivided into three groups in order to look for any systematic variation of cluster luminosities within the Galaxy. These groups are (1) outlying clusters with $|b| \geqslant 10°$, (2) those

TABLE XIII. Apparent moduli, luminosities, corrected colors,[a] and magnitudes.[a]

| NGC | M | $(m-M)_{pg}$ | $(m-M)_V$ I | $(m-M)_V$ II | $M_{P_t}$ | $M_{V_t}$ | $(P-V)_c$ I | $(P-V)_c$ II | $V_{to}$ I | $V_{to}$ II |
|---|---|---|---|---|---|---|---|---|---|---|
| 2419 | | 19.4 | 19.3 | | <−7.9 | <−8.4 | 0m50 | | <10.5 | |
| 4147 | | 17.1 | 17.1 | | −6.4 | −6.9 | 0.48 | | 10.2 | |
| 4590 | 68 | 16.1 | 15.7 | | −7.2 | −7.7 | 0.49 | | 8.0 | |
| 5024 | 53 | 16.7 | 16.7 | | −8.4 | −8.9 | 0.50 | | 7.7 | |
| 5053 | | 16.4 | 16.4 | | −6.0 | −6.5 | 0.52 | | 9.8 | |
| 5272 | 3 | 15.7 | 15.7 | 15.6 | −8.9 | −9.4 | 0.56 | 0.49 | 6.3 | 6.2 |
| 5466 | | 16.4 | 16.3 | | −6.6 | −7.1 | 0.50 | | 8.8 | |
| 5634 | | 17.1 | 17.1 | 17.0 | <−6.7 | <−7.2 | 0.53 | 0.49 | <9.7 | <9.6 |
| 5694 | | 17.7 | 17.6 | | −6.8 | −7.3 | 0.47 | | 9.8 | |
| 5824 | | ... | ... | | ... | ... | 0.49 | 0.46 | 8.6 | 8.5 |
| 5897 | | 16.2 | 16.1 | | (−7.2) | (−7.7) | 0.50 | | (8.0) | |
| 5904 | 5 | 15.2 | 15.1 | | −8.6 | −9.2 | 0.56 | | 5.7 | |
| 5986 | | ... | ... | | ... | ... | 0.61 | 0.51 | 7.2 | 6.9 |
| 6093 | 80 | 16.0 | 15.9 | 15.8 | −7.9 | −8.5 | 0.62 | 0.55 | 6.9 | 6.7 |
| 6121 | 4 | 14.0 | 13.7 | 13.6 | −7.2 | −7.8 | 0.58 | 0.51 | 4.9 | 4.7 |
| 6144 | | 16.0 | 15.8 | | −6.2 | −6.8 | 0.64 | 0.61 | 8.5 | 8.4 |
| 6171 | 107 | 16.2 | 15.9 | 15.8 | −7.0 | −7.6 | 0.69 | 0.56 | 7.4 | 7.0 |
| 6205 | 13 | 14.8 | 14.8 | | −8.4 | −9.0 | 0.57 | 0.54 | 5.8 | |
| 6218 | 12 | 15.2 | 15.0 | | −7.7 | −8.2 | 0.56 | 0.53 | 6.1 | 6.0 |
| 6229 | | 17.7 | 17.6 | | −7.6 | −8.2 | 0.57 | 0.54 | 9.2 | 9.1 |
| 6254 | 10 | 15.2 | 15.0 | 14.9 | −7.8 | −8.4 | 0.62 | 0.51 | 6.1 | 5.8 |
| 6266 | 62 | 16.7 | 16.3 | 16.2 | −9.1 | −9.6 | 0.54 | 0.43 | 5.5 | 5.2 |
| 6273 | 19 | 16.0 | 15.6 | | −8.2 | −8.7 | 0.49 | | 5.7 | |
| 6284 | | 17.3 | 17.1 | 17.0 | −7.4 | −8.0 | 0.70 | 0.57 | 8.4 | 8.0 |
| 6287 | | 17.3 | 16.9 | 16.7 | −6.7 | −7.2 | 0.72 | 0.51 | 8.3 | 8.7 |
| 6293 | | 16.7 | 16.3 | | −7.4 | −7.9 | 0.48 | | 7.3 | |
| 6304 | | ... | ... | | ... | ... | 0.74 | 0.53 | 7.1 | 6.5 |
| 6316 | | ... | ... | | ... | ... | 0.69 | 0.48 | 7.7 | 7.1 |
| 6325 | | ... | ... | | ... | ... | 0.73 | 0.56 | 8.6 | 8.1 |
| 6333 | | 16.4 | 16.0 | | −7.7 | −8.2 | 0.46 | | 7.9 | |
| 6341 | 92 | 15.2 | 15.2 | | −8.1 | −8.6 | 0.50 | | 6.4 | |
| 6342 | | ... | ... | | ... | ... | 0.86 | 0.65 | 9.1 | 8.5 |
| 6355 | | ... | ... | | ... | ... | 0.82 | 0.65 | 8.1 | 7.6 |
| 6356 | | 17.2 | 16.9 | 16.7 | −7.7 | −8.4 | 0.78 | 0.58 | 7.6 | 7.0 |
| 6401 | | ... | | | | | 0.65: | 0.48: | 8.3: | 7.8: |
| 6402 | 14 | 16.7 | 16.2 | 16.1 | −8.0 | −8.6 | 0.60 | 0.50 | 6.1 | 5.8 |
| 6426 | | 17.8 | 17.5 | | <−4.2 | <−4.8 | 0.57 | 0.51 | <11.9 | <11.7 |
| 6440 | | ... | ... | | ... | ... | 0.71 | 0.57 | 6.2 | 5.8 |
| 6453 | | ... | ... | | ... | ... | 0.59: | 0.42: | 8.6: | 8.1: |
| 6517 | | ... | ... | | ... | ... | 0.57 | 0.50 | 7.2 | 7.0 |
| 6522 | | 17.8 | 17.3 | | −8.2 | −8.7 | 0.54 | | 7.2 | |
| 6528 | | ... | ... | | ... | ... | 0.86 | 0.65 | 8.3 | 7.7 |
| 6539 | | ... | ... | | ... | ... | 0.57 | 0.50 | 6.5 | 6.3 |
| 6544 | | ... | ... | | ... | ... | 0.62 | 0.51 | (6.4) | (6.1) |
| 6553 | | ... | ... | | ... | ... | 0.67 | 0.46 | 6.1 | 5.5 |
| 6569 | | ... | ... | | ... | ... | 0.77 | 0.56 | 7.7 | 7.1 |
| 6624 | | ... | ... | | ... | ... | 0.79 | 0.59 | 7.8 | 7.2 |
| 6626 | 28 | 15.6 | 15.3 | 15.2 | −7.7 | −8.3 | 0.63 | 0.56 | 6.0 | 5.8 |
| 6637 | 69 | ... | ... | | ... | ... | 0.80 | 0.59 | 7.5 | 6.9 |
| 6638 | | 17.5 | 17.2 | 17.1 | −7.4 | −8.0 | 0.68 | 0.55 | 8.4 | 8.0 |
| 6652 | | ... | ... | | ... | ... | 0.78 | 0.61 | 8.9 | 8.4 |
| 6656 | 22 | 14.2 | 13.8 | | −8.2 | −8.6 | 0.45 | 0.41 | 3.9 | 3.8 |
| 6681 | 70 | ... | ... | | ... | ... | (0.59) | 0.56 | (8.1) | 8.1 |
| 6712 | | 16.5 | 16.2 | 16.0 | −7.3 | −7.9 | 0.70 | 0.52 | 7.1 | 6.6 |
| 6715 | 54 | 17.4 | 17.2 | | −9.0 | −9.5 | 0.53 | 0.49 | 7.2 | 7.1 |
| 6723 | | 15.3 | ... | 15.2 | −7.5 | −8.0 | (0.61) | 0.54 | (7.2) | (7.0) |
| 6760 | | 17.4 | 16.4 | | −6.7 | −7.2 | 0.59 | 0.52 | 6.3 | 6.1 |
| 6779 | 56 | 16.3 | 16.1 | 16.0 | −7.3 | −7.8 | 0.50 | 0.46 | 7.5 | 7.4 |
| 6809 | 55 | 14.5 | 14.4 | | −7.7 | −8.2 | 0.48 | | 6.1 | |
| 6838 | 71 | 14.6: | 14.5: | 14.3: | −5.4: | −5.6: | 0.81 | 0.61 | 7.9 | 7.3 |
| 6864 | 75 | 18.1 | 18.0 | 17.9 | −8.8 | −9.4 | 0.64 | 0.50 | 8.4 | 8.0 |
| 6934 | | 16.9 | 16.9 | 16.8 | −7.2 | −7.8 | 0.62 | 0.55 | 9.1 | 8.9 |
| 6981 | 72 | 17.0 | ... | 17.0 | −7.0 | −7.8 | (0.57) | 0.57 | (9.4) | 9.4 |
| 7006 | | 18.8 | 18.7 | | −7.5 | −8.0 | 0.47 | | 10.3 | |
| 7078 | 15 | 15.9 | 15.8 | | −8.9 | −9.4 | 0.52 | | 6.2 | |
| 7089 | 2 | 16.2 | 16.1 | | −9.1 | −9.6 | 0.50 | | 6.3 | |
| 7099 | 30 | 15.5 | 15.5 | | −7.4 | −7.2 | 0.48 | | 7.6 | |

[a] Numbers in parentheses are uncorrected (colors) or uncertain (magnitudes).

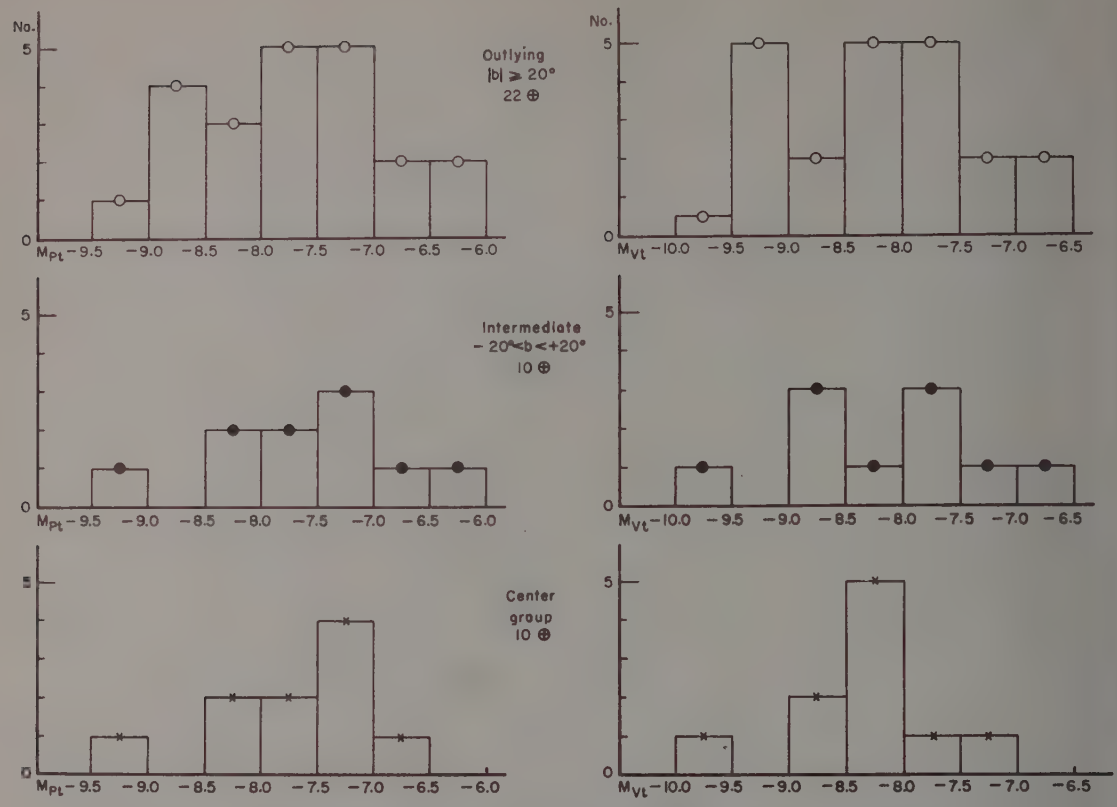


FIG. 14. Histograms for three groupings of globular cluster total absolute magnitudes, in photographic light (left) and visual (right), computed with the assumption that $M_P=0.0$ for cluster-type (RR Lyr) variables.

of intermediate concentration with $-20°<b<+20°$, and (3) those in the direction around the galactic center. The histograms for the frequencies for the three groups combined are given in the lower part of Fig. 20, for comparison with similar data for M31 (Sec. XII).

The small number of clusters in the intermediate and center groups, 10 each, is not encouraging for refined analysis. Nevertheless, there is little suggestion that cluster luminosities are significantly different in different parts of the Galaxy. So far as they go, the frequency distributions look rather similar for the three groups, and the average absolute magnitudes in the penultimate column of Table XV are remarkably the same. Thus the over-all means in photographic and visual light, −7.7 and −8.2, respectively, may be fairly stable, statistical quantities as distance indicators, for example, of the galactic center (Sec. XIII).

TABLE XIV. Comparison of total absolute visual magnitudes.

| NGC | M | $V_t$ | $(m-M)'_V$ | $M'_{Vt}$ | $M_{Vt}$ | Δ mag. |
|---|---|---|---|---|---|---|
| 4147 | ··· | 10.2 | 16.8 | −6.6 | −6.9 | 0.3 |
| 4147 | ··· | 10.2 | 17.1 | −6.9 | −6.9 | 0.0 |
| 5272 | 3 | 6.4 | 15.7 | −9.3 | −9.4 | 0.1 |
| 5904 | 5 | 5.9 | 15.1 | −9.2 | −9.2 | 0.0 |
| 6205 | 13 | 5.9 | 14.7 | −8.8 | −9.0 | 0.2 |
| 6254 | 10 | 6.6 | 14.8 | −8.2 | −8.4 | 0.2 |
| 6341 | 92 | 6.5 | 15.2 | −8.7 | −8.6 | 0.1 |
| 6656 | 22 | 5.1 | 14.0 | −8.9 | −8.6 | 0.3 |
| 7078 | 15 | 6.4 | 15.9 | −9.5 | −9.4 | 0.1 |
| 7089 | 2 | 6.5 | 16.2 | −9.7 | −9.6 | 0.1 |

## Colors

The frequencies of the corrected, integrated-light colors, $(P\text{-}V)_c$, are given in Table XVI, and are shown as histograms in Fig. 15; the poor-data cases of 6401 and 6453 are omitted as for the luminosities, and this material also has been subdivided into three groups, according to concentration of the clusters toward the galactic plane and center.

Comparison of the histograms obtained from alternatives I and II shows, as expected, that alternative II produces frequency distributions having pronounced peaks, especially for the outlying and intermediate cluster groups. The small assumed intrinsic color variation also tends to suppress any systematic differences between the groups. For example, the histograms resulting from alternative I suggest rather definitely that the clusters become redder, both with concentration toward the galactic plane and with location around the center. This effect, however, is

TABLE XV. Distribution of luminosities of galactic globular clusters.

| Luminosity Interval | −9.9 −9.5 | −9.4 −9.0 | −8.9 −8.5 | −8.4 −8.0 | −7.9 −7.5 | −7.4 −7.0 | −6.9 −6.5 | −6.4 −6.0 | Total No. | ⟨M⟩ (mag.) | σ (mag.) |
|---|---|---|---|---|---|---|---|---|---|---|---|
| Outlying $\lvert b\rvert \geq 20°$ | | 1 | 4 | 3 | 5 | 5 | 2 | 2 | 22 | −7.7 | 0.8 |
| | 1 | 5 | 2 | 5 | 5 | 2 | 2 | | 22 | −8.2 | 0.8 |
| Intermediate $-20° < b < +20°$ | | 1 | 0 | 2 | 2 | 3 | 1 | 1 | 10 | −7.5 | 0.75 |
| | 1 | 0 | 3 | 1 | 3 | 1 | 1 | | 10 | −8.1 | 0.7 |
| Center Group | | 1 | 0 | 2 | 2 | 4 | 1 | | 10 | −7.75 | 0.6 |
| | 1 | 0 | 2 | 5 | 1 | 1 | | | 10 | −8.3 | 0.6 |
| All | | 3 | 4 | 7 | 9 | 12 | 4 | 3 | 42 | −7.7 | 0.8 |
| | 3 | 5 | 7 | 11 | 9 | 4 | 3 | | 42 | −8.2 | 0.8 |

closely related to the way in which color excesses were estimated, particularly for clusters of unknown spectral type: by the assumption of types F5, G0, and G5 for such clusters in the three groups. Moreover, nearly half of the center group clusters are unobserved for spectral type. Thus until further photometric or spectroscopic work is done for them, we cannot conclude with confidence from our data that the closer globular clusters are to the galactic plane and center, the redder is their intrinsic color. But this is an interesting possibility pertaining to galactic evolution.

The frequency distributions of the corrected colors for 65 clusters regardless of group are given in the last two lines of Table XVI; they are shown as histograms in the lower part of Fig. 19, for comparison with the colors of the M31 clusters. Here, however, we wish to discuss only these combined data for the galactic globular clusters. For alternative II, the frequency distribution has a fairly symmetrical, prominent maximum about a mean $(P\text{-}V)_c = +0.52$ mag., with a small dispersion $\sigma = 0.05$ mag. While we do not rule out such a result on the basis of the present material, there are

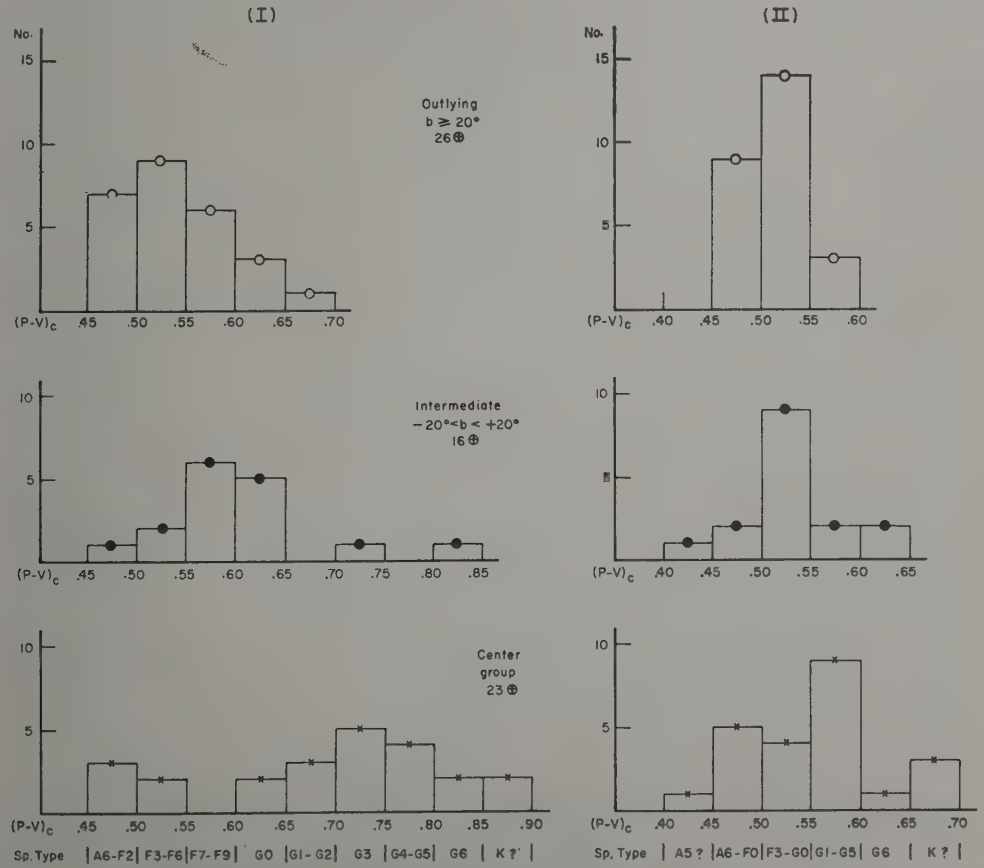


FIG. 15. Histograms for three groupings of globular cluster colors corrected for color excess by alternatives I and II.

TABLE XVI. Distribution of corrected colors of galactic globular clusters.

| $(P\text{-}V)_c$ Interval | | +0.40 +0.44 | 0.45 0.49 | 0.50 0.54 | 0.55 0.59 | 0.60 0.64 | 0.65 0.69 | 0.70 0.74 | 0.75 0.79 | 0.80 0.84 | 0.85 0.89 | Total No. | $\langle P\text{-}V\rangle_c$ (mag.) | $\sigma$ (mag.) |
|---|---|---|---|---|---|---|---|---|---|---|---|---|---|---|
| Outlying $\lvert b\rvert \geq 20°$ | I | | 7 | 9 | 6 | 3 | 1 | | | | | 26 | +0.53 | 0.06 |
| | II | | 9 | 14 | 3 | | | | | | | 26 | +0.51 | 0.03 |
| Intermediate $-20° < b < +20°$ | I | | 1 | 2 | 6 | 5 | 0 | 1 | 0 | 1 | | 16 | +0.60 | 0.08 |
| | II | 1 | 2 | 9 | 2 | 2 | | | | | | 16 | +0.52 | 0.05 |
| Center Group | I | | 3 | 2 | 0 | 2 | 3 | 5 | 4 | 2 | 2 | 23 | +0.69 | 0.12 |
| | II | 1 | 5 | 4 | 9 | 1 | 3 | | | | | 23 | +0.55 | 0.06 |
| All | I | | 11 | 13 | 12 | 10 | 4 | 6 | 4 | 3 | 2 | 65 | +0.60 | 0.11 |
| | II | 2 | 16 | 27 | 14 | 3 | 3 | | | | | 65 | +0.52 | 0.05 |

some reasons to view it skeptically. If the three clusters (NGC 6681, 6723, 6981) used to define alternative II are found to have earlier spectral types by future and better spectroscopic work, or fail to have their relatively blue colors confirmed by further photometry, then this particular path of color excess estimation is invalidated. If so, there would then be stronger support for alternative I, which conforms much more to the expectation that appreciably redder intrinsic colors accompany later spectral types. For this reason, we regard more favorably the color-frequency histogram resulting from alternative I. It does not have nearly so high a maximum, and it is unsymmetrical with a long tail toward redder colors. Moreover, unless the unobserved clusters materially modify the frequencies, it seems unlikely to us that the most frequent color, about $(P\text{-}V)_c = +0.5$ mag., or the range from +0.45 to +0.90 mag., will change drastically. The corresponding dispersion

TABLE XVII. Corrected moduli, distances, linear diameters, and mean surface brightnesses.

| NGC | M | $(m-M)_c$ I | $(m-M)_c$ II | $r$(kpc) I | $r$(kpc) II | $D_{0.9}$(pc) I | $D_{0.9}$(pc) II | $\langle SB\rangle^a$ I | $\langle SB\rangle^a$ II |
|---|---|---|---|---|---|---|---|---|---|
| 2419 | | 18.9 | | 60 | | | | | |
| 4147 | | 17.1 | | 26 | | 26 | | +0.2 | |
| 4590 | 68 | 15.4 | | 12 | | 22 | | −1.0 | |
| 5024 | 53 | 16.7 | | 22 | | 53 | | −0.3 | |
| 5053 | | 16.3 | | 18 | | ... | | ... | |
| 5272 | 3 | 15.7 | 15.4 | 14 | 12 | 38 | 32 | −1.5 | −1.8 |
| 5466 | | 15.9 | | 15 | | ... | | ... | |
| 5634 | | 17.0 | 16.8 | 25 | 23 | ... | | ... | |
| 5694 | | 17.2 | | 28 | | 19 | | −0.9 | |
| 5824 | | ... | | ... | | ... | | ... | |
| 5897 | | 15.7 | | 14 | | (64) | | (+1.3) | |
| 5904 | 5 | 14.9 | | 9.5 | | 30 | | −1.8 | |
| 5986 | | ... | | ... | | ... | | ... | |
| 6093 | 80 | 15.5 | 15.2 | 13 | 11 | 33 | 28 | −0.9 | −1.3 |
| 6121 | 4 | 12.7 | 12.4 | 3.5 | 3.0 | 23 | 20 | −1.0 | −1.3 |
| 6144 | | 15.3 | 15.2 | 11 | | 36 | | +1.0 | |
| 6171 | 107 | 15.1 | 14.6 | 10 | 8.3 | 37 | 31 | +0.2 | −0.2 |
| 6205 | 13 | 14.8 | 14.7 | 9.1 | 8.7 | 34 | 33 | −1.4 | |
| 6218 | 12 | 14.4 | 14.3 | 7.6 | 7.2 | 48 | 45 | +0.2 | 0.0 |
| 6229 | | 17.4 | 17.3 | 30 | 29 | 31 | 30 | −0.8 | |
| 6254 | 10 | 14.5 | 14.1 | 7.9 | 6.6 | 37 | 31 | −0.6 | −1.0 |
| 6266 | 62 | 15.1 | 14.7 | 10 | 8.7 | 26 | 22 | −2.6 | −2.9 |
| 6273 | 19 | 14.4 | | 7.6 | | 21 | | −2.1 | |
| 6284 | | 16.5 | 16.0 | 20 | 16 | 33 | 27 | −0.4 | −0.8 |
| 6287 | | 15.7 | 14.9 | 14 | 9.5 | 24 | 16 | −0.3 | −1.2 |
| 6293 | | 15.2 | | 11 | | 20 | | −1.4 | |
| 6304 | | ... | | ... | | ... | | ... | |
| 6316 | | ... | | ... | | ... | | ... | |
| 6325 | | ... | | ... | | ... | | ... | |
| 6333 | | 14.8 | | 9.1 | | 21 | | −1.6 | |
| 6341 | 92 | 15.1 | | 10 | | 36 | | −0.8 | |
| 6342 | | ... | | ... | | ... | | ... | |
| 6355 | | ... | | ... | | ... | | ... | |
| 6356 | | 16.1 | 15.3 | 17 | 11 | 31 | 20 | −1.0 | −1.9 |
| 6401 | | ... | | ... | | ... | | ... | |

TABLE XVII—*Continued*

| NGC | M | $(m-M)_c$ I | $(m-M)_c$ II | $r$(kpc) I | $r$(kpc) II | $D_{0.9}$(pc) II | $D_{0.9}$(pc) II | $\langle SB\rangle$[a] I | $\langle SB\rangle$[a] II |
|---|---|---|---|---|---|---|---|---|---|
| 6402 | 14 | 14.7 | 14.3 | 8.7 | 7.2 | 27 | 23 | −1.4 | −1.8 |
| 6426 | | 16.7 | 16.5 | 22 | 20 | ... | | ... | |
| 6440 | | ... | ... | ... | | ... | | ... | |
| 6453 | | ... | ... | ... | | ... | | ... | |
| 6517 | | ... | ... | ... | | ... | | ... | |
| 6522 | | 15.9 | | 15 | | 18 | | −2.4 | |
| 6528 | | ... | | ... | | ... | | ... | |
| 6539 | | ... | | ... | | ... | | ... | |
| 6544 | | ... | | ... | | ... | | ... | |
| 6553 | | ... | | ... | | ... | | ... | |
| 6569 | | ... | | ... | | ... | | ... | |
| 6624 | | ... | | ... | | ... | | ... | |
| 6626 | 28 | 14.3 | 14.0 | 7.2 | 6.3 | 20 | 17 | −1.8 | −2.1 |
| 6637 | 69 | ... | | ... | | ... | | ... | |
| 6638 | | 16.4 | 15.9 | 19 | 15 | 24 | 19 | −1.1 | −1.6 |
| 6652 | | ... | | ... | | ... | | ... | |
| 6656 | 22 | 12.6 | 12.5 | 3.3 | 3.2 | 25 | 24 | −1.6 | |
| 6681 | 70 | ... | | ... | | ... | | ... | |
| 6712 | | 15.2 | 14.5 | 11 | 7.9 | 39 | 28 | +0.1 | −0.7 |
| 6715 | 54 | 16.7 | 16.6 | 22 | 21 | 31 | 29 | −2.1 | −2.4 |
| 6723 | | ... | 15.0 | 10 | | 34 | | −0.4 | |
| 6760 | | 13.6 | 13.4 | 5.2 | 4.8 | 13 | 12 | −1.6 | −1.8 |
| 6779 | 56 | 15.4 | 15.2 | 12 | 11 | 35 | 32 | −0.1 | −0.3 |
| 6809 | 55 | 14.2 | | 6.9 | | 42 | | −0.1 | |
| 6838 | 71 | 14.1: | 13.3: | 6.6: | 4.6: | 20: | 14: | +0.4: | +0.3: |
| 6864 | 75 | 17.8 | 17.3 | 36 | 29 | 51 | 41 | −0.8 | −1.4 |
| 6934 | | 16.9 | 16.6 | 24 | 21 | 23 | 20 | −1.0 | −1.3 |
| 6981 | 72 | ... | 17.0 | 25 | | 47 | | +0.6 | |
| 7006 | | 18.3 | | 46 | | 40 | | 0.0 | |
| 7078 | 15 | 15.6 | | 13 | | 36 | | −1.6 | |
| 7089 | 2 | 15.9 | | 15 | | 30 | | −2.2 | |
| 7099 | 30 | 15.5 | | 13 | | 26 | | −0.8 | |

[a] Unit of $\langle SB\rangle$ is $M_V/pc^2$.

$\sigma=0.11$ mag., with such a skew distribution, may not be very meaningful.

## Distances and Diameters

With the values of $A_V$ listed in Table X and of $(m-M)_V$ in Table XIII, corrected distance moduli were computed. These are given as $(m-M)_c$ in Table XVII, with corresponding distances in kiloparsecs, $r$(kpc). On the basis of these distances, linear diameters containing 0.9 of the total light, $D_{0.9}$, were computed from the angular diameters $d_{0.9}$ in Table IV, and, finally, the mean absolute surface brightness, $\langle SB\rangle$, from $M_{V_t}+5\log D_{0.9}$. Results from these calculations are plotted in Fig. 16 for alternatives I and II, with $M_{V_t}$ as abscissa.

Figure 16 shows, first, that there is little over-all difference in the character of the plots for the two different ways used to estimate color excesses; except in a few individual cases, averages for I and II would be satisfactory. Considering, next, the linear diameters containing 0.9 the total light, we note they are nearly independent of luminosity in the range from $M_{V_t}=-6.8$ to $-9.6$ and in the diameter range from about 20 to 50 pc. There is some indication of systematic difference between the three groups of clusters: for those with $|b|\geqslant 20°$, $-20°<b<+20°$, and the 10 clusters near the galactic center direction, the mean diameters are $\langle D\rangle_{0.9}=34$, 28, and 22 pc, respectively. While this trend may be real, there exists the possibility that it is due to increasing field star density, which makes more uncertain those diameter determinations for clusters in rich star fields. The mean absolute surface brightnesses, on the other hand, show a marked correlation with the absolute magnitudes, which is to be expected from the small range in linear diameter compared to the much larger range in luminosity. The intrinsically brightest clusters appear to have mean surface brightnesses more than 3 mag. brighter than the least luminous clusters.

## XI. CLUSTERS IN THE M31 GROUP

### Magnitudes and Colors

We consider here the magnitudes $V$, in this case equivalent to $V_t$ and the color indices $(P\text{-}V)$ and $(V\text{-}I)$ from Table VII, which are plotted in Figs. 17 and 18.

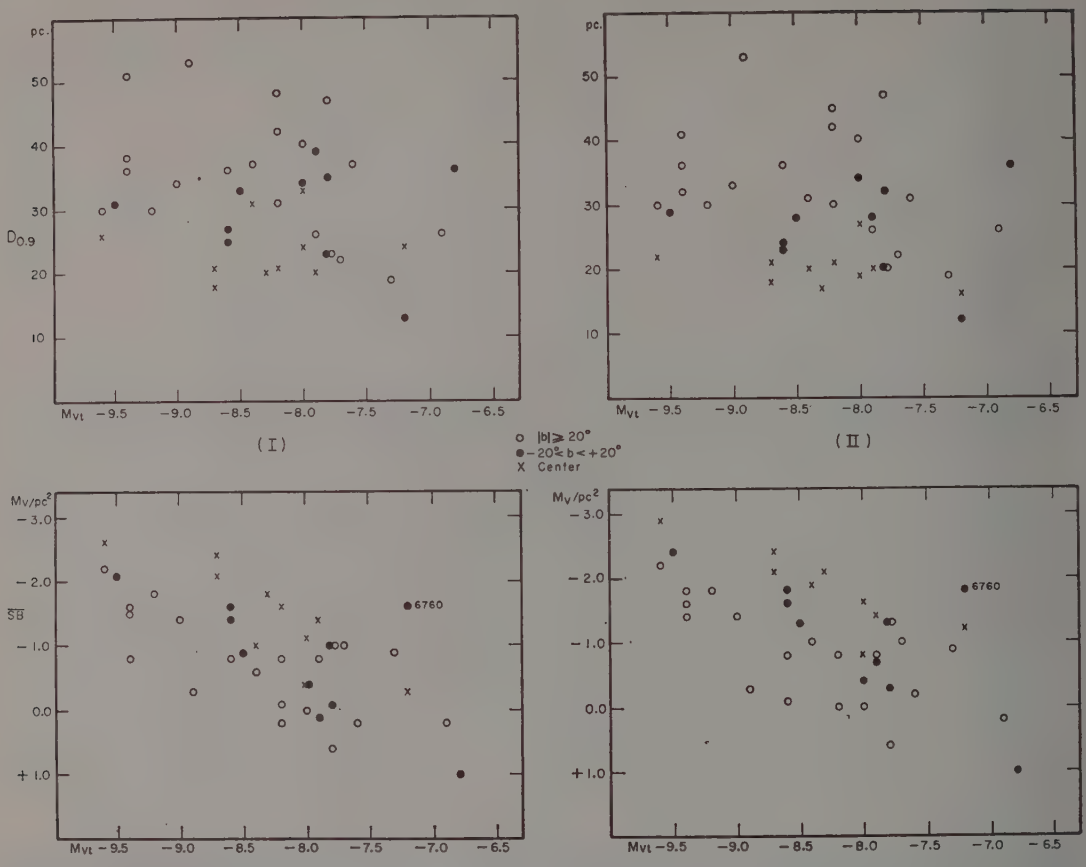


FIG. 16. Linear diameters for 0.9 total light (above) and corresponding mean absolute surface brightnesses (below), for three groups of globular clusters, plotted against total absolute visual magnitudes; results are shown separately for alternative I (left) and II (right).

Although this sample is incomplete, especially for the fainter objects, it has the advantage of including 79 clusters all presumably at nearly the same distance.

Looking, first, at the lower left part of Fig. 17, we find that there are eight objects with $(P\text{-}V)<+0.50$ mag. Four of these are in M33 and have already been mentioned in Sec. VII. Here we wish to note that the brightest one in M33, Mc with $V=15.97$, is apparently more than two magnitudes fainter than the brightest cluster in M31, M II with $V=13.75$. Even with allowance for as much as 0.5 mag. local reddening in M33, it seems probable that the upper limit of luminosity for clusters in M33 is significantly lower than that in M31. Of the remaining four clusters with $(P\text{-}V)<+0.50$ mag., one is H VIII in NGC 205 and the other three are H5, H7 and H21 in M31. Although the latter appear in the spiral structure, their location in the principal plane is necessarily uncertain because of possible projection. Object H5, however, was observed in three colors, and if plotted in Fig. 10 would be associated with the galactic open clusters. For this reason it was observed with the Crossley nebular spectrograph. A five-hour exposure recorded only a narrow trace without conspicuous absorption lines, and a continuum somewhat stronger shortward of H and K than found previously for objects M II, III, IV, and VI (Mayall and Eggen 1953). If these three relatively bluer objects in M31 are, in fact, like open clusters of higher luminosity, they probably are not greatly reddened, for the colors of the galactic open clusters listed in Table VI range up to $(P\text{-}V)=+0.90$ mag.

Considering, next, those objects with $(P\text{-}V)\gtrsim+0.50$ mag. in Fig. 17, we note a fairly high concentration in the approximate range $+0.5<(P\text{-}V)<+1.0$ mag., and a few redder ones that tend to be fainter with increasing color index, the most extreme case being B327 with $V=16.97$ and $(P\text{-}V)=+1.94$ mag. There appears to be, in fact, a fairly well-defined sloping right-hand boundary, as would be found for the highest luminosity clusters increasingly dimmed and reddened by interstellar matter in M31. The effect is indicated in the figure by the dashed lines connecting those points corresponding to clusters that are brightest for their colors; the dotted line shows, with less certainty, the similar effect expected for clusters of high to normal luminosity.

Except for the reddest clusters, it is, of course, im-

TABLE XVIII. Distribution of colors of M31 clusters.

| $(P\text{-}V)$ Interval | +0.50 +0.54 | 0.55 0.59 | 0.60 0.64 | 0.65 0.69 | 0.70 0.74 | 0.75 0.79 | 0.80 0.84 | 0.85 0.89 | Total No. | $\langle P\text{-}V \rangle$ (mag.) | $\sigma$ (mag.) |
|---|---|---|---|---|---|---|---|---|---|---|---|
| Outlying only | 3 | 5 | 1 | 5 | 3 | 1 | 2 | 4 | 24 | +0.68 | 0.12 |
| $+0.50 \leqslant (P\text{-}V) < +0.90$ | 3 | 6 | 5 | 9 | 11 | 4 | 11 | 7 | 56 | +0.72 | 0.10 |

possible without further information to identify individually those clusters of small or moderate reddening, because of the ranges in true color and brightness. Nevertheless, their influence as a group may be avoided by considering only those clusters which appear in Fig. 4 to be sufficiently outlying that little or no space-reddening from the spiral structure seems probable. There are 24 of the observed objects that may reasonably be placed in this category, and they are indicated in Table VII by the superscript a, and in Figs. 17 and 18 by encircled dots. Their range in color is from $(P\text{-}V) = +0.50$ to $+0.89$ mag. (inclusive), which may correspond closely to the true range because the sample is of fair size. The frequencies in 0.05 mag. intervals, means and dispersions for both the outlying clusters and for all those with $+0.50 < (P\text{-}V) < +0.90$ mag., are given in Table XVIII, and their distribution is shown as the histogram in the upper part of Fig. 19.

This distribution in color for these M31 clusters does not indicate a well-defined maximum within the $(P\text{-}V)$ color range of 0.40 mag. Although there may be some slight suggestion of subsidiary maxima at about $(P\text{-}V) = 0.72$ and 0.82 mag., these data are not relevant regarding the existence of "blue"- and "red"-color groups of clusters, as suggested by Kron and Gascoigne (1952), nor do they indicate a clear separation into "halo" and "disk-type" globular clusters, as identified by Morgan (1956). Our data, however, are observationally biased toward the apparently brightest objects, and the possibility is by no means excluded that obser-

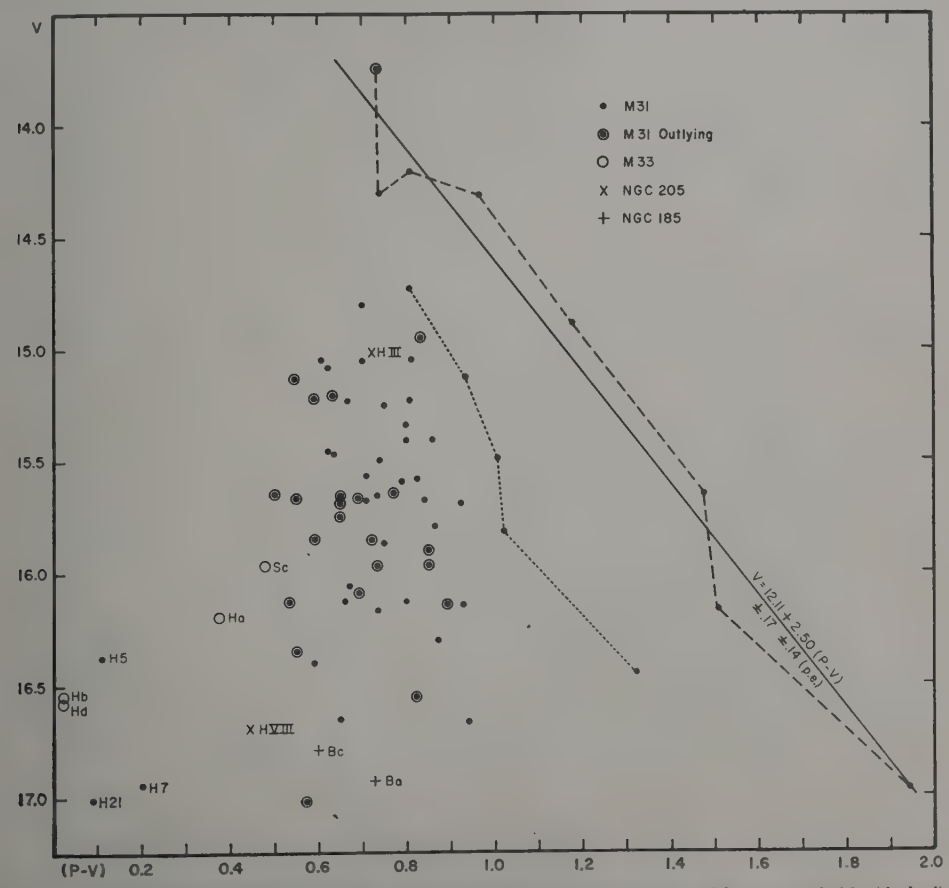


FIG. 17. Color-magnitude diagram for star clusters observed in the M31 group, with some probable (dashed) and possible (dotted) reddening runs indicated.

vations of the many fainter clusters may reveal groups like those mentioned. Also, there is little tendency for the outlying clusters to be systematically bluer than those seen projected over the spiral; in fact, six outlying ones have $(P\text{-}V)>+0.80$ mag. Hence the use of these objects, most of which probably are bonafide globular star clusters, as indicators of small space reddening by interstellar matter either from the Galaxy or in M31 seems likely to be unsatisfactory, or, at best, attended with results of low precision.

## Color Excess and Absorption

If it is assumed that the eight clusters corresponding to those points in Fig. 17 connected by the dashed lines are the highest luminosity clusters of nearly the same color, $(P\text{-}V)\sim 0.7$ mag., then it is possible to estimate the ratio of $V$ absorption to $(P\text{-}V)$ color excess in M31. A least-squares solution for the relationship between $V$ and $(P\text{-}V)$ gave the following result with probable errors: $V=12.11\pm 0.17+(2.50\pm 0.14)(P\text{-}V)$, which is represented by the solid straight line drawn in Fig. 17.

Thus these M31 data give $A_V/E_{(P-V)}=2.50\pm 0.14$, a value somewhat smaller than that derived by Stebbins (1950) from the integrated light of small areas around the nuclear region: 3.0 (when reduced to visual). It is also smaller than the values usually obtained from space-reddened stars in the Galaxy. Hiltner and Johnson (1956), for example, found a ratio of $3.0\pm 0.2$ on their (B-V) color system that has nearly the same color base-line as $(P\text{-}V)$. Although a slope of 3.0 would not represent so well these few reddest clusters observed in M31, the difference in the ratios, $0.50\pm 0.24$, is too poorly determined to suggest seriously that the absorbing material in M31 differs significantly from that in the Galaxy. Similar conclusions have been reached by Holmberg (1950) for NGC 5195, and by Sérsic (1958) for NGC 5128.

Color excesses and total absorptions may also be estimated, with low precision, for the few individually reddest clusters represented in Figs. 17 and 18, if a "normal" or intrinsic color index is assumed for them. Moreover, since some of these were observed in both the $(P\text{-}V)$ and $(V\text{-}I)$ color systems, comparison of the results provides a useful internal check on the procedure. For this purpose we use, first, the $(P\text{-}V)$ data for the 12 objects in M31 with $(P\text{-}V)\geqslant +0.90$ mag., and assume that their mean intrinsic color is $\langle P\text{-}V\rangle_0 = +0.70$ mag., which is the average of the two mean values in Table XVIII. For each of these clusters, the visual absorption, $A_V$, was computed from $2.9[(P\text{-}V) -0.70]=2.9\,E_{(P-V)}=A_V$, where the factor 2.9 from Sec. VIII was used because it is probably less subject to observational selection error than the factor 2.5 found from M31. Next, from the three-color plot of Fig. 18, it seemed reasonable to obtain an average intrinsic $(V\text{-}I)$ color from the 12 clusters represented in the rectangle, since among these points are five referring to outlying clusters. Thus, for these 12 clusters $\langle V\text{-}I\rangle_0=+0.86$ mag., and the corresponding $\langle P\text{-}V\rangle_0$

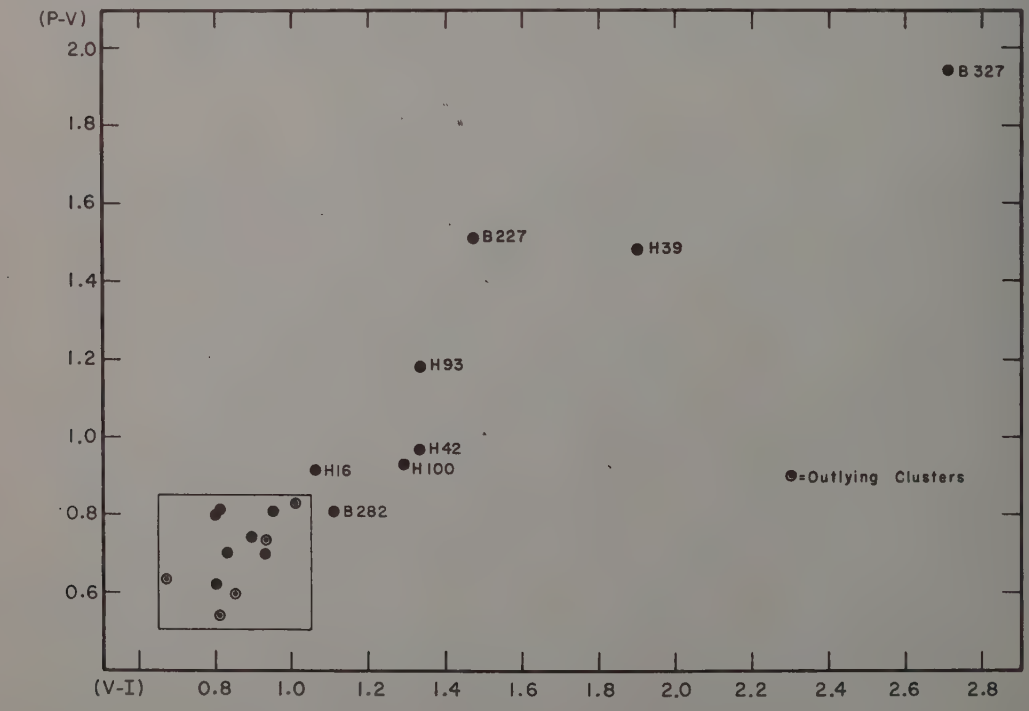


FIG. 18. Three-color (two color-index) diagram for star clusters in M31.

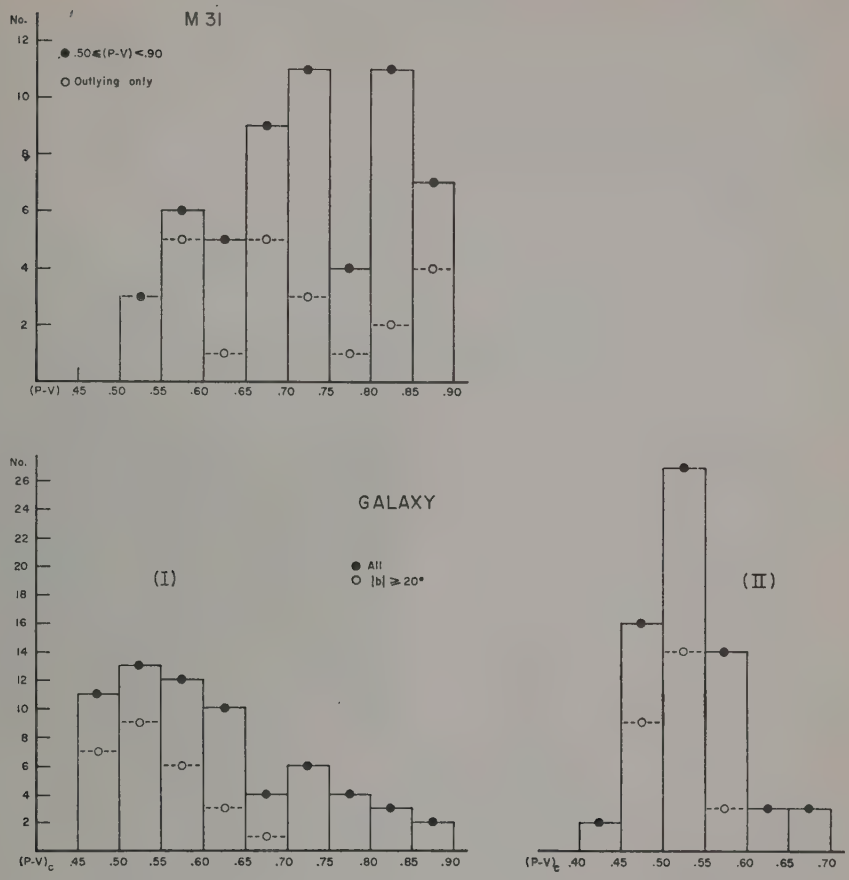


FIG. 19. Comparison of histograms of colors of star clusters in M31 and of globular clusters in the Galaxy; for the latter the colors are corrected for color excess by alternatives I and II.

$=+0.71$ mag., which agrees satisfactorily with that from the preceding grouping. For the remaining nine clusters with $(V\text{-}I)>+1.00$ mag., the visual absorption was found from

$$2.3[(V\text{-}I)-0.86]=2.3\,E_{(V-I)}=2.3\,E_{(V-I)}=A_V,$$

where the factor 2.3 was obtained as described in Sec. VIII. Table XIX gives the results from this procedure.

The agreement between $A_V$ from the two different color systems seems generally satisfactory, except for B227. This object is located on the edge of a dark lane, and evidently the $(V\text{-}I)$ observations (Fig. 18) were more affected than the $(P\text{-}V)$ ones (Fig. 17). If this discrepant $(V\text{-}I)$ case is omitted, the last three columns of the table give, respectively, the mean, $\langle A\rangle_V$, rounded to the nearest 0.05 mag., the corresponding $\langle E\rangle_{(P-V)}$ by division by 2.9, and the corrected colors, $(P\text{-}V)_c$. The mean corrected color for these 13 objects is $\langle P\text{-}V\rangle_c=0.68$ mag., which is 0.03 mag. smaller than $\langle P\text{-}V\rangle_0$ because of the use of a factor of 2.9 instead of 2.5.

This treatment of the M31 photometric data indicates that interstellar matter in the spiral may have reddened a few of the observed clusters by about a magnitude and dimmed them by several magnitudes. On the whole, however, most of the clusters in this sample do not appear to be strongly reddened by local absorption, as Baade (1950) had noted previously from his color-filter photographs.

## Luminosities

It is evident from Fig. 17 that the apparently brightest clusters in M31 attain high luminosities. For $V<14.5$, an apparent distance modulus of 24.6 (Sandage 1958), and without any correction for possible local absorption in the spiral, there are four clusters having $M_V<-10$; namely, M II, B282, H12, and H42. Of these, only M II is outlying and, if unreddened, it has $M_V=-10.8$, the position of H12 in Fig. 17 does not suggest that it is reddened, while the locations of B282 and H42 in Fig. 17 suggest that they are. If the $V$ magnitudes for the two latter clusters and for the others in Table XIX are corrected by the tabulated values of $\langle A\rangle_V$, then the following 10 clusters have $M_{V_c}\leqslant-10.0$:

| Cluster | $M_{V_c}$ | Cluster | $M_{V_c}$ |
|---|---|---|---|
| H12 | −10.3 | H100 | −10.3 |
| H32 | −10.0 | B227 | −10.8 |
| H39 | −11.2 | B282 | −11.0 |
| H42 | −11.2 | B327 | −11.5: |
| H93 | −11.0 | MII | −10.8 |

TABLE XIX. Color excess and absorption for M31 clusters.

| Cluster | $E_{(P-V)}$ $\langle P\text{-}V\rangle_0=+0^m.70$ | $A_V$ | $E_{(V-I)}$ $\langle V\text{-}I\rangle_0=+0^m.86$ | $A_V$ | $\langle A_V\rangle$ | $\langle E\rangle_{(P-V)}$ | $(P\text{-}V)_c$ |
|---|---|---|---|---|---|---|---|
| H 16 | $0^m.22$ | $0^m.64$ | $0^m.20$ | $0^m.46$ | $0^m.55$ | $0^m.19$ | $0^m.73$ |
| B 282 | ...[a] | ...[a] | 0.25 | 0.58 | 0.60 | 0.21 | 0.60 |
| H 38 | 0.23 | 0.67 | ... | ... | 0.70 | 0.24 | 0.69 |
| H 100 | 0.23 | 0.67 | 0.43 | 0.99 | 0.85 | 0.29 | 0.64 |
| B 259 | 0.24 | 0.70 | ... | ... | 0.70 | 0.24 | 0.70 |
| H 42 | 0.27 | 0.78 | 0.47 | 1.08 | 0.95 | 0.33 | 0.64 |
| H 97 | 0.31 | 0.90 | ... | ... | 0.90 | 0.31 | 0.70 |
| B 258 | 0.32 | 0.93 | ... | ... | 0.95 | 0.33 | 0.69 |
| H 93 | 0.48 | 1.39 | 0.47 | 1.08 | 1.25 | 0.43 | 0.75 |
| H 32 | 0.62 | 1.80 | ... | ... | 1.80 | 0.62 | 0.70 |
| H 39 | 0.78 | 2.26 | 1.04 | 2.39 | 2.30 | 0.79 | 0.69 |
| B 227 | 0.81 | 2.35 | (0.61) | (1.40) | 2.35 | 0.81 | 0.70 |
| B 327 | 1.24 | 3.60 | 1.85 | 4.25 | 3.90 | 1.34 | 0.60 |

[a] Not included because $(P\text{-}V)=+0.81<0.90$ mag.

The upper limit of luminosity for clusters in M31 appears from these results to be of the order of $M_V=-11$. The highest luminosity of $-11.5$ for B327, however, is to be regarded as very uncertain, because this object was the faintest observed, with $P=18.9$. Also, if the intrinsic colors of any of these clusters are redder than the assumed mean value of $\langle P\text{-}V\rangle_c=0.70$ mag., their listed luminosities will become fainter by $\Delta\langle P\text{-}V\rangle_0\times 2.9$, which amounts to 0.6 mag. if, for example, $\langle P\text{-}V\rangle_0=0.90$ mag. In order to show the influence of these uncertain absorption effects on the luminosity frequencies, we give the latter for: (1) outlying clusters only, (2) clusters with $+0.50\leqslant(P\text{-}V)<+0.90$ mag. uncorrected for absorption, and (3) clusters with $(P\text{-}V)\geqslant+0.50$ mag. including those corrected for absorption as described in the foregoing. Table XX contains these three sets of frequencies in 0.5 mag. intervals, and the distribution for (1) and (2) is shown graphically as a histogram in the upper right part of Fig. 20; the upper left part gives the histogram of frequencies for $P$-magnitudes.

These frequencies suggest that the luminosities of these M31 clusters have a well-defined maximum around $M_V=-9$, with a moderate dispersion of $\sigma=0.6$ mag. if the highly space-reddened ones are disregarded. This result, however, could be considerably affected by observational selection, because the observing program included mainly those objects of photographic magnitude 16.5 and brighter. Thus the frequencies for $M_V=-8$ and fainter are hardly represented in the sample. On the other hand, the 24 outlying clusters, whose census probably is almost complete, give nearly the same distribution. Obviously, observations of more and fainter clusters are needed to establish more reliably the fainter part of the luminosity function.

## XII. COMPARISON OF GLOBULAR CLUSTERS IN THE GALAXY AND IN M31

### Colors

In the left-hand side of Fig. 19, the scales of abscissae, or $(P\text{-}V)$ colors, have been aligned vertically in order to compare the color frequency distributions of globular clusters in M31 and in the Galaxy. In the histogram for M31, only those clusters are included that have $0.50\leqslant(P\text{-}V)<0.90$ mag., and in that for the Galaxy the $(P\text{-}V)_c$ colors are those corrected on the basis of alternate I. These two histograms indicate that in M31 a substantial majority of the clusters have colors in the range from $(P\text{-}V)=0.65$ to 0.90 mag., whereas in the Galaxy a large proportion of the globular clusters have colors in the range from $(P\text{-}V)=0.45$ to 0.65 mag. Whether this systematic difference is real, and not due to observational selection of clusters in M31 and to incorrect color excesses for clusters in the Galaxy, probably remains to be determined by future work. It does not seem probable to us, however, that reasonably different procedures for deriving color excesses for the galactic globular clusters would produce a distribution of colors comparable to that in M31. Many of the galactic globulars with $|b|>20°$ are in the range of $(P\text{-}V)_c=0.45$ to 0.65, and they are so little reddened that it does not make too much difference how their color excesses are estimated. Also, although most of the clusters with $(P\text{-}V)_c=0.65$ to 0.90 mag. are located around the center, the observing program included a large fraction of the known number, and observations of additional ones could hardly produce a frequency maximum comparable or higher than that in the bluer range. If alternate II is used to estimate color excesses, there is even less possibility of getting a maximum in the redder range. As for the clusters in M31, since uncorrected colors were used in the histogram, we cannot rule out the possibility that many of those seen in projection over the spiral may be reddened by amounts averaging 0.25 mag. in $(P\text{-}V)$. Nevertheless, a substantial percentage would have to be reddened by this amount in order to produce a frequency maximum in the range from $(P\text{-}V)_c=0.45$ to 0.65 mag. This condition seems improbable if half are located in front of the principal plane containing the absorbing material, and half in back. Possibly a more promising way to get a higher

TABLE XX. Luminosity distribution of M31 clusters.

| $M_V$ Interval | $-11.5$ $-11.1$ | $-11.0$ $-10.6$ | $-10.5$ $-10.1$ | $-10.0$ $-9.6$ | $-9.5$ $-9.1$ | $-9.0$ $-8.6$ | $-8.5$ $-8.1$ | $-8.0$ $-7.6$ | $-7.5$ $-7.1$ | Total No. | $\langle M_V\rangle$ (mag.) | $\sigma$ (mag.) |
|---|---|---|---|---|---|---|---|---|---|---|---|---|
| Outlying | ... | 1 | 0 | 1 | 3 | 12 | 5 | 1 | 1 | 24 | $-8.8$ | 0.63 |
| $+0.50\leqslant(P\text{-}V)<+0.90$ | ... | 1 | 2 | 5 | 14 | 20 | 11 | 2 | 1 | 56 | $-9.0$ | 0.61 |
| Incl. 12 Corr. for Abs. | 3 | 4 | 2 | 8 | 16 | 20 | 12 | 2 | 1 | 68 | $-9.2$ | (0.80 |

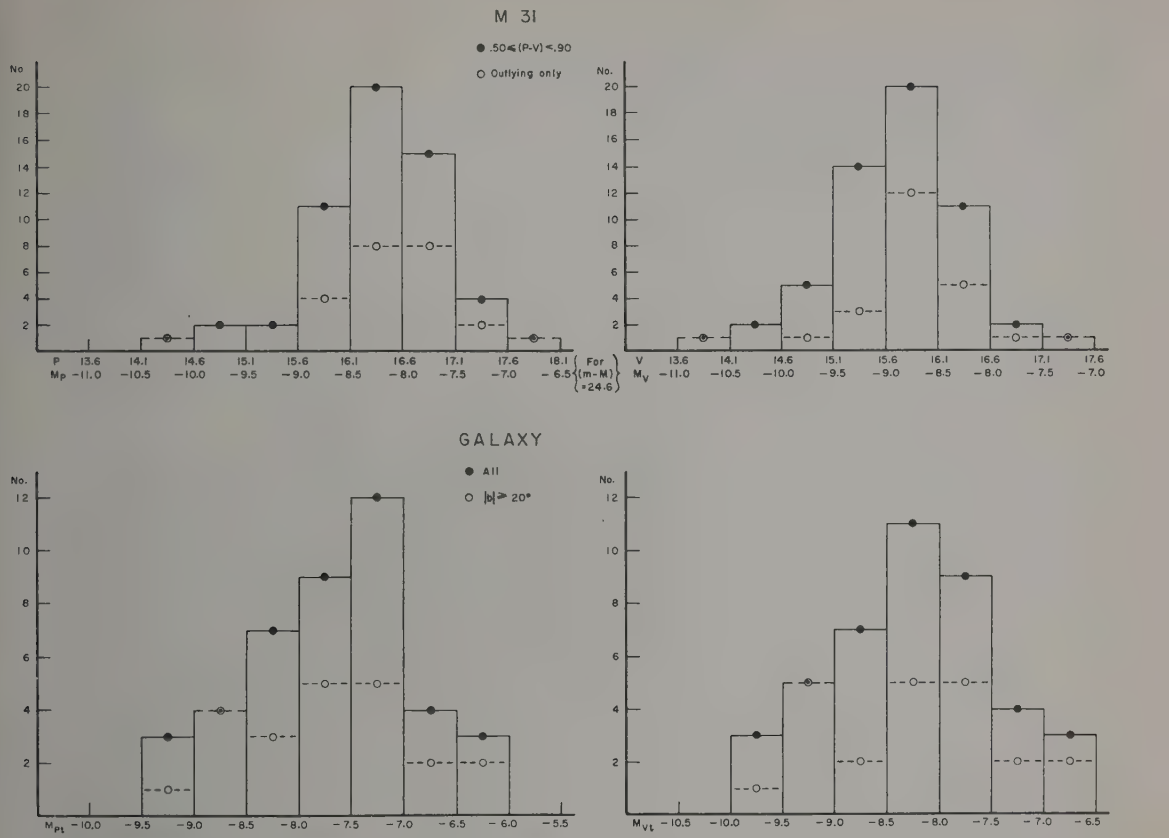


FIG. 20. Comparison of the histograms of absolute photographic (left) and visual (right) magnitudes of star clusters in M31 (above) and of globular clusters in the Galaxy (below), computed with the assumption that $M_P = 0.0$ for cluster-type (RR Lyr) variables.

maximum in the bluer range would be to observe the remaining two-thirds of the clusters known in M31. Since nearly all of these are fainter than photographic magnitude 16.5, however, it is also probable that many will be considerably reddened, and some will be open clusters, with the result that inference of their intrinsic colors will be a difficult and uncertain procedure. Until such additional data are available, we conclude that the present results give some support for a systematically different color frequency distribution, in the sense that the clusters in M31 may be intrinsically redder, by 0.2 to 0.3 mag. on the average, than the globular clusters in the Galaxy.

## Luminosities

In Fig. 20, the left-hand side shows the frequency distributions in photographic light, and the right-hand side in visual light, of the apparent magnitudes of the clusters in M31 (above) and of the absolute magnitudes of globular clusters in the Galaxy (below). In this figure the maximum frequencies are vertically aligned, with the result that the scale of abscissae have a constant difference of 23.6 mag. in photographic light and 24.1 in visual light. The bearing of these figures on the distance modulus of M31 is considered in the next section, which is a discussion of globular clusters as distance indicators.

Considering, first, the brighter side of the luminosity distributions represented in Fig. 20, we note that the histograms for the M31 clusters appear to fall off faster and to extend to higher luminosities, than the ones for the galactic globular clusters. This characteristic, if real, probably is due to the fact that for M31 this program included all but the most heavily absorbed high luminosity clusters, whereas for the Galaxy the intrinsically brightest ones in the southern hemisphere are not included. [*Note added in proof.* We regret having overlooked, when writing this section, the important paper by S. C. B. Gascoigne and E. J. Burr (*Monthly Notices Roy. Astron. Soc.* **116**, 570, 1956) on 47 Tucanae and $\omega$ Centauri. From photoelectric photometry they found $M_{Pi} = -10.0$ for 47 Tuc and $-10.4$ for $\omega$ Cen. If these values were included in the lower left histogram of Fig. 17, the agreement between the luminosity distributions for the Galaxy and M31 would be much improved.] This kind of observational selection argues

against making a too-detailed comparison of the high-luminosity "tails"; about all we are willing to conclude is that the present data do not indicate any substantial difference in this respect between M31 and the Galaxy. Second, we note that all the histograms show fairly well-defined maxima, but, as stated in Sec. XI, those in M31 probably are misleading, if not spurious, because of the lack of observations for the great bulk of clusters fainter than photographic magnitude 16.5. For the Galaxy, on the other hand, the frequency distributions are reasonably complete (about 60%), and as significant as permitted by our present knowledge of distance moduli, and by the assumption of $M_P=0.0$ for cluster-type (RR Lyrae) variables.

## XIII. GLOBULAR CLUSTERS AS DISTANCE INDICATORS

In this section we consider how the photometric data obtained in the present work may be used to estimate the distance moduli of the Andromeda nebula (M31), Magellanic Clouds, and the galactic center. This was one of the original aims of the program, which, if successful, could be extended with larger telescopes to other, more distant galaxies. A few of these have been resolved into outlying objects whose colors, distribution, order of luminosity, and possible nonstellar character suggest they probably are globular clusters (Bowen 1952, Baum 1955). Since they are among the highest-luminosity objects in the systems, their importance as distance indicators is obvious.

### Andromeda Nebula (M31)

For this spiral we use the results shown in Fig. 20, in which the scales of abscissae have been adjusted to make the maximum frequencies coincide. In photographic light (left), the correspondence gives $P-M_{Pt}=23.6$ mag. when the filled circles are used. If only the open circles were used, which means only outlying objects in M31 and high-latitude clusters in the Galaxy, then a lining up of maxima would give $P-M_{Pt}=24.1$ mag. This latter figure is undoubtedly preferable, because in M31 the observations are complete only to $P\sim16.5$ mag., while in the Galaxy the distances of the high-latitude clusters are best determined. In visual light (right), the maxima given by the filled circles yield $V-M_{Vt}=24.1$ mag., while the open-circle maxima could give either 24.1 or 24.6 mag., depending on how the sharper maximum for M31 is placed with respect to the broader one for the Galaxy.

Thus the foregoing comparison of apparent magnitudes of star clusters in M31 with absolute magnitudes of globular clusters in the Galaxy gives a difference ranging from 23.6 to 24.6 mag. If these objects are comparable in luminosity, then a reasonably conservative estimate of the M31 distance modulus is $(m-M)=24.1\pm0.5$ mag., based on the premise that $M_P=0.0$ for cluster-type (RR Lyrae) variables, and with no correction for galactic absorption in the direction of M31. Although in the past estimates of this correction have ranged up to 0.7 mag., there now seems to be little justification for them, because of the work of Code and Houck (1956). From three-color observations, they found that the colors of several of the brightest stars in an outer spiral arm, distant 75′ from the nucleus, are bluer than the galactic OB stars. On the other hand, there may be reason to revise the deduced modulus downward by 0.5 to 0.6 mag., because of recent work on the luminosities of cluster-type variables and of RR Lyrae (Pavlovskaya 1953, 1954; Arp 1958; Sandage and Eggen 1959; Baum *et al.* 1959); if so, then our result would become $(m-M)\sim23.5\pm0.5$ mag. However, since the luminosities of cluster-type variables in the high-latitude or halo-type globular clusters may be closer to $M_P=+0.2$ mag. than to an uncertain mean in the range of $M_P$ from about $+0.2$ to $+1.0$ mag., we conclude that the M31 distance modulus, as estimated from its probable globular clusters, falls within the range $(m-M)=23.5$ to 24.0 mag., with an uncertainty of 0.5 mag.

### Magellanic Clouds

Since only five probable globular clusters were observed in the Small Cloud and six (including the poor-data case of NGC 2121) in the Large Cloud, we cannot construct any significant luminosity distributions for estimation of separate distance moduli for the two systems. This procedure, however, has been used for 97 SMC clusters by de Vaucouleurs (1959), who employed small-scale photographic photometry, with Gascoigne and Kron's (1952) photoelectric cluster data as standards. Instead, we note that the mean, uncorrected apparent total magnitudes are $\langle P_t\rangle=11.6$ or 10.9, and $\langle V_t\rangle=11.0$ or 10.2 mag., for the Small or Large Cloud, respectively. Thus there is an average systematic difference of 0.7 or 0.8 mag. between these Cloud clusters, with those in the SMC being fainter. This difference has already been noted before (Kron 1956), and also seems to be confirmed by de Vaucouleurs' photographic results. Nevertheless, the photoelectric data are presently too few to place such a difference beyond question, so in this discussion we shall use the over-all means of $\langle P\rangle_t=11.2$ and $\langle V\rangle_t=10.6$ mag. We next review some of the data bearing on correction of these values for galactic and local Cloud absorption.

Until a few years ago, it was customary to use galactic absorption corrections of $A_{pg}=0.3$ or 0.4 mag., computed either (Shapley 1951, de Vaucouleurs 1954) from Harvard galaxy counts fitted to a cosecant law, or $A_{pg}=0.4$ to 0.6 mag. calculated (Thackeray and Wesselink 1953) from Oort's (1938) discussion of Hubble's (1934) data. Lack of more suitable photometric results left no alternative to this procedure, which was known to be unsatisfactory because of the considerable unevenness in the background galaxy population: poor

TABLE XXI. Comparison of results for galactic globular clusters.

| NGC | Apert. | $V_J$ | $V_{KM}$ | J-KM | $(P\text{-}V)_J$ | J-KM | NGC | Apert. | $V_J$ | $V_{KM}$ | J-KM | $(P\text{-}V)_J$ | J-KM |
|---|---|---|---|---|---|---|---|---|---|---|---|---|---|
| 2419 | 138″ | 11m05 | 10m97 | +0m08 | +0m57 | −0m07 | 6553 | 106″ | (9m37) | 9m44 | (−0m07) | +1m50 | +0m11 |
| 5904 | 250 | 6.67 | 6.45 | +0.22 | 0.66 | +0.03 | 6569 | 250 | (9.10) | 8.90 | (+0.20) | 1.24 | +0.13 |
| 6205 | 49 | ... | ... | ... | 0.56 | −0.01 | 6624 | 250 | 8.51 | 8.45 | +0.06 | 0.99 | −0.01 |
| 6205 | 82 | 7.85 | 8.08 | −0.13 | 0.58 | +0.01 | 6626 | 250 | 7.49 | 7.29 | +0.20 | 1.05 | +0.08 |
| 6205 | 250 | 6.54 | 6.46 | +0.08 | 0.60 | +0.03 | 6638 | 106 | 9.55 | 9.66 | −0.11 | 1.08 | +0.12 |
| 6218 | 250 | 7.95 | 7.70 | +0.25 | 0.79 | +0.02 | 6656 | 250 | 6.38 | 6.39 | −0.01 | 0.99 | +0.13 |
| 6254 | 250 | 7.51 | 7.39 | +0.12 | 0.88 | +0.09 | 6809 | 82 | 9.78 | 9.66 | +0.12 | 0.60 | +0.05 |
| 6273 | 250 | 7.33 | 7.26 | +0.07 | 0.98 | +0.08 | 6809 | 250 | 7.62 | 7.43 | +0.19 | 0.66 | +0.11 |
| 6293 | 250 | 8.77 | 8.65 | +0.12 | 0.92 | +0.06 | 7006 | 82 | 11.08 | 11.08 | 0.00 | 0.66 | +0.05 |
| 6304 | 250 | (8.77) | 8.82 | (−0.05) | 1.22 | 0.00 | 7006 | 250 | 10.63 | 10.76 | −0.13 | 0.77 | +0.16 |
| 6316 | 250 | (9.25) | 9.36 | (−0.11) | 1.10 | −0.07 | 7078 | 82 | 7.52 | 7.38 | +0.14 | 0.62 | +0.03 |
| 6341 | 250 | 6.97 | 6.92 | +0.05 | 0.53 | 0.00 | 7078 | 250 | 6.88 | 6.73 | +0.15 | 0.62 | +0.03 |
| 6402 | 106 | (8.86) | 9.09 | (−0.23) | 1.27 | +0.15 | 7089 | 82 | 7.63 | 7.74 | −0.11 | 0.62 | +0.05 |
| 6402 | 250 | (8.20) | 8.06 | (+0.14) | 1.20 | +0.08 | 7089 | 106 | 7.41 | 7.48 | −0.07 | 0.62 | +0.05 |
| 6517 | 49 | (11.80) | 11.75 | (+0.05) | (1.71) | (+0.04) | 7089 | 250 | 6.88 | 6.76 | +0.12 | 0.62 | +0.05 |
| 6522 | 49 | 9.99 | 9.62 | +0.37 | 1.08 | +0.06 | 7099 | 82 | 8.65 | 8.67 | −0.02 | 0.51 | +0.03 |
| 6522 | 250 | 8.75 | 8.71 | +0.04 | +1.04 | +0.02 | 7089 | 250 | 7.95 | 7.86 | +0.09 | +0.53 | +0.05 |

around the Small Cloud and rich around the Large (Shapley 1957). The question has more recently been considered by Feast, Thackeray and Wesselink (1958) and by Arp (1958), on the basis of photoelectric observations of colors of stars in the galactic foreground and in the Clouds, but they obtained somewhat different answers. The Pretoria workers found $A_{pg}=0.2$ to 0.8 mag., depending on assumptions made for the intrinsic colors of the stars observed. They concluded that "the early-type supergiants studied in the two clouds suffer a small but definite amount of absorption, partly due to galactic dust and partly due to dust within the Clouds themselves," but they refrained from quoting any average values. Arp, on the other hand, in his extensive program of southern hemisphere photometry at the Cape, found that some faint, early-type galactic stars yielded a reddening of $+0.01\pm0.01$ mag. in the SMC field, and $+0.04\pm0.02$ mag. in the LMC field. He obtained significant reddening, among the stars observed, for only two of six supergiants identified in the SMC. Thus he confirmed local absorption within the Clouds, but not through the Galaxy in the directions to them.

The foregoing review suggests that there may be little, if any, galactic absorption towards the Clouds, but that some objects within them are locally reddened and obscured. Of the Cloud globular clusters observed photoelectrically in this program, nearly all are outlying or fringe objects. Only one cluster, NGC 1835 at one end of the central bar in the LMC, is an interior object, but its color, $(P\text{-}V)=+0.61$ mag., seems normal. Thus these 11 clusters probably are negligibly locally reddened in the Clouds. We shall, therefore, apply no corrections for galactic or Cloud absorption to the mean apparent magnitudes, $\langle P\rangle_t=11.2$ and $\langle V\rangle_t=10.6$ mag., of these Cloud clusters. If they are of the same luminosity as those in the Galaxy, for which we found (Sec. X, Table XV) $\langle M\rangle_{Pt}=-7.7$ and $\langle M\rangle_{Vt}=-8.2$ mag., then the estimated distance moduli from the two colors are $(m-M)_P=18.9$ and $(m-M)_V=18.8$ mag. Since first-decimal accuracy can hardly be expected in these values, we prefer to round off the mean to 19, and to estimate its uncertainty at 0.5 mag.

## Galactic Center

We estimate this distance in two ways: (1) from the group of globular clusters seen in the general direction of the center, and (2) from the central bulge RR Lyrae variables studied by Baade (1951, 1953) in the field of NGC 6522.

1. With the omission of the two poor-data cases of NGC 6401 and 6453, there are 23 clusters, identified by the superscript letter b in Table VI, which appear to form a fairly compact group around the direction to the galactic center. For this group the mean corrected total apparent visual magnitude, obtained from the individual values of $V_{tc}$ in Table XIII, is $\langle V\rangle_{tc}=7.5$ or 7.1 mag., for color-excess alternates I or II, respectively. From Table XV and the discussion in Sec. X, it seems reasonable to assume for this center group that $\langle M\rangle_{Vt}=-8.2$ mag., which gives distance moduli of $m-M=15.7$ (I) or 15.3 (II) mag., and corresponding distances of 13.8 or 11.5 kpc. How uncertain these figures may be is difficult to determine. Their formal probable errors, if computed from those of $\langle V\rangle_{tc}$ and $\langle M\rangle_{Vt}$, are of the order of $\pm0.1$ to $\pm0.2$ mag., which are unrealistic because they do not include the more serious uncertainties in zero-point and sampling. Some indication of the latter may be obtained from the 10 clusters in the group for which individual corrected moduli are available (Table XVII). The corresponding mean distances (and ranges) are $\langle r\rangle=13.0$(7.2 to 20) or 10.9(6.3 to 16) kpc, for color excess alternates I or II, respectively. With such large ranges, the group means are probably not very trustworthy, although

their formal probable errors are only ±1.0 I and ±0.7 II kpc. We conclude from these results that this group of clusters indicates a galactic center distance of the order of 12.5 kpc, with an estimated uncertainty of 1.5 kpc.

2. From photographic photometry based on photoelectric standards (Stebbins, Whitford, and Johnson 1950), Baade (1951) found that the most frequent apparent magnitude of a large number of RR Lyrae variables in a field at $l=328°$, $b=-4°$ is $m_{pg}=17.5$ mag. From the fact that the frequency maximum is steep and of small spread, he concluded that these variables are located in the galactic nuclear bulge. Thus they could be used to estimate the distance to the galactic center, with certain assumptions. The first is that $M_{pg}=0.0$ for these variables, the second that their space absorption is the same as that of the globular cluster NGC 6522 in the same field. Using Stebbins and Whitford's unpublished photoelectric color measurements of this cluster. Baade derived an absorption of $A_{pg}=2.8$ mag. A few years later, following further work, Baade (1953) presented revised values of 17.3 and 2.75 mag., or $m-M=14.6$ mag. and a galactic center distance of 8.16 kpc, which has subsequently been widely used. Since the crucial point is how the absorption correction is obtained from the observed color of NGC 6522, we shall make an estimate based on our data for this cluster. From Table X the color excess for NGC 6522 is $\langle E\rangle_{(P-V)}=0.48$ mag., which multiplied by 4 gives $A_{pg}=1.92$ mag. Thus for $M_{pg}=0.0$ for RR Lyrae variables, the corrected distance modulus is $m-M=17.3-1.9=15.4$ mag., or a distance of 12.0 kpc. Again, it is difficult to assess the accuracy of this result by a formal probable error calculation, but if the color excess error is ±0.1 mag., then the modulus is uncertain by at least ±0.4 mag. and the distance by ±1.2 kpc.

Although these two ways of estimating the galactic center distance give results accordant to better than 1 kpc, such close agreement is undoubtedly accidental because of the several shaky assumptions and systematic errors involved. Nevertheless, our results lead to a galactic center distance nearly 50% greater than that in current use, unless the zero-point for luminosities of RR Lyrae variables is considerably revised. Thus, to obtain a galactic center distance as small as 8.2 kpc from our data and procedure, it would be necessary to use $M_P\sim+0.9$ or +0.8 mag. for RR Lyrae variables. This revision has already been suggested, as mentioned in the above discussion of the M31 modulus, and future work may establish it. If so, then the different photographic space-absorption correction for NGC 6522 found by Baade, 2.8 mag., and by us, 1.9 mag., will serve as an illustration of how difficult it is to get reliable color excesses and absorptions for obscured galactic center objects, especially when they are of composite character and of uncertain intrinsic color (Whitford 1960).

## ADDENDUM

During preparation of this paper for publication, some new photoelectric photometry of star clusters was reported: by Johnson (1959) for 27 galactic globular clusters, and by Hiltner (1960), for 46 star clusters in M31 and M33—23 in each system. In both cases the observations were made on the $U$, $B$, $V$ system. After conversion of their results to our $P$, $V$ system according to the relationships given in Sec. III, we have the comparison for objects in common as shown in Tables XXI and XXII.

In Table XXI the columns headed $V_J$ and $(P\text{-}V)_J$ contain magnitudes and colors by Johnson reduced to our $P$, $V$ system; those in parentheses represent conversions in the color range where the transfer formulae are not well determined. The column headed $V_{KM}$ gives our magnitudes for the apertures used by Johnson, listed in the second column. For this purpose we used the same luminosity distribution curves that gave the total magnitudes and diameters in Table IV. The two columns of differences, in the sense J-KM, yield average systematic differences and AD's, respectively, of +0.06 and 0.10 mag. in the magnitudes, and +0.05 and 0.04 mag. in the colors. The largest difference in the integrated magnitudes is +0.37 mag. for NGC 6522 measured with the 49″ aperture; however, this difference is

TABLE XXII. Comparison of results for extragalactic star clusters.

| Cluster | $V_H$ | H-KM | $(P\text{-}V)_H$ | H-KM | Cluster | $V_H$ | H-KM | $(P\text{-}V)_H$ | H-KM |
|---|---|---|---|---|---|---|---|---|---|
| | | | | M31 | | | | | |
| H 5 | 16m27 | −0m10 | +0m31 | +0m20 | H 94 | 15m88 | −0m02 | +0m89 | +0m04 |
| 26 | 15.54 | −0.03 | 0.89 | +0.18 | 99 | 15.74 | +0.08 | 0.69 | +0.04 |
| 27 | 15.68 | 0.00 | 0.76 | +0.05 | 106 | 15.17 | +0.12 | 0.75 | −0.06 |
| 42 | 14.33 | +0.01 | 1.08 | +0.11 | 112 | 15.43 | −0.04 | 0.66 | +0.03 |
| 44 | 15.10 | +0.14 | 0.88 | +0.55 | 115 | 15.57 | −0.01 | 0.93 | +0.11 |
| 55 | 15.60 | −0.04 | 0.90 | +0.13 | 116 | 15.46 | +0.05 | 0.91 | +0.05 |
| 57 | 16.05 | +0.08 | 0.90 | +0.05 | B 231 | 15.30 | +0.04 | 0.82 | +0.07 |
| 64 | 14.77 | +0.04 | 0.84 | +0.03 | 258 | 15.80 | −0.02 | 1.17 | +0.15 |
| 73 | 15.50 | +0.09 | 0.90 | +0.10 | 282 | 14.25 | +0.04 | +0.88 | +0.07 |
| 76 | 15.68 | +0.03 | +0.56 | +0.06 | | | | | |
| | | | | M33 | | | | | |
| Ha=*e* | 16.21 | +0.02 | +0.70 | +0.33 | Hb=*d* | 16.67 | +0.13 | +0.11 | +0.09 |

only +0.04 mag. for the 250″ aperture. All the other integrated magnitude differences fall in the satisfactorily small range from −0.23 to +0.25 mag. On the other hand, the differences in integrated color range from −0.07 to +0.16 mag., which, although not so good, may serve as an indication of the difficulties, and hence of the lack of high precision, of integrated-light and large-aperture photometry in rich star fields of nonuniform density.

In the discussion of his data on the basis of the same intrinsic color, $(B\text{-}V)=+0.60$ or $(P\text{-}V)=+0.52$ mag., for all globular star clusters, Johnson found for NGC 6522 a maximum color excess of $E_{(B-V)}=+0.53$ mag. and a total blue absorption of $A_B=+2.1$ mag.; this value agrees satisfactorily with ours of $A_{pg}=+1.9$ mag., as deduced in Sec. XIII. Johnson also compared his estimate with Baade's (1958), but the comparison was made with the misprinted value of +2.15 on page 329, instead of with the correct number +2.75 on page 61 of the cited reference.

In Table XXII the columns headed $V_H$ and $(P\text{-}V)_H$ contain magnitudes and colors determined by Hiltner and reduced to our $P$, $V$ system. For M31 the average systematic differences and AD's are, respectively, +0.02 and 0.05 mag. in the magnitudes, and +0.08 and 0.08 mag. in the colors. The magnitudes thus agree very well, but not the colors, which seem to have an appreciable systematic error. If 0.08 mag. is subtracted from the differences, the AD becomes 0.05 mag., which would be satisfactory. Since we cannot account for such a systematic difference, however, we do not wish to consider it as a correction to either series of observation; instead, we should be inclined to take averages from the two sets. For M33 only two clusters were observed in common, and the difference of +0.33 mag. between the measurements of color for Ha=Hiltner's *e*, is especially large. Nevertheless, Hiltner's much more extensive material for M33 leaves little doubt that its star clusters are systematically bluer and fainter than most of those observed in M31, as we had concluded previously (Secs. VII and XI) from fewer data. This result thus emphasizes again that there are significantly different types of star clusters in different types of of galaxies.

Lastly, Sandage and Wallerstein (1960) have published their detailed study of NGC 6356, a cluster in Morgan's (1959) spectroscopic group having moderately strong metallic lines. From three-color photoelectric observations and from spectrograms of 12 early-type stars in the same field, they found color excesses ranging from $E_{(B-V)}=0.0$ to 0.9 mag. Using these, they adopted a value of $E_{(B-V)}=0.5\pm0.1$ mag. for the cluster. Their estimate may be compared with our alternate ones of $E_{(P-V)}=0.28$ (I) or 0.48 (II); the agreement seems about as good as may be expected, considering the different assumptions involved. For RR Lyrae $M_V=0.0$ they also derived an apparent modulus of $(m-M)_V=17.7$, compared to our mean of 16.8 (Table XIII). Since the latter modulus depends upon Dr. Helen S. Hogg's (1953) preliminary photographic measurements of brightest stars in NGC 6356, the photoelectric data indicate a correction of +0.9 mag. to the photographic. Accordingly, our corrected moduli and distances (Table XVII) for this cluster should be revised to: $(m-M)_c=17.0$ (I) or 16.2 (II), and $r$(kpc)=25 (I) or 17 (II), compared to Sandage and Wallerstein's estimates of $(m-M)_c=16.2$ and $r$(kpc)=17.4. On the *ad hoc* assumption that NGC 6356 is close to the galactic nucleus, they suggested that their values obtained from RR Lyrae $M_V=+0.9$, $(m-M)_c=15.3$ and $r$(kpc) = 11.5, are to be preferred.

ACKNOWLEDGMENT

We are indebted to S. C. B. Gascoigne and to Joel Stebbins for permission to make use of the photometric and colorimetric data of the open clusters. These data originated in a joint project undertaken by Gascoigne and Kron at the Lick Observatory in 1956; much of the observing, however, was done by Stebbins and Kron.

REFERENCES

Arp, H. C. 1955, *Astron. J.* **60**, 317.
——. 1958, *ibid.* **63**, 118.
——. 1958, *Handbuch der Physik* (Springer-Verlag, Berlin), Vol. 51, p. 75.
Baade, W. 1944, *Astrophys. J.* **100**, 137.
——. W. 1951, *Publs. Univ. Michigan Obs.* **10**, 16.
——. 1953, *Symposium on Astrophysics* (University of Michigan, Ann Arbor, Michigan), p. 25.
——. 1958, *Le Probleme de Populations Stellaires* (Pontificiae Academiae Scientiarum Scripta Varia, Vatican City), Vol. 16.
Baade, W. and Hubble, E. 1939, *Publs. Astron. Soc. Pacific* **51**, 40.
Baade, W. and Mayall, N. U. 1950, *Problems of Cosmical Aerodynamics* (Central Air Documents Office, Dayton, Ohio), p. 166.
Baum, W. A. 1955, *Publs. Astron. Soc. Pacific* **67**, 328.
——. 1959, *Astrophys. J.* **130**, 749.
Becker, W. 1938, *Z. Astrophys.* **15**, 225.
Bowen, I. S. 1952, *Carnegie Inst. Washington Yearbook* **51**, 19.
——. 1956, *ibid.* **55**, 48.
Christie, W. H. 1940, *Astrophys. J.* **91**, 8.
Code, A. D. and Houck, T. E. *Astron. J.* **61**, 173.
de Vaucouleurs, G. 1954, *Australian J. Sci. Suppl.* **17**, 7.
——. 1959, *Publs. Astron. Soc. Pacific* **71**, 202.
Eggen, O. J. 1951, *Astrophys. J.* **114**, 141.
——. 1955, *Astron. J.* **60**, 65.
Feast, M. W., Thackeray, A. D., and Wesselink, A. J. 1958, *Observatory* **78**, 156.
Gascoigne, S. C. B. and Kron, G. E. 1952, *Publs. Astron. Soc. Pacific* **64**, 196.
Hiltner, W. A. 1960, *Astrophys. J.* **131**, 163.
Hogg, H. S. 1953, *David Dunlap Obs.*, Communication No. **34**.
——. 1959, *Handbuch der Physik* (Springer-Verlag, Berlin), Vol. 53, p. 166.
Holmberg, E. 1950, *Lund Obs. Meddelanden*, Ser. II, No. **170**.
Hubble, E. 1932, *Astrophys. J.* **76**, 44.
——. 1934, *ibid.* **79**, 8.
Johnson, H. L. 1952, *Astrophys. J.* **116**, 272.
——. 1953, *ibid.* **117**, 313.
Johnson, H. L. and Morgan, W. W. 1951, *Astrophys. J.* **114**, 522.
Keenan, P. C. 1940, *Astrophys. J.* **91**, 113.
Kron, G. E. 1956, *ibid.* **68**, 230.
——. 1958, *ibid.* **70**, 285.
Kron, G. E., Greeby, R. W. and Willson, J. R. 1956, *Publs. Astron. Soc. Pacific* **68**, 544.

Kron, G. E. and Smith, J. L. 1951, *Astrophys. J.* **113**, 324.
Kron, G. E., White, H. S. and Gascoigne, S. C. B. 1953, *Astrophys. J.* **118**, 502.
Mayall, N. U. 1946, *Astrophys. J.* **104**, 290.
Mayall, N. U. and Eggen, O. J. 1953, *Publs. Astron. Soc. Pacific* **65**, 24.
Morgan, W. W. 1956, *Publs. Astron. Soc. Pacific* **68**, 509.
——. 1959, *Astron. J.* **64**, 432.
Morgan, W. W., Harris, D. L., and Johnson, H. L. 1953, *Astrophys. J.* **118**, 92.
Mowbray, A. G. 1946, *Astrophys. J.* **104**, 47.
Nassau, J. J. and Mac Rae, D. A. 1955, *Astrophys. J.* **121**, 32.
Nassau, J. J. and Seyfert, C. K. 1945, *Astrophys. J.* **102**, 377.
Oort, J. 1938, *Bull. Astron. Inst. Neth.* **8**, 233.
Pavlovskaya, P. 1953, *Variable Stars* (U.S.S.R.) **9**, 233; 1954, **9**, 349.
Sandage, A. R. 1958, *Astrophys. J.* **127**, 513.
Sandage, A. R. and Eggen, O. J. 1959, *Monthly Notices Roy. Astron. Soc.* **119**, 255.
Sandage, A. R. and Wallerstein, G. 1960, *Astrophys. J.* **131**, 598.
Sawyer, H. B. 1947, *David Dunlap Obs. Publ.* **1**, 383.
Seares, F. H. and Joyner, M. C. 1945, *Astrophys. J.* **101**, 15.
Sersic, J. L. 1958, *Observatory* **78**, 24.
Shane, C. D. and Wirtanen, C. A. 1954, *Astron. J.* **59**, 285.
Shapley, H. 1951, *Publs. Univ. Michigan Obs.* **10**, 79.
——. 1953, *Proc. Natl. Acad. Sci. U. S.* **39**, 358.
——. 1957, *The Inner Metagalaxy* (Yale University Press, New Haven, Connecticut) pp. 97–100.
Shapley, H. and Sayer, A. R. 1935, *Proc. Natl. Acad. Sci. U. S.* **21**, 593.
Stebbins, J. 1933, *Proc. Natl. Acad. Sci. U. S.* **19**, 222.
Stebbins, J. and Whitford, A. E. 1936, *Astrophys. J.* **84**, 132.
——. 1937, *ibid.* **86**, 247.
——. 1945, *ibid.* **102**, 318.
Stebbins, J., Whitford, A. E. and Johnson, H. L. 1950, *Astrophys. J.* **112**, 469.
Thackeray, A. D. and Wesselink, A. J. 1953, *Nature* **171**, 693.
Whitford, A. E. 1960, *Publs. Astron. Soc. Pacific* (to be published).

# Effect of Precession and Nutation on the Orbital Elements of a Close Earth Satellite

YOSHIHIDE KOZAI
*Smithsonian Astrophysical Observatory and Harvard College Observatory, Cambridge, Massachusetts*
(Received August 26, 1960)

Perturbations due to the motion of the equatorial plane of the earth are derived for the orbital elements of a close earth satellite. It is suggested that, for precise studies of satellite motion, a system be adopted in which the inclination and the argument of perigee are referred to the equator of date, and the longitude of the node is measured from a fixed point along a fixed plane and then along the equator of date.

## INTRODUCTION

IN a previous paper (Kozai 1959b) we studied the motion of an artificial satellite by assuming that the equator of the earth is fixed to an inertial system of reference.

However, the earth is moving around the sun, and because of precession and nutation the equatorial plane is not fixed in space. The effect of the orbital motion of the earth can be taken into account as direct perturbations due to the sun and the moon (Kozai 1959a). The effects of precession and nutation, which are studied in the present paper, may be regarded as indirect luni-solar perturbations.

## DISTURBING FUNCTION

The declination $\delta$ appearing in the expression for the gravitational potential of the earth,

$$U=\frac{GM}{r}\left[1+\frac{A_2}{r^2}(\tfrac{1}{3}-\sin^2\delta)+\cdots\right], \tag{1}$$

is measured from the instantaneous equator of the earth. However, the equator of the earth undergoes precessional and nutational motions in inertial space. Therefore, in solving the satellite equations of motion in inertial space, several time-dependent terms are introduced in the expression for the earth's potential. It is the purpose of this paper to examine the dynamical terms introduced by these time-dependent terms.

The equator at a certain initial epoch is adopted as the fixed plane. The argument of latitude, the argument of perigee, the longitude of the ascending node, and the inclination with respect to this fixed plane are denoted by $L$, $\psi$, $N$, and $J$, and those with respect to the equator of date are denoted respectively by $u$, $\omega$, $\Omega$, and $i$ (Fig. 1). The longitudes of the node $N$ and $\Omega$ are measured from the fixed equinox $E$ at the initial epoch. In Fig. 1, two angles $\theta$ and $N_0$ represent the inclination and the longitude of the ascending node of the equator of date referred to the fixed plane.

The mutual inclination of the two equators $\theta$ is assumed to be a very small angle, so that its square $\theta^2$ can be neglected in the following discussion. Then, between the two sets of elements the following relations hold:

$$\begin{aligned} J-i&=\theta\cos(N-N_0),\\ N-\Omega&=-\theta\cot J\sin(N-N_0),\\ \psi-\omega&=\theta\csc J\sin(N-N_0). \end{aligned} \tag{2}$$

The declination $\delta$ is expressed by the elements referred to the fixed plane as follows:

$$\sin\delta=\sin L[\sin J-\theta\cos J\cos(N-N_0)]-\theta\cos L\sin(N-N_0).$$

Introducing this relation into Eq. (1) leads to a potential function which is not symmetric about the equator of the fixed coordinate system.

In relation to the short-periodic perturbations due to the oblateness of the earth, the effect of the motion of the equator is very small and can be neglected. The most important effect comes from the secular part of the disturbing function. This is given by

$$R=\frac{A_2}{a^2}\frac{GM}{a}(1-e^2)^{-\frac{3}{2}}[(\tfrac{1}{3}-\tfrac{1}{2}\sin^2 J)+\tfrac{1}{2}\theta\sin 2J\cos(N-N_0)]. \tag{3}$$

The terms of the first part of $R$ are of the same form as those given for the secular part in the previous paper (Kozai 1959b) except for a difference in the definitions of the inclination. The term in the second part of $R$ arises from the fact that the axis of symmetry of the potential field deviates from the pole of the fixed coordinate system by the angle $\theta$.

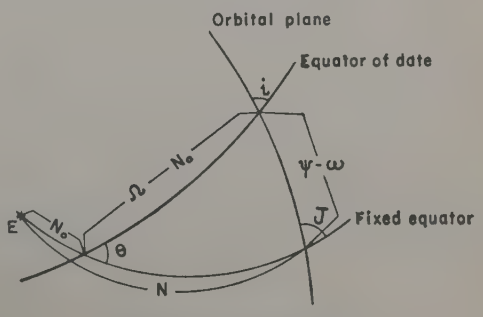


FIG. 1. Equators and orbit.

PERTURBATIONS

Equations expressing the variations of the orbital elements with the disturbing function $R$ show that the semi-major axis $a$ and the eccentricity $e$ are constant and, of course, they have the same values in the two systems of coordinates.

The variations of the other four elements produced by the term proportional to $\theta$ in $R$ are then given by the differential equations

$$\begin{aligned}
&\frac{d\cdot\delta J}{dt}=\frac{A_2}{p^2}n\theta\cos J\sin(N-N_0),\\
&\frac{d\cdot\delta N}{dt}=\frac{A_2}{p^2}n\left[\theta\frac{\cos 2J}{\sin J}\cos(N-N_0)+\sin J\cdot\delta J\right],\\
&\frac{d\cdot\delta\psi}{dt}=\frac{A_2}{p^2}n\left[\theta\left(\frac{\cos J\cos 2J}{\sin J}-\tfrac{3}{2}\sin 2J\right)\cos(N-N_0)\right.\\
&\qquad\qquad\left.+5\sin J\cos J\cdot\delta J\right],\\
&\frac{d\cdot\delta M}{dt}=\frac{3}{2}\frac{A_2}{p^2}n(1-e^2)^{\frac{1}{2}}\sin 2J[\theta\cos(N-N_0)-\delta J],
\end{aligned}\tag{4}$$

where $\delta J$ in the right-hand sides is derived from the first of these equations, and

$$p=a(1-e^2).$$

Now let us denote obliquities of the fixed and moving equators to the ecliptic by $\epsilon$ and $\epsilon'$, respectively, and the angular distance between the two equators measured along the ecliptic by $\sigma$. The ecliptic may be assumed to be fixed over several years. As angles $\theta$, $\sigma$, and $\epsilon-\epsilon'$ are very small, the following relations hold:

$$\begin{aligned}
&\theta\sin N_0=\sigma\sin\epsilon',\\
&\theta\cos N_0=\epsilon'-\epsilon.
\end{aligned}\tag{5}$$

The principal terms whose coefficients are larger than one tenth of a second of arc in the expressions of $\sigma\sin\epsilon'$ and $\epsilon-\epsilon'$ are

$$\begin{aligned}
&\sigma\sin\epsilon'=6''.86\sin\Omega_{\leftmoon}+0''.51\sin 2L_\odot+20''.04T+A,\\
&\epsilon'-\epsilon=9''.21\cos\Omega_{\leftmoon}+0''.55\cos 2L_\odot+B,
\end{aligned}\tag{6}$$

where $\Omega_{\leftmoon}$ and $L_\odot$ are, respectively, the longitude of the ascending node of the lunar orbit referred to the ecliptic, and the mean longitude of the sun. In the expressions (6) $T$ denotes years from the initial epoch, and $A$ and $B$ are additional constant terms chosen so that the two quantities $\sigma\sin\epsilon'$ and $\epsilon'-\epsilon$ may vanish at the initial epoch.

Then $\theta\cos(N-N_0)$ and $\theta\sin(N-N_0)$, appearing in the right-hand sides of the differential equations (4), have the following form:

$$\begin{aligned}
\theta\cos(N-N_0)=&\,8''.0\cos(N-\Omega_{\leftmoon})+1''.2\cos(N+\Omega_{\leftmoon})\\
&+0''.5\cos(N-2L_\odot)+20''.04T\sin N\\
&+C\cos(N-\Omega_0),\\
\theta\sin(N-N_0)=&\,8''.0\sin(N-\Omega_{\leftmoon})+1''.2\sin(N+\Omega_{\leftmoon})\\
&+0''.5\sin(N-2L_\odot)-20''.04T\cos N\\
&+C\sin(N-\Omega_0),
\end{aligned}\tag{7}$$

where $C$ and $\Omega_0$ are constants related to $A$ and $B$ by

$$\begin{aligned}
A&=C\sin\Omega_0,\\
B&=C\cos\Omega_0.
\end{aligned}$$

On the assumption that $N$ is a known function of time and that $\dot N=-A_2n\cos J/p^2$, the expression of $\delta J$ is derived by the usual method of approximation as follows:

$$\begin{aligned}
\delta J=&\,8''.0\frac{\dot N}{\dot N-\dot\Omega_{\leftmoon}}\cos(N-\Omega_{\leftmoon})+1''.2\frac{\dot N}{\dot N+\dot\Omega_{\leftmoon}}\cos(N+\Omega_{\leftmoon})\\
&+0''.5\frac{\dot N}{\dot N-2n_\odot}\cos(N-2L_\odot)+20''.04T\sin N\\
&+C\cos(N-\Omega_0)+\frac{3''.14}{\dot N}\cos N,
\end{aligned}\tag{8}$$

where $\dot N$, $\dot\Omega_{\leftmoon}$, and $n_\odot$ are, respectively, the daily mean motions of $N$, $\Omega_{\leftmoon}$, and $L_\odot$ expressed in degrees, and

$$\begin{aligned}
\dot\Omega_{\leftmoon}&=-0^\circ.053,\\
n_\odot&=0^\circ.986.
\end{aligned}$$

For a typical close earth satellite whose inclination is not near 90°, all terms except for $\cos(N-2L_0)$ have nearly the same period, and both $\dot N/(\dot N-\dot\Omega_{\leftmoon})$ and $\dot N/(\dot N+\dot\Omega_{\leftmoon})$ are near unity.

From Eqs. (8) and (2), inequalities appearing in the inclination to the equator of date are derived as follows:

$$\begin{aligned}
\delta i=&\,8''.0\frac{\dot\Omega_{\leftmoon}}{\dot N-\dot\Omega_{\leftmoon}}\cos(N-\Omega_{\leftmoon})-1''.2\frac{\dot\Omega_{\leftmoon}}{\dot N+\dot\Omega_{\leftmoon}}\cos(N+\Omega_{\leftmoon})\\
&+1''.0\frac{n_\odot}{\dot N-2n_\odot}\cos(N-2L_\odot)+\frac{3''.14}{\dot N}\cos N.
\end{aligned}\tag{9}$$

In this expression (9), terms having large amplitudes in (8) have disappeared. And, if $\dot N=-3^\circ$, the largest term in (9) is the last one, with an amplitude of 1″.

If the mean value of $i$ is adopted as the inclination appearing in the expression of $\dot N$, $\psi$, and $n$ as in the previous paper, $\delta J$ in the right-hand sides of (4) can be written as $\delta i+\theta\cos(N-N_0)$, since the relation

between $J$ and $i_0$ is

$$J=i_0+\delta i+\theta\cos(N-N_0),$$

where $i_0$ is the mean value of $i$.

Then $\delta N$, $\delta\psi$, and $\delta M$ are easily derived from Eqs. (4) as follows:

$$\begin{aligned}\delta N&=-F\cot i-G\tan i,\\ \delta\psi&=F\csc i+5G\sin i,\\ \delta M&=3G(1-e^2)^{\frac{1}{2}}\sin i,\end{aligned}\tag{10}$$

where

$$\begin{aligned}F=&8''.0\frac{\dot N}{\dot N-\dot\Omega_\mathbb{C}}\sin(N-\Omega_\mathbb{C})+1''.2\frac{\dot N}{\dot N+\dot\Omega_\mathbb{C}}\sin(N+\Omega_\mathbb{C})\\ &+0''.5\frac{\dot N}{\dot N-2n_\odot}\sin(N-2L_\odot)-20''.04T\cos N\\ &+\frac{3''.14}{\dot N}\sin N+C\sin(N-\Omega_0),\end{aligned}\tag{11}$$

$$\begin{aligned}G=&8''.0\frac{\dot N\dot\Omega_\mathbb{C}}{(\dot N-\dot\Omega_\mathbb{C})^2}\sin(N-\Omega_\mathbb{C})-1''.2\frac{\dot N\dot\Omega_\mathbb{C}}{(\dot N+\dot\Omega_\mathbb{C})^2}\sin(N+\Omega_\mathbb{C})\\ &+1''.0\frac{\dot N n_\odot}{(\dot N-2n_\odot)^2}\sin(N-2L_\odot)+\frac{3''.14}{\dot N}\sin N.\end{aligned}$$

By combining Eqs. (2) and (10) expressions of inequalities in the elements referred to the moving equator are derived as

$$\begin{aligned}\delta\Omega&=-H\cot i-G\tan i,\\ \delta\omega&=H\csc i+5G\sin i,\end{aligned}\tag{12}$$

where

$$\begin{aligned}H=&8''.0\frac{\dot\Omega_\mathbb{C}}{\dot N-\dot\Omega_\mathbb{C}}\sin(N-\Omega_\mathbb{C})-1''.2\frac{\Omega_\mathbb{C}}{\dot N+\Omega_\mathbb{C}}\sin(N+\Omega_\mathbb{C})\\ &+1''.0\frac{n_\odot}{\dot N-2n_\odot}\sin(N-2L_\odot)+\frac{3''.14}{\dot N}\sin N.\end{aligned}$$

The amplitudes in the expressions of $\delta\Omega$ and $\delta\omega$ are clearly much smaller than those in $\delta N$ and $\delta\psi$ for a typical close satellite.

## DISCUSSION

As an example, numerical expressions are given here for a case in which $\dot N=-3°.0$ and $i=45°$.

$$\begin{aligned}\delta i=&0''.1\cos(N-\Omega_\mathbb{C})-0''.2\cos(N-2L_\odot)-1''.0\cos N,\\ \delta\Omega=&-0''.2\sin(N-\Omega_\mathbb{C})+0''.3\sin(N-2L_\odot)+2''.0\sin N,\\ \delta\omega=&0''.5\sin(N-\Omega_\mathbb{C})-0''.6\sin(N-2L_\odot)-4''.9\sin N,\\ \delta M=&(1-e^2)^{\frac{1}{2}}[0''.2\sin(N-\Omega_\mathbb{C})-0''.2\sin(N-2L_0)\\ &-2''.1\sin N].\end{aligned}$$

The coefficients in these expressions are very small, but not negligible for some satellites. Furthermore, if a fixed equator is adopted as the reference plane, inequalities appearing in the orbital elements become much larger.

The difference between the perturbations appearing in the two coordinate systems is, in essence, the following. In the fixed coordinate system, the precession and nutation lead to an asymmetric potential field and produce secular perturbations which typically amount to something more than 20 seconds of arc during the course of a year. By a shift to a coordinate system attached to the moving equator of date, the major perturbations are eliminated and the typical values are reduced to several seconds of arc.

The writer therefore suggests that, for the analysis of a close earth satellite, the inclination and the argument of perigee can most conveniently be referred to the equator of date, and the longitude of the node be measured from a fixed point. Explicitly, the node should be measured from the equinox of an initial epoch along the fixed equator to the ascending node of the moving equator, and then along this equator. Note the assumption that the initial epoch, to which the fixed equator is referred, is not far from the date.

This system of coordinates has already been adopted by G. Veis and C. Moore of the Smithsonian Astrophysical Observatory in their orbital improvement program for artificial satellites, and the orbital elements given in the Smithsonian Special Reports are referred to this system.

## REFERENCES

Kozai, Y. 1959a, *Smithsonian Astrophys. Obs. Special Rept.* No. 22, 7–10.

——. 1959b, *Astron. J.* **64**, 367–377.

# On the Motion of a Satellite in the Vicinity of the Critical Inclination

BORIS GARFINKEL
*Ballistic Research Laboratories, Aberdeen Proving Ground, Maryland*
(Received September 20, 1960)

The paper treats the motion of a particle in the potential field

$$V=-1/r+J_2P_2(\sin\theta)/r^3+J_4P_4(\sin\theta)/r^5,$$

with $J_2$ and $J_4$ assumed to be small quantities of the first and the second orders, respectively, and with the value of the orbital inclination $i$ lying in a neighborhood of $\tan^{-1}2\sim63^\circ.4$. The method of attack is based on the removal of the short-periodic terms from the Hamiltonian by the von Zeipel method, followed by a Taylor series expansion of the energy integral up to quantities of the second order. As far as the Delaunay variables $G'$, $g'$ are concerned, the motion then becomes formally identical with that of a simple pendulum, and the solution is reduced to elliptic functions. In this form all the essential features of the motion are clearly revealed.

## 1. INTRODUCTION

THE published solutions (Brouwer 1959, Garfinkel 1959, Kozai 1959) of the satellite problem generally contain long-periodic terms with a critical divisor $5\cos^2i-1$, where $i$ is the "mean" orbital inclination. Such a solution therefore fails to represent the motion with sufficient accuracy in some neighborhood

$$|i-i_*|\leq w, \quad i_*=\tan^{-1}2, \tag{1}$$

of the singularity at $i=i_*$. A nonsingular solution, as given by the author in his 1959 lectures at the Summer Institute in Dynamical Astronomy, is reproduced here with a few simplifications. The method involves the removal of the short-periodic terms from the Hamiltonian, followed by a Taylor series expansion of the energy integral.

Let the problem be defined by the potential

$$V=-1/r+J_2P_2(\sin\theta)/r^3+J_4P_4(\sin\theta)/r^5, \tag{2}$$

with the constants $J_2$ and $J_4$ satisfying the relations $0\leq J_2\ll1$, $J_4=O(J_2^2)$, and with the orbital inclination $i$ lying in a sufficiently small neighborhood (1).

## 2. THE NEW HAMILTONIAN

A canonical transformation based on the von Zeipel (1916) method is used to remove the short-periodic terms from the Hamiltonian. The new Hamiltonian may be readily obtained from the author's earlier paper (1959) with two modifications:

(1) Since the long-periodic terms in that paper had been removed along with those of short period, the former must now be restored. This is achieved by setting $S_1^*=0$ on page 357.

(2) Since the long-periodic terms have been shown to be independent of the parameters $c_1$, $c_2$, $c_3$ of the intermediary orbit that was used there as a first approximation, these parameters may now be set equal to zero. Useful checks are then provided by a comparison with the new Hamiltonian $F'$ of Brouwer (1959) who had used as a first approximation the Kepler ellipse, with $c_1=c_2=c_3=0$.

If $c_i=0$, there follows $g_{21}=0$, $\mu=\lambda_1=\lambda_2=1$; furthermore, if $S_1^*=0$, the new Hamiltonian $F'(L',G',g')$ can be written

$$F'=\bar{F}'+F^{*\prime}=\tfrac{1}{2}L^{-2}+\bar{R}_1+\bar{R}_2+\bar{\Phi}+R_2^*+\Phi^*, \tag{3}$$

where $R_1$ and $R_2$ are the portions of the disturbing function of orders $J_2$ and $J_4$, respectively, $\Phi$ is of order $J_2^2$, and the bar and the star denote the secular and the long-period parts of the variable, respectively. It is understood that the Delaunay variables $L$, $G$, $g$ occurring as the arguments in the right-hand member of (3) are to be replaced by the new variables $L'$, $G'$, $g'$. The quantities $\bar{R}_1$, $\bar{R}_2$, $\bar{\Phi}$, $R_2^*$, $\Phi^*$ are given respectively by the equations (28), (91), (68), (95), (80) of the author's earlier paper (1959), with $c_i=0$, $2k=J_2$, $k'=J_4$:

$$\bar{R}_1=(1/4)J_2nG^{-3}(3y^2-1), \tag{4}$$

$$\bar{R}_2=(-3/128)J_4nG^{-7}(5-3x^2)(3-30y^2+35y^4), \tag{5}$$

$$\bar{\Phi}=(3/128)J_2^2nG^{-7}[-5+4x+5x^2+y^2(10-24x-18x^2)+y^4(35+36x+5x^2)], \tag{6}$$

$$R_2^*=(15/64)J_4nG^{-7}e^2\sin^2i(1-7y^2)\cos2g, \tag{7}$$

$$\Phi^*=(3/64)J_2^2nG^{-7}e^2\sin^2i(1-15y^2)\cos2g, \tag{8}$$

with the abbreviations

$$x=(1-e^2)^{\frac{1}{2}}=G/L, \quad y=\cos i=H/G, \quad n=L^{-3}. \tag{9}$$

The expressions (3)–(8) agree, as they should, with Brouwer's (1959), who removed $l'$ from the Hamiltonian in the first of his two von Zeipel transformations. Since $l'$ is absent from $F'$, we have $L'=\text{const}$, so that our problem is reduced to one degree of freedom, with $G'$, $g'$ appearing as conjugate variables.

The quantity $F^{*\prime}$ and the derivatives of $\bar{R}_1$ with respect to $G$ will be needed in the next section. By the addition of (7) and (8),

$$F^{*\prime}=R_2^*+\Phi^*=-\tfrac{3}{32}J_2^2nG^{-7}e^2\times\sin^2i\cos2g[b-2b_0(5y^2-1)], \tag{10}$$

with the constants $b$ and $b_0$ defined by

$$b=1+J_4/J_2^2, \qquad b_0=1-7b/4, \tag{11}$$

where $b$ is the Vinti index (Garfinkel 1959, Vinti 1959). From (1) it follows that the quantity $\Delta$ defined by $\Delta=|5\cos^2 i-1|$ satisfies the inequality $\Delta\lesssim 4w$; accordingly $\Delta$ is a small quantity, say of $O(J_2^k)$, with the number $k$ to be specified later. Then $\sin^2 i=\frac{4}{5}+O(J_2^k)$, and (10) can be written

$$F^{*\prime}=-(3/40)J_2^2 bne^2G^{-7}\cos 2g+O(J_2^{2+k}). \tag{12}$$

Next, by the differentiation of (4) with respect to $G$,

$$\bar{R}_{1G}=-\tfrac{3}{4}J_2 nG^{-4}(5y^2-1)=O(J_2^{1+k}), \qquad \bar{R}_{1GG}=\tfrac{3}{2}J_2 nG^{-5}+O(J_2^{1+k}). \tag{13}$$

## 3. THE ENERGY INTEGRAL

Since $t$ is absent from $F'$,

$$F'=\text{const} \tag{14}$$

is the integral of energy. Let $\delta$ be defined by

$$\delta=G'-G'', \tag{15}$$

where $G''$ is a constant to be chosen later, and let $F'$ be expanded about $G''$ in a Taylor series in powers of $\delta$. In view of (3), Eq. (14) becomes

$$\bar{F}'_{G''}\delta+\tfrac{1}{2}\bar{F}'_{G''G''}\delta^2+F^{*\prime}+\cdots+c=0, \tag{16}$$

with the constant term $\bar{F}'(G'')$ absorbed in the constant $c$. The dominant terms in (16) are given by

$$\bar{F}'_{G''}=\bar{R}_{1G''}+\cdots\equiv B+\cdots, \qquad \bar{F}'_{G''G''}=\bar{R}_{1G''G''}+\cdots\equiv B'+\cdots, \qquad F^{*\prime}(G'')=A\cos 2g', \tag{17}$$

where $A$, $B$, $B'$ are constants corresponding to the dominant terms in (12) and (13):

$$A=-(3/40)J_2^2 bne^2G^{-7}, \qquad B=-(3/4)J_2 nG^{-4}(5\cos^2 i-1)=O(J_2^{1+k}), \qquad B'=(3/2)J_2 nG^{-5}>0. \tag{18}$$

It is understood here that $L$, $G$ are to be replaced by $L'$, $G''$ wherever they occur in (18) and (9). Now (16) can be approximated by

$$A\cos 2g'+B\delta+\tfrac{1}{2}B'\delta^2+c=0, \tag{19}$$

Note that if $i=i_*$, then $B=0$ from (18), and $\delta=O|A/B'|^{\frac{1}{2}}=O(J_2^{\frac{1}{2}})$; on the other hand, if $i\neq i_*$, then $\delta=O(B/B')=O(J_2^k)$. It is therefore natural to choose $k=\frac{1}{2}$, so that the quantities $|5\cos^2 i-1|$ and $\delta$ are both of order $(J_2)^{\frac{1}{2}}$. Then all the terms of (19) are of the second order in $J_2$, and the terms rejected are of $O(J_2^{\frac{1}{2}})$.

The canonical equation in $G'$,

$$\dot{G}'=F_{g'}=-2A\sin 2g'+O(J_2^{\frac{5}{2}}), \tag{20}$$

becomes, in view of (15), to $O(J_2^2)$,

$$\dot{\delta}=-2A\sin 2g', \tag{21}$$

which, together with (19), determines $\delta$ and $g'$ as functions of the time.

In the classical solution $A$ is proportional to the coefficient of the singular long-periodic term. When either $e=0$ or $b=0$ in (18), this term vanishes, and the problem of singularity disappears. Indeed, with $A=0$, (21) is satisfied by $\delta=\text{const}$, while the canonical equation in $g'$,

$$\dot{g}'=-F'_{G'}=-B+O(J_2^2), \tag{22}$$

has the solution $g'=-Bt$, with $-B$ in (18) furnishing the classical expression for the secular rate of the argument of the pericenter, to the order $J_2^{\frac{3}{2}}$. Without any loss of generality, it can therefore be assumed here that $A\neq 0$.

## 4. CHANGE OF VARIABLES

It will appear later that the location of the point of stable equilibrium depends on the sign of the Vinti index $b$ (Garfinkel 1959, Vinti 1959). To make the equations of motion independent of $b$, define a new variable $\xi$:

$$\xi=g'-\tfrac{1}{4}\pi(1+\operatorname{sgn} A). \tag{23}$$

If $b>0$, then $A<0$ and $\xi=g'$; on the other hand, if $b<0$, then $A>0$ and $\xi=g'-\frac{1}{2}\pi$. Therefore $\cos 2g'=-\operatorname{sgn} A\cos 2\xi$, so that (19) becomes

$$-|A|\cos 2\xi+B\delta+\tfrac{1}{2}B'\delta^2+c=0. \tag{24}$$

Now let $G''$ and the origin of time be so chosen that

$$\delta(0)=0, \quad \xi(0)=0. \tag{25}$$

Then $c=|A|$, and (24) can be written

$$2|A|\sin^2\xi+B\delta+\tfrac{1}{2}B'\delta^2=0. \tag{26}$$

It has been shown that $\delta$ is of order $(J_2)^{\frac{1}{2}}$. Noting that $A\neq 0$ and that $B'>0$, define new constants:

$$C=|5/J_2 b|^{\frac{1}{2}}, \qquad \alpha=-B/|4AB'|^{\frac{1}{2}}=(5\cos^2 i-1)(p/2e)C, \qquad \omega_0=|4AB'|^{\frac{1}{2}}=\tfrac{3}{2}J_2^{\frac{1}{2}}ne p^{-3}|b/5|^{\frac{1}{2}}, \tag{27}$$

where $p=a(1-e^2)=G^2$, and a new variable $\eta$:

$$\eta=|B'/4A|^{\frac{1}{4}}\delta-\alpha. \tag{28}$$

Note that the parameter $\alpha$ is a measure of the difference $|i-i_*|$, and that $\eta$ is a linear function of $G'$; the scale has been magnified so that both $\alpha$ and $\eta$ are of order unity. In terms of the new variables the equations of motion (26), (21), and the initial conditions (25)

become

$$\sin^2\xi+\eta^2=\alpha^2,$$
$$\dot\eta=\tfrac{1}{2}\omega_0\sin 2\xi, \qquad (29)$$
$$\xi(0)=0, \quad \eta(0)=-\alpha.$$

## 5. SOLUTION OF THE EQUATIONS OF MOTION

Equations (29) are identical in form with the equations of motion of a simple pendulum. If $\theta$ is the central angle, $\omega_0$ the angular frequency of zero oscillations, and $\alpha^2$ is the ratio of the actual energy to that required to raise the pendulum to the top, perfect analogy is established by

$$\theta=2\xi, \quad \dot\theta/\omega_0=-2\eta, \quad \ddot\theta+\omega_0^2\sin\theta=0. \qquad (30)$$

The phase-plane orbits are furnished by the contour lines of the function

$$f(\xi,\eta)=\sin^2\xi+\eta^2. \qquad (31)$$

Since $f$ is a periodic function of $2\xi$, the domain may be confined to $-\frac{1}{2}\pi<\xi\leq\frac{1}{2}\pi$. The stationary points of $f$ are furnished by the condition $f_\xi=f_\eta=0$, which is satisfied by the two points $M$ and $S$:

$$M: \quad \xi=0, \quad \eta=0; \quad \alpha=0$$
$$S: \quad \xi=\tfrac{1}{2}\pi, \quad \eta=0; \quad |\alpha|=1. \qquad (32)$$

That $M$ is a minimum point of $f$ and that $S$ is a saddle point follow from the values of the second partial derivatives of $f$. With the substitution $2\xi=\theta$ the phase-plane diagram becomes identical with that of a simple pendulum, as given in the standard textbooks of mechanics (e.g., Goldstein 1950). The contour lines passing through $S$,

$$\eta=\pm\cos\xi, \qquad (33)$$

separate the domain into two regions: (1) The libration region $|\alpha|<1$, where $\xi(t)$ is periodic, and the orbits are closed curves enclosing $M$, the point of stable equilibrium, and (2) the circulation region $|\alpha|>1$, where $\xi(t)$ is monotonic, and the orbits are open curves; the advance or the regression of the argument of the pericenter occurs as $\alpha>1$ or $\alpha<-1$, respectively.

The formal solution of (29) is

$$\sin\xi=\alpha\,\mathrm{sn}(\omega_0 t,|\alpha|)=\mathrm{sn}(\alpha\omega_0 t,1/|\alpha|),$$
$$\eta=-\alpha\,\mathrm{cn}(\omega_0 t,|\alpha|)=-\alpha\,\mathrm{dn}(\alpha\omega_0 t,1/|\alpha|). \qquad (34)$$

The first form is convenient when $|\alpha|<1$, the second when $|\alpha|>1$; in either case the indicated modulus $\kappa$ of the elliptic functions is less than unity. Note that, in view (27) and (17)

$$\alpha\omega_0=-B=-\bar R_{1G''}, \qquad (35)$$

so that the product $\alpha\omega_0$ in (34) is the classical rate of advance of the argument of the pericenter.

In the limiting case $|\alpha|=1$, (34) becomes

$$\sin\xi=\tanh(\alpha\omega_0 t),$$
$$\eta=-\alpha\,\mathrm{sech}(\alpha\omega_0 t). \qquad (36)$$

This is an asymptotic orbit described in infinite time; as $t\to\infty$, it follows that $\xi\to\pi/2$, $\eta\to 0$, so that the configuration approaches the saddle point $S$, which is a point of unstable equilibrium. It is noteworthy that the stable and the unstable points are situated on the line $\xi=0$ and on the line $\xi=\frac{1}{2}\pi$, respectively. These are the line of nodes $g'=0$, $\pi$ and the line $g'=\pi/2$, $3\pi/2$ if $b>0$, and vice versa if $b<0$. The latter inequality holds for the earth with the commonly accepted values of $J_2$ and $J_4$. From (27), the condition $|\alpha|=1$ implies

$$|i-i_*|\sim\tfrac{1}{4}|5\cos^2 i-1|=\frac{e}{2p}|J_2 b/5|^{\frac{1}{2}}\equiv w_0. \qquad (37)$$

The "width" $w_0$ of the libration region is thus only a small fraction of the width $w$ of the "resonance" region defined in our earlier paper by

$$w=\frac{e}{2p}\left|\frac{1}{120}b\right|^{\frac{1}{2}}. \qquad (38)$$

Indeed,

$$w_0/w=2|6J_2|^{\frac{1}{2}}\sim 0.16,$$
$$\max w=1^\circ, \quad \max w_0=560'', \qquad (39)$$

the numerical values corresponding to $p=1+e$, $e=1$, and $J_2=1.08\times10^{-3}$, $J_4=-1.71\times10^{-6}$, with $b=-0.47$ (O'Keefe *et al.* 1959). Somewhat smaller values of $w$ and $w_0$ correspond to $J_4=(-1.3\pm0.2)10^{-6}$ (King-Hele 1959), with the resulting value $b=-0.1\pm0.2$.

The general behavior of the phase orbits can be summarized as follows. As $i$ increases from 0 to $\pi/2$, $\alpha$ decreases from $+\infty$ to $-\infty$. The value $i=i_*\sim63.^\circ4$ corresponds to $\alpha=0$, with the orbit degenerating into a point $M$. Let $\bar\xi$ and $\xi^*$ denote the linear and the periodic portions of $\xi$, and $\omega$ the common angular frequency of $\xi^*$ and $\eta$. (1) In the libration region $|\alpha|<1$,

$$\kappa=|\alpha|, \quad \bar\xi=0, \quad \xi^*=\sin^{-1}(\alpha\,\mathrm{sn}\,\omega_0 t),$$
$$\omega=(\pi/2K)\omega_0,$$
$$0\leq|\xi|\leq\sin^{-1}|\alpha|, \qquad (40)$$
$$0\leq|\eta|\leq|\alpha|,$$

where $K$ is the complete elliptic integral of the first kind. As $|\alpha|$ increases from 0 to 1, $\omega$ decreases from $\omega_0$ to zero; the secular rate remains zero. The amplitudes of $\xi$ and $\eta$ increase from zero to $\pi/2$ and 1, respectively. (2) In the circulation region $|\alpha|>1$:

$$\kappa=1/|\alpha|, \quad \dot{\bar\xi}=(\pi/2K)\alpha\omega_0,$$
$$\xi^*=\sin^{-1}(\mathrm{sn}\,\alpha\omega_0 t)-(\pi/2K)\alpha\omega_0 t,$$
$$\omega=(\pi/K)\alpha\omega_0, \qquad (41)$$
$$0\leq|\xi^*|\leq\sin^{-1}\{\alpha[1-(\pi/2K)^2]^{\frac{1}{2}}\}$$
$$-\mathrm{sn}^{-1}\{\alpha[1-(\pi/2K)^2]^{\frac{1}{2}}\}, \ (\alpha^2-1)^{\frac{1}{2}}\leq|\eta|\leq|\alpha|.$$

As $|\alpha|$ increases from 1 to $\infty$, $\omega$ and $\dot{\xi}$ increase from zero, asymptotically approaching $2\alpha\omega_0$ and $\alpha\omega_0$, respectively. Since $\alpha\omega_0=-\bar{R}_{1G}$, these results agree with the classical theory as $|\alpha|\to\infty$. The amplitudes of $\xi^*$ and $\eta$ increase from zero, asymptotically approaching $(8\alpha^2)^{-1}$ and $(4\alpha)^{-1}$, respectively. The latter values are derived from (41) with the aid of a Fourier series for sn (Whittaker and Watson 1952), and the relations (42).

$$\xi^*=\tfrac{1}{8}\kappa^2\sin(\pi/K)\alpha\omega_0 t+\cdots,\quad \kappa=1/|\alpha|,$$
$$\tfrac{1}{2}[\alpha-(\alpha^2-1)^{\frac{1}{2}}]=(4\alpha)^{-1}+\cdots. \tag{42}$$

(3) The asymptotic orbit, $|\alpha|=1$, separating the libration and the circulation regions, is described with an infinite period. On this orbit the angular frequency $\omega$ is minimized at value zero, the amplitudes of the oscillation are maximized, and the secular rate $\dot{\xi}$ vanishes, as $|\alpha|$ ranges from $\infty$ to 0.

## 6. COMPARISONS AND CHECKS

In a recent paper Hori (1960) treated the problem by removing the long-periodic terms from the Hamiltonian $F'$ by the method of von Zeipel, but with the generating function $S$ expanded in powers of $(J_2)^{\frac{1}{2}}$. With this modification of the classical solution the singularities are avoided. Although he carries out the expansion $S=S_0+S_{\frac{1}{2}}+S_1+\cdots$ explicitly only as far as $S_{\frac{1}{2}}$, higher-order terms can be obtained if desired. His derivative $S_{\frac{1}{2}g'}$ is equal to our $\delta$, and the results are equivalent to order $(J_2)^{\frac{1}{2}}$.

Further checks of the theory are furnished by a comparison of (42) with the dominant long-period terms in Eqs. (84) and (99) of our earlier paper (1959). For the combined effect of the second and the fourth spherical harmonics these equations yield:

$$\delta^*g'=\tfrac{1}{10}J_2be^2G^{-4}(5\cos^2i-1)^{-2}\sin 2g'+\cdots,$$
$$\delta^*\log G'=\tfrac{1}{10}J_2be^2G^{-4}(5\cos^2i-1)^{-1}\cos 2g'+\cdots, \tag{43}$$

with $L$, $G$, replaced by $L'$, $G''$ wherever they occur as arguments in the right-hand member. An agreement between (43) and (42) is established with the aid of (27) and (28), and the relation $G=\sqrt{p}$. Thus the "resonance" and the classical solutions asymptotically merge into each other.

The form of the solution adopted here clearly reveals all the essential features of the motion; i.e., the libration, the asymptotic orbit, and the interchange of the stable and the unstable points with change of sign of the Vinti index. The latter phenomenon has a perfect analogy in a simple pendulum, where such an interchange is governed by the sign of the acceleration of gravity.

## REFERENCES


Brouwer, D. 1959, *Astron. J.* **64**, 378.
Garfinkel, B. 1959, *Astron. J.* **64**, 353.
Goldstein, H. 1950, *Classical Mechanics* (Addison-Wesley Publishing Company, Inc., Reading, Massachusetts), p. 290.
Hori, G. 1960, *Astron. J.* **65**, 291.
King-Hele, D. G. 1959, *Xth International Astronautical Congress*, London.
Kozai, Y. 1959, *Astron. J.* **64**, 367.
O'Keefe, J. A., Eckles, Ann, and Squires, R. K. 1959, *Science* **129**, 565–566.
Vinti, J. P. 1959, *J. Research Natl. Bur. Standards* **63B**, 105.
von Zeipel, H. 1916, *Ark. Mat. Astr. Fys.* **11**, No. 1.
Whittaker, E. T. and Watson, G. N. 1952, *A Course in Modern Analysis* (Cambridge University Press, New York), p. 510.

# The System of VV Cephei

LAURENCE W. FREDRICK*
*Flower and Cook Observatory, University of Pennsylvania, Philadelphia and Sproul Observatory, Swarthmore College, Swarthmore, Pennsylvania*

(Received September 9, 1960)

The system of VV Cephei is studied by combining photometric, spectroscopic and astrometric information. The absolute parallax is shown to be approximately 0".005. The inclination of the orbit is very nearly 90° and the size of the giant M component is on the order of 600 solar radii. Discrepancies between the spectroscopic data and the astrometric and photometric data are discussed and suggestions are made to explain or resolve the discrepancies.

## INTRODUCTION

THE system of VV Cephei presents a rare opportunity in that it may be studied as an astrometric, spectroscopic, and eclipsing binary. Gaposchkin (1937) and Goedicke (1938) have presented data on the spectroscopic orbit and van de Kamp (1951) has given results of a provisional study of the astrometric material. The present study brings the Sproul astrometric material up to date and combines it with an analysis of the photoelectric light curves obtained during the recent eclipse.

## ASTROMETRY

The system has been observed at the Sproul Observatory in every season starting in 1938. A total of 1126 measurable plates have been taken on 316 nights until the end of 1958. The exposure times run between one and two minutes as VV Cephei is reduced by $5^m.76$ by means of a rotating sector. Data for the reference stars used in the astrometric reductions are given in the following. The dependence values Dep are given to show the balance of the reference frame, Dia is the diameter of the image in millimeters on the average plate and $\Delta m$ is the magnitude difference from reference star 2. The spectra are by Vyssotsky (interobservatory communication) who notes that star 1 is extremely reddened.

| Star | Dep | Diam (mm) | $\Delta m$ | $m_v$ | Sp |
|---|---|---|---|---|---|
| 1 | 0.334 | 0.068 | +0.08 | 10.68 | G |
| 2 | 0.213 | 0.076 | ··· | 10.60 | K0 |
| 3 | 0.210 | 0.098 | −0.38 | 10.22 | B8 |
| 4 | 0.243 | 0.081 | −0.03 | 10.57 | F5 |
| VV Cep | ··· | 0.073 | +0.05 | 10.65 | M2 |

The observations, measurements and reductions were carried out in the usual Sproul fashion (van de Kamp 1942). Because of the enormous amount of material, the nights have been combined to form normal points where the night weights have a sum of approximately twelve. Thus each normal point on the average contains four night's observations. The normal points are given in Table I, where the columns are (1) the year of observation, (2) the interval of observation for the normal point, (3) the sum of the weights, (4) the mean epoch reckoned from 1950.00, (5) and (6) the mean parallax factors in $\alpha$ and $\delta$, (7) and (8) the mean elliptical rectangular coordinates in $X$ and $Y$ (for periastron passage 1951.2), (9) the mean displacement $\xi$ in $\alpha$, and (10) the mean displacement $\eta$ in $\delta$. The values of $\xi$ and $\eta$ are given in units of $10^{-4}$ mm and a color effect in $\xi$ (Lippincott 1957) has already been allowed for. Figure 1 presents the astrometric data plotted as yearly normal points in order to minimize the parallax effect. The orbital motion is clearly superimposed on the proper motion.

In order to reduce the computational time to a minimum, ten supernormal points were formed. This virtually eliminates any parallactic effects and allows the material to be represented by the equations of condition where the bars indicate that supernormal points are being used and the symbols have their usual meaning (van de Kamp 1951).

$$\bar{\xi}=c_x+\mu_x t+(B)x+(G)y; \quad \bar{\eta}=c_y+\mu_y t+(A)x+(F)y.$$

Least-squares solutions for the unknowns were made using $P=20^y.34$, $e=0.20$, and $T=1942.56$, these elements being adopted from the papers of Gaposchkin and Goedicke cited earlier. The reliability of the results were then tested by varying the eccentricity. The sum of the squares of the residuals from these solutions indicate that either the eccentricity is zero or that the astrometric material can better be fitted by assuming a different value of $P$ or $T$. Since $P$ is probably known with an accuracy far greater than $T$, it was assumed that $T$ should be investigated.

Using the yearly normal points shown in Fig. 1, the proper motion in $x$ and in $y$ was removed graphically and $T$ and $e$ were determined by means of displacement curves (van de Kamp 1947), thus yielding $T=1951$ and $e=0.50$. The eccentricity was then varied through a large range, and least-squares solutions were made using the supernormal points. The sum of the squares of the residuals suggest that $T=1951.2$ and $e=0.50$ should be used.

Adopting $P=20^y.34$, $e=0.5$, and $T=1951.2$, a solution was then made using the normal points in Table I and the equations of condition.

* Now at Lowell Observatory.

TABLE I. Astrometric normal points.

| Year | Interval | $w$ | $t$ | $P_\alpha$ | $P_\delta$ | $x$ | $y$ | $\xi$ | $\eta$ |
|---|---|---|---|---|---|---|---|---|---|
| 1938 | Jul. 7–Aug. 15 | 16 | −11.41 | +.23 | +.96 | −1.37 | +.42 | − 7 | −18 |
| | Aug. 26–Sep. 4 | 13 | −11.34 | −.18 | +.94 | −1.38 | +.41 | −18 | −49 |
| | Oct. 15–Nov. 9 | 6 | −11.18 | −.85 | +.28 | −1.40 | +.38 | + 1 | −24 |
| 1939 | Jul. 2–Aug. 6 | 13 | −10.46 | +.50 | +.86 | −1.45 | +.26 | − 1 | −20 |
| | Aug. 12–Sep. 3 | 12 | −10.35 | −.09 | +.96 | −1.46 | +.24 | +18 | − 3 |
| | Sep. 5–Sep. 21 | 11 | −10.30 | −.40 | +.84 | −1.46 | +.24 | 0 | −19 |
| | Nov. 16–Dec. 7 | 8 | −10.10 | −.91 | −.17 | −1.47 | +.20 | − 7 | −20 |
| 1940 | Jun. 22–Jul. 9 | 11 | − 9.50 | +.68 | +.75 | −1.49 | +.09 | + 3 | −19 |
| | Jul. 14–Jul. 21 | 12 | − 9.46 | +.50 | +.88 | −1.49 | +.09 | +10 | −17 |
| | Aug. 1–Aug. 5 | 11 | − 9.41 | +.25 | +.97 | −1.50 | +.08 | +15 | −15 |
| | Aug. 9–Aug. 20 | 11 | − 9.38 | +.07 | +.98 | −1.50 | +.07 | 0 | −17 |
| | Sep. 2–Sep. 15 | 11 | − 9.32 | −.29 | +.90 | −1.50 | +.06 | +20 | − 9 |
| | Sep. 18–Oct. 10 | 11 | − 9.26 | −.58 | +.70 | −1.50 | +.05 | − 4 | −33 |
| | Oct. 12–Nov. 28 | 12 | − 9.16 | −.85 | +.16 | −1.50 | +.03 | + 1 | −21 |
| 1941 | Jun. 27–Aug. 3 | 11 | − 8.46 | +.48 | +.86 | −1.49 | −.09 | +12 | + 6 |
| | Aug. 8–Aug. 17 | 14 | − 8.39 | +.12 | +.98 | −1.49 | −.10 | +15 | + 9 |
| | Aug. 29–Sep. 9 | 15 | − 8.32 | −.26 | +.91 | −1.49 | −.12 | − 7 | 16 |
| | Oct. 11–Nov. 17 | 10 | − 8.19 | −.81 | +.33 | −1.49 | −.14 | − 1 | − 1 |
| 1942 | Jul. 16–Aug. 8 | 12 | − 7.44 | +.40 | +.92 | −1.45 | −.27 | −16 | + 5 |
| | Aug. 27–Oct. 8 | 15 | − 7.29 | −.40 | +.80 | −1.43 | −.30 | −15 | + 6 |
| 1943 | Jul. 1–Sep. 6 | 12 | − 6.42 | +.28 | +.88 | −1.36 | −.44 | −17 | 0 |
| | Sep. 13–Nov. 18 | 11 | − 6.20 | −.73 | +.39 | −1.34 | −.48 | − 5 | +12 |
| 1944 | Jul. 24–Sep. 2 | 15 | − 5.39 | +.10 | +.96 | −1.22 | −.60 | − 2 | + 7 |
| | Oct. 22–Dec. 4 | 9 | − 5.13 | −.88 | −.02 | −1.18 | −.63 | −14 | +17 |
| 1945 | Jun. 23–Jul. 12 | 11 | − 4.49 | +.65 | +.78 | −1.06 | −.71 | − 2 | +11 |
| | Aug. 12–Sep. 28 | 11 | − 4.31 | −.19 | +.88 | −1.03 | −.74 | − 6 | + 1 |
| | Oct. 16–Nov. 18 | 17 | − 4.19 | −.83 | +.34 | −1.00 | −.75 | −16 | +17 |
| 1946 | Jun. 27–Jul. 18 | 8 | − 3.47 | +.56 | +.83 | − .84 | −.82 | − 6 | − 8 |
| | Jul. 31–Aug. 12 | 12 | − 3.40 | +.21 | +.98 | − .82 | −.82 | −15 | +17 |
| | Aug. 24–Aug. 31 | 12 | − 3.34 | −.13 | +.96 | − .80 | −.83 | −10 | +13 |
| | Oct. 3–Nov. 27 | 9 | − 3.18 | −.78 | +.30 | − .76 | −.84 | − 4 | + 5 |
| 1947 | Jul. 13–Aug. 11 | 12 | − 2.43 | +.34 | +.94 | − .55 | −.86 | − 3 | − 2 |
| | Oct. 20–Oct. 26 | 9 | − 2.19 | −.84 | +.36 | − .48 | −.87 | −12 | − 1 |
| 1948 | Jul. 8–Sep. 16 | 12 | − 1.39 | +.12 | +.88 | − .21 | −.83 | −13 | 0 |
| | Oct. 21–Nov. 14 | 11 | − 1.17 | −.88 | +.22 | − .14 | −.81 | −13 | − 1 |
| 1949 | Aug. 9–Aug. 10 | 6 | − 0.40 | +.16 | +.98 | + .14 | −.67 | −30 | −16 |
| | Sep. 20–Sep. 25 | 12 | − 0.27 | −.53 | +.76 | + .18 | −.63 | − 9 | −13 |
| | Oct. 1–Oct. 13 | 12 | − 0.23 | −.70 | +.57 | + .20 | −.62 | −10 | − 2 |
| | Oct. 20–Nov. 20 | 12 | − 0.15 | −.90 | +.09 | + .22 | −.60 | − 6 | − 7 |
| 1950 | Jul. 18–Aug. 9 | 12 | + 0.57 | +.34 | +.94 | + .43 | −.31 | +14 | + 6 |
| | Sep. 17–Oct. 6 | 12 | + 0.74 | −.58 | +.71 | + .46 | −.24 | + 5 | + 9 |
| | Oct. 13–Oct. 30 | 15 | + 0.80 | −.81 | +.41 | + .47 | −.20 | + 3 | − 5 |
| | Nov. 1–Nov. 18 | 14 | + 0.86 | −.92 | +.07 | + .48 | −.18 | + 8 | + 6 |
| 1951 | Jul. 31–Sep. 15 | 11 | + 1.66 | −.17 | +.90 | + .46 | +.24 | + 3 | + 9 |
| | Sep. 23–Oct. 5 | 11 | + 1.74 | −.60 | +.69 | + .45 | +.28 | + 2 | − 6 |
| | Oct. 13–Nov. 20 | 13 | + 1.82 | −.84 | +.29 | + .43 | +.32 | − 1 | 0 |
| 1952 | Jun. 25–Jul. 13 | 12 | + 2.50 | +.68 | +.74 | + .24 | +.58 | +18 | + 9 |
| | Jul. 15–Aug. 19 | 12 | + 2.60 | +.20 | +.95 | + .21 | +.61 | +11 | +10 |
| | Aug. 23–Sep. 1 | 13 | + 2.56 | −.12 | +.96 | + .19 | +.63 | +17 | + 6 |
| | Sep. 5–Oct. 5 | 11 | + 2.72 | −.45 | +.80 | + .17 | +.65 | +14 | +11 |
| | Oct. 6–Oct. 23 | 13 | + 2.80 | −.79 | +.44 | + .14 | +.67 | + 9 | +15 |
| | Oct. 24–Oct. 30 | 11 | + 2.83 | −.87 | +.28 | + .13 | +.68 | + 7 | +15 |
| | Nov. 12–Nov. 24 | 9 | + 2.88 | −.93 | −.06 | + .11 | +.69 | − 5 | −12 |
| 1953 | Jul. 5–Oct. 3 | 12 | + 3.68 | −.28 | +.72 | − .16 | +.82 | +10 | −10 |
| | Oct. 7–Oct. 12 | 12 | + 3.77 | −.72 | +.56 | − .21 | +.83 | + 9 | − 2 |
| | Oct. 16–Nov. 1 | 12 | + 3.82 | −.84 | +.32 | − .22 | +.83 | + 2 | − 7 |
| | Nov. 2–Nov. 19 | 12 | + 3.87 | −.92 | +.01 | − .24 | +.84 | + 3 | − 3 |

TABLE I. (Continued)

| Year | Interval | $w$ | $t$ | $P_\alpha$ | $P_\delta$ | $x$ | $y$ | $\xi$ | $\eta$ |
|---|---|---|---|---|---|---|---|---|---|
| 1954 | Jul. 27–Aug. 13 | 12 | + 4.59 | +.26 | +.96 | − .48 | +.87 | + 8 | 0 |
| | Aug. 14–Aug. 31 | 14 | + 4.64 | −.06 | +.97 | − .49 | +.87 | + 4 | + 6 |
| | Sep. 2–Sep. 29 | 12 | + 4.72 | −.47 | +.79 | − .51 | +.87 | − 4 | + 5 |
| | Oct. 23–Nov. 15 | 15 | + 4.84 | −.90 | +.15 | − .55 | +.86 | 0 | + 4 |
| 1955 | Jul. 13–Aug. 6 | 9 | + 5.56 | +.40 | +.92 | − .76 | +.84 | + 2 | +10 |
| | Aug. 27–Sep. 21 | 11 | + 5.69 | −.35 | +.86 | − .79 | +.83 | + 1 | + 1 |
| | Sep. 28–Oct. 17 | 14 | + 5.77 | −.69 | +.59 | − .81 | +.82 | − 2 | + 8 |
| | Oct. 20–Nov. 18 | 12 | + 5.84 | −.88 | +.21 | − .83 | +.82 | 0 | +11 |
| 1956 | Jul. 28–Aug. 22 | 10 | + 6.57 | +.32 | +.88 | −1.00 | +.75 | − 1 | +17 |
| | Sep. 21–Nov. 5 | 12 | + 6.80 | −.77 | +.39 | −1.05 | +.73 | − 8 | +13 |
| | Nov. 6–Nov. 27 | 11 | + 6.87 | −.92 | 0 | −1.06 | +.72 | − 4 | + 5 |
| 1957 | Sep. 11–Oct. 11 | 10 | + 7.76 | −.64 | +.63 | −1.22 | +.60 | −16 | +21 |
| | Oct. 20–Dec. 2 | 8 | + 7.84 | −.88 | −.02 | −1.23 | +.59 | −13 | +20 |
| 1958 | Jun. 26–Jul. 1 | 12 | + 8.49 | +.73 | +.70 | −1.32 | +.49 | + 4 | +24 |
| | Aug. 9–Aug. 21 | 14 | + 8.62 | +.05 | +.98 | −1.34 | +.47 | −22 | +20 |
| | Nov. 7–Nov. 12 | 12 | + 8.86 | −.92 | +.06 | −1.36 | +.43 | − 6 | +21 |

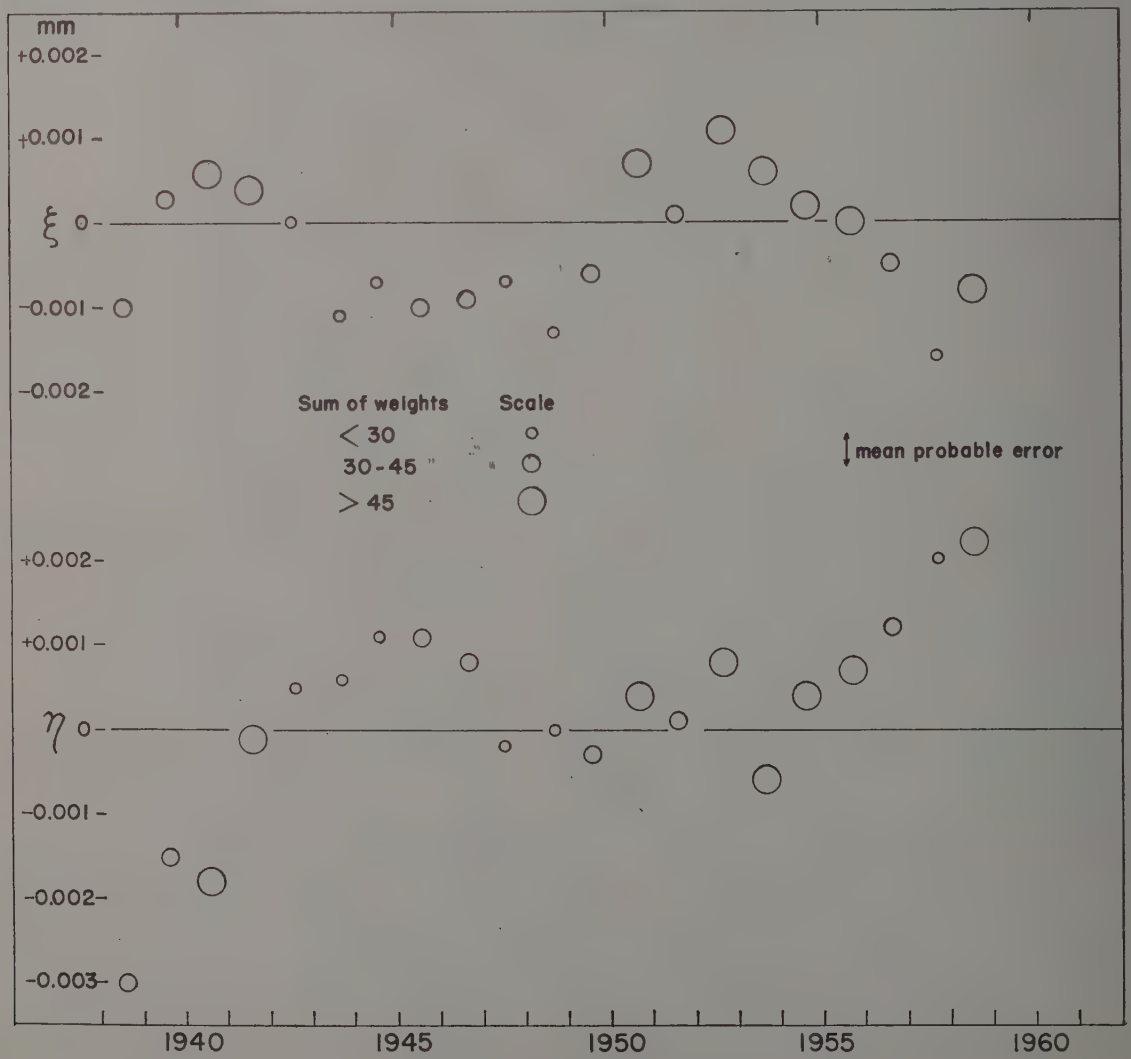


FIG. 1. Mean yearly displacements $\xi$ (R.A.) and $\eta$ (Dec.).

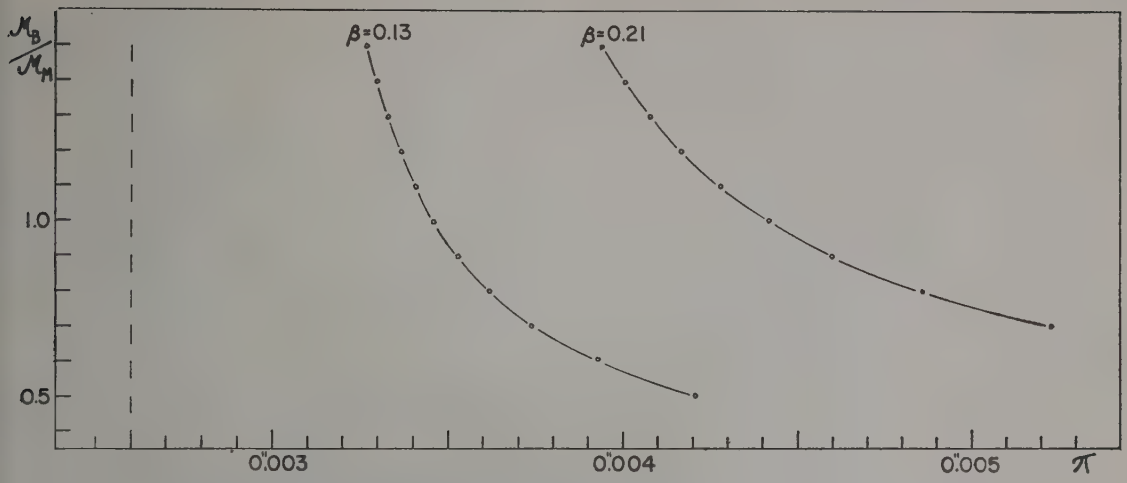


FIG. 2. The parallax $\pi$ as a function of mass ratio for the extreme values of $\beta$ and for $a_1=13.3$ a.u. Dashed line on the left is the limiting value for $\pi$.

$$\xi = c_x + \mu_x t + \pi_x P_\alpha + (B)x + (G)y,$$
$$\eta = c_y + \mu_y t + \pi_y P_\delta + (A)x + (F)y.$$

The coefficients determined by the method of least squares are

| | | |
|---|---|---|
| $c_x$ | $=+0.00027$ mm | |
| $c_y$ | $=-0.00017$ | |
| $\mu_x$ | $=-0.00009=-0''.0017$/yr | $\pm 0''.0008$ |
| $\mu_y$ | $=+0.00023=+0.0043$/yr | $\pm 0.0007$ |
| $\pi_x$ | $=+0.00046=+0.0086$ | $\pm 0.0026$ |
| $\pi_y$ | $=+0.00024=+0.0044$ | $\pm 0.0029$ |
| $(B)$ | $=+0.00071=+0.0134$ | $\pm 0.0036$ |
| $(G)$ | $=+0.00116=+0.0219$ | $\pm 0.0063$ |
| $(A)$ | $=-0.00063=-0.0119$ | $\pm 0.0037$ |
| $(F)$ | $=-0.00098=-0.0185$ | $\pm 0.0063$. |

The conversion to seconds of arc is made by using the Sproul scale factor, 18".87/mm. The coefficients $(B)$, $(G)$, $(A)$, and $(F)$ yield the elements

$$\alpha = 0.00178\text{mm} = 0''.0336 \pm 0''.0030$$
$$i = \pm 90°39'$$
$$\omega = +302°$$
$$\Omega = +133°.$$

The values of the relative parallax in $x$ and $y$ are in good agreement. Assuming the present parallax determinations from 1951 on have no systematic errors, a study by Miss Lippincott (1957) would correct the value of the relative parallax in $x$ to 0".0041, which is in excellent agreement with the value in $y$. Adopting this correction the combined relative parallax is

$$\pi_r = +0''.0042 \pm 0''.0020.$$

The reduction to absolute parallax may be made by using the precepts of the Vyssotskys (1948) yielding

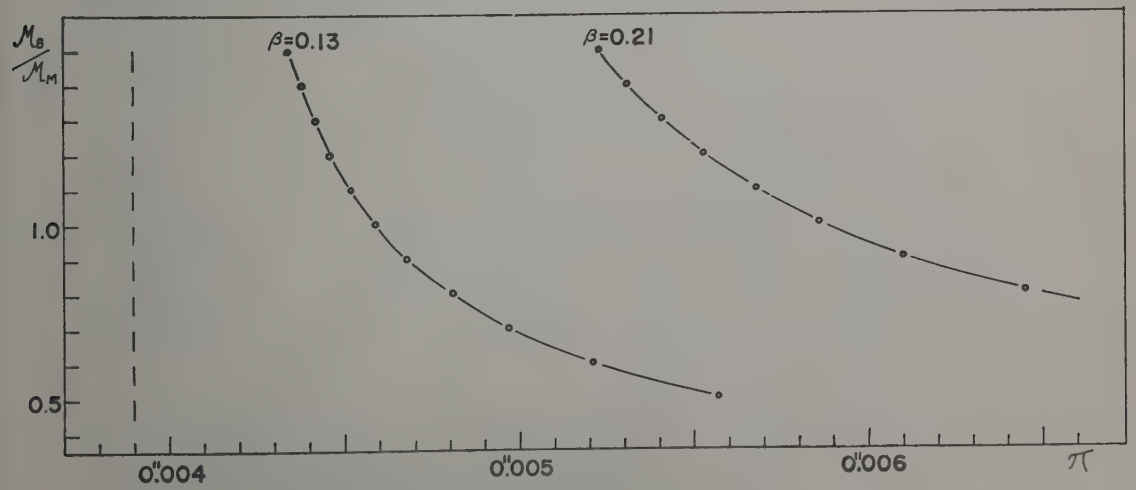


FIG. 3. Same as Fig. 2 except here $a_1=10$ a.u.

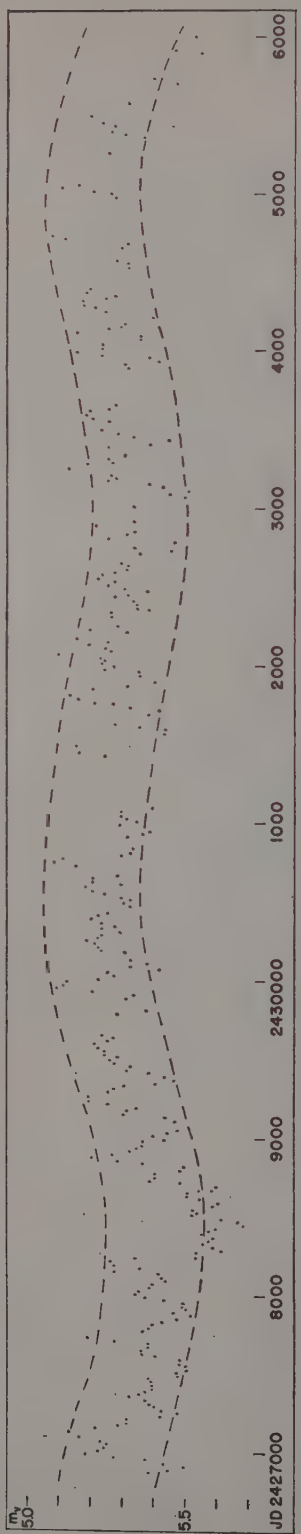


FIG. 4. Twenty-day means of visual observations by McLaughlin. The long-term $M'$ wave is indicated by the dashed line.

a correction of +0".0010 or by using the precepts of Binnendijk (1943) yielding a correction of +0".0015. The value +0".0012 is adopted here, giving for the combined absolute parallax,

$$\pi_a = +0''.0054 \pm 0''.0023.$$

This is a direct trigonometric parallax. Another and more reliable value for the parallax may be derived using the amplitudes of the photocentric orbit given in the foregoing.

The fractional distance $\beta$ of the M star to the photocenter is given by (van de Kamp 1951)

$$\beta = l_B/(l_M + l_B),$$

where the subscripts M and B refer to the M- and B-type stars involved. Normalizing $l_M + l_B$ to unit light gives $\beta = l_B$. This can then be obtained from the depth of eclipse curve given in Fig. 12 and discussed later. At the effective wavelength of the Sproul refractor we find $0.13 < \beta < 0.21$, the uncertainty arising from the intrinsic light variations, which will be discussed later.

For a given mass ratio $\mathfrak{M}_B/\mathfrak{M}_M$, there is the mass function $B_2 = \mathfrak{M}_B/(\mathfrak{M}_M + \mathfrak{M}_B)$. The spectroscopic orbit gives $a_1$. Since $a = a_1/B_2$, the substitution can be made in $\alpha = (B_2 - \beta)a$ which gives

$$\alpha = (1 - \beta/B_2)a_1,$$

where $\alpha$ is the semi-major axis of the photocentric orbit with respect to the center of mass. The parallax, which is here called a dynamical parallax $\pi_d$, then follows directly from the relation

$$\pi_d = \alpha''/\alpha.$$

Adopting Goedicke's value for $a_1 \sin i$, since the inclination is very nearly 90°, there results $a_1 = 13.3$ a.u. If the relation for $\pi_d$ is written in the form

$$\pi_d = \alpha''/(1 - \beta/B_2)a_1,$$

it is possible to investigate $\pi_d$ as a function of the mass ratio. Figure 2 exhibits this for the extreme values of $\beta$. It is easily seen that for this value of $a_1$ the lower limit for the parallax is 0".0026.

## SPECTROSCOPY

A new analysis for the spectroscopic elements will soon be available from the Michigan material. From a small-scale reproduction of the radial velocities the author has derived the following elements using the method of Lehmann-Filhes as presented by Smart (1951):

$$\omega = 200°$$
$$e = 0.2$$
$$V_0 = -18.2 \text{ km/sec}$$
$$T = \text{JD } 2430500$$
$$a_1 \sin i = 15.2 \times 10^6 \text{ km}.$$

TABLE II. Variable and comparison stars.

| Star | | BD No. | R.A. (1950) | Dec. | $m_v$ | Spectra |
|---|---|---|---|---|---|---|
| VV Cephei | Variable | +62°2007 | $21^h55^m14^s$ | +63°23′13″ | 5.25 | M2 |
| 20 Cephei | Comparison | +62°2029 | $22^h03^m29^s$ | +62°32′28″ | 5.14 | K5 |
| ··· | Check | +62°1994 | $21^h51^m10^s$ | +62°28′35″ | 6.25 | B8 |

It follows that $a_1=10$ a.u. A plot of $\pi_d$ as a function of mass ratio is given in Fig. 3 for $a_1=10$ a.u. Here the lower limit for the parallax is 0″.0039.

For a range in the mass ratio of 0.7 to 1.0 it is evident that the parallax lies between 0″.004 and 0″.006. The new spectroscopic material will probably favor the smaller value of $a_1$ and hence the larger value for the parallax. In what follows $\pi=0''.005$ is used.

## PHOTOMETRY

McLaughlin made visual estimates of the magnitude of VV Cephei on 1539 nights from June 1932 to May 1957. These observations have been averaged over twenty-day intervals and are plotted in Fig. 4. Examination of this figure shows very pronounced peaks. There are 25 such peaks within the 8380-day interval giving an average time between peaks of 349 days. The peaks have an average amplitude of $0^m.3$. There is also a much longer term variation (here called the $M'$ wave) of the order of 13.7 years with an amplitude of something like $0^m.15$. It is to be noted that the recent eclipse occurred near the top, but on the downward slope, of this long-term variation.

The system of VV Cephei has been observed photoelectrically at the Flower and Cook Observatory. The Pierce photometer (Biltzstein 1958) coupled with the 15-inch siderostat was used for most of the observations. The photometer was not used as a dual photometer for these observations. This photometry is defined by the following filters:

| Filter | Type | Wavelength | Halfwidth |
|---|---|---|---|
| Yellow | Interference | 5295 A | 55 A |
| Green | Interference | 4890 | 50 |
| Blue | Interference | 4290 | 65 |
| Ultraviolet | Glass | 3800 | 290 |

The interference filters were fabricated by Baird-Atomic, Inc. and purchased through a grant from the Swarthmore College Faculty Research Fund. The transmission intensities were traced on a Beckman spectrometer and are shown in Fig. 5.

Observations were made on 131 nights. The observations were made in the order: sky, comparison star, variable, comparison star, variable, etc., in all wave-

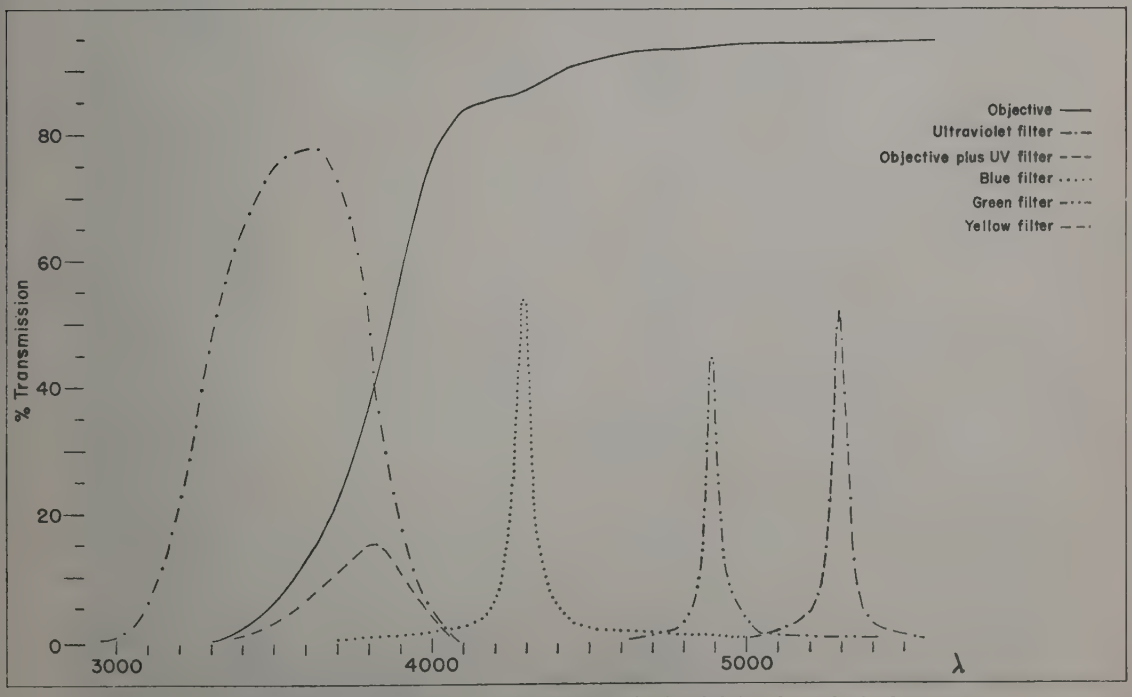


FIG. 5. Transmission characteristics of the filters and objective defining the author's photometry.

TABLE III. Photometric normal points.

| Yellow | | | Green | | | Blue | | | Ultraviolet | | |
|---|---|---|---|---|---|---|---|---|---|---|---|
| JD Epoch | $\Delta m$ | $n$ | Epoch | $\Delta m$ | $n$ | Epoch | $\Delta m$ | $n$ | Epoch | $\Delta m$ | $n$ |
| 2435438.5328 | −0.117 | 3 | .5355 | +0.013 | 3 | .5484 | −0.164 | 2 | | | |
| 5441.4838 | −0.114 | 3 | .4854 | +0.025 | 3 | .4868 | −0.144 | 3 | .5359 | −1.222 | 2 |
| 5442.5249 | −0.129 | 2 | .5271 | +0.003 | 2 | .5289 | −0.158 | 2 | .4868 | −1.369 | 3 |
| 5448.5134 | −0.175 | 2 | .5148 | −0.065 | 2 | .5159 | −0.255 | 2 | .4680 | −1.414 | 2 |
| 5452.4847 | −0.149 | 2 | .4859 | −0.016 | 2 | .4873 | −0.255 | 2 | | | |
| 2435679.8075 | +0.024 | 3 | | | | .8562 | +0.446 | 1 | .8289 | −0.317 | 2 |
| 5681.7797 | −0.019 | 6 | .7574 | +0.162 | 4 | .7788 | +0.447 | 3 | .7384 | −0.237 | 3 |
| 5682. | | | | | | | | | .7505 | −0.254 | 3 |
| 5683.7799 | 0.000 | 5 | .8018 | +0.162 | 3 | .8268 | +0.421 | 3 | .7874 | −0.233 | 5 |
| 5684.7156 | −0.022 | 3 | | | | | | | .6973 | −0.125 | 2 |
| 5685.7652 | +0.002 | 10 | .7553 | +0.216 | 4 | .7778 | +0.488 | 3 | .7936 | −0.171 | 10 |
| 5700.6702 | +0.005 | 4 | | | | | | | | | |
| 5701.7498 | +0.018 | 8 | | | | | | | .7596 | +0.004 | 2 |
| 5703.7695 | +0.030 | 5 | | | | | | | | | |
| 5708.7133 | +0.023 | 7 | .7494 | +0.155 | 3 | .7134 | +0.521 | 3 | .6947 | −0.035 | 4 |
| 2435709.7143 | +0.022 | 8 | | | | | | | .7108 | +0.043 | 4 |
| 5710.7274 | +0.023 | 5 | | | | | | | .7011 | +0.052 | 4 |
| 5711. | | | | | | | | | .7454 | +0.066 | 5 |
| 5713.6864 | +0.006 | 1 | | | | | | | .6480 | +0.157 | 3 |
| 5715.6799 | +0.010 | 1 | | | | | | | | | |
| 5721. | | | | | | | | | .6610 | +0.108 | 4 |
| 5725.6626 | +0.024 | 5 | .6186 | +0.168 | 2 | .6846 | +0.533 | 3 | .6323 | +0.067 | 5 |
| 5726.6515 | +0.033 | 6 | .6782 | +0.185 | 3 | .6910 | +0.545 | 2 | .7134 | +0.107 | 7 |
| 5729.6638 | +0.018 | 14 | | | | | | | | | |
| 5735.6367 | +0.062 | 6 | .6760 | +0.205 | 1 | .6380 | +0.584 | 6 | .6605 | +0.142 | 3 |
| 5737.6453 | +0.072 | 4 | | | | .6454 | +0.598 | 4 | .6457 | +0.140 | 3 |
| 5738.6251 | +0.054 | 1 | | | | .6239 | +0.568 | 1 | .6227 | +0.081 | 1 |
| 5754.5871 | +0.168 | 1 | | | | .5883 | +0.703 | 1 | .5913 | +0.203 | 1 |
| 5755.5784 | +0.178 | 1 | | | | .6036 | +0.702 | 1 | .6038 | +0.232 | 1 |
| 5756.5819 | +0.183 | 8 | | | | .5830 | +0.704 | 9 | .6079 | +0.301 | 4 |
| 5758.6203 | +0.198 | 1 | | | | .6212 | +0.675 | 1 | .6221 | +0.327 | 1 |
| 5762.5500 | +0.185 | 1 | | | | .5749 | +0.711 | 1 | | | |
| 6019. | | | | | | | | | .7807 | +0.575 | 4 |
| 6020. | | | | | | | | | .7667 | +0.608 | 2 |
| 6021. | | | | | | | | | .7860 | +0.613 | 12 |
| 6022. | | | | | | | | | .7942 | +0.594 | 9 |
| 6025. | | | | | | | | | .7871 | +0.576 | 7 |
| 6027. | | | | | | | | | .7336 | +0.525 | 1 |
| 6030. | | | | | | | | | .7618 | +0.488 | 1 |
| 6034. | | | | | | | | | .7415 | +0.475 | 2 |
| 6035. | | | | | | | | | .7858 | +0.433 | 4 |
| 6037. | | | | | | | | | .7181 | +0.470 | 2 |
| 2436038. | | | | | | | | | .7408 | +0.400 | 3 |
| 6039. | | | | | | | | | .7470 | +0.432 | 2 |
| 6040. | | | | | | | | | .7574 | +0.451 | 6 |
| 6051. | | | | | | .7571 | +0.682 | 2 | .7232 | +0.378 | 5 |
| 6052.7218 | −0.019 | 5 | | | | .7245 | +0.673 | 4 | .7675 | +0.524 | 5 |
| 6053.7557 | −0.026 | 2 | | | | .7676 | +0.659 | 2 | .7833 | +0.490 | 1 |
| 6056.7093 | −0.031 | 5 | | | | .7127 | +0.658 | 6 | .7538 | +0.501 | 4 |
| 6061.7185 | −0.034 | 5 | .7246 | +0.172 | 4 | .7203 | +0.670 | 5 | .6716 | +0.511 | 4 |
| 6062.7312 | −0.054 | 2 | .7321 | +0.162 | 2 | .7330 | +0.647 | 2 | .7021 | +0.498 | 2 |
| 6063.7135 | −0.055 | 5 | .7144 | +0.178 | 5 | .7135 | +0.666 | 4 | .6635 | +0.527 | 5 |
| 6074.6792 | −0.053 | 5 | .6818 | +0.191 | 4 | .6783 | +0.663 | 5 | .7312 | +0.541 | 7 |
| 6078.6368 | −0.047 | 7 | .6379 | +0.167 | 7 | .6428 | +0.654 | 7 | .6641 | +0.545 | 5 |
| 6087.6279 | +0.014 | 7 | .6288 | +0.224 | 7 | .6296 | +0.691 | 7 | .6631 | +0.571 | 4 |
| 6101.5842 | +0.106 | 5 | .5850 | +0.320 | 5 | .5860 | +0.765 | 5 | .6082 | +0.585 | 4 |
| 6106.5894 | +0.145 | 2 | .5908 | +0.372 | 2 | .5923 | +0.781 | 2 | .6255 | +0.673 | 1 |
| 6107.5438 | +0.143 | 3 | .5447 | +0.355 | 3 | .5456 | +0.781 | 3 | .5666 | +0.603 | 1 |
| 6108.6038 | +0.139 | 2 | .6047 | +0.368 | 2 | .6056 | +0.793 | 2 | .6285 | +0.650 | 2 |
| 6109.5715 | +0.166 | 6 | .5724 | +0.374 | 6 | .5733 | +0.796 | 6 | .6085 | +0.648 | 4 |
| 6115.5919 | +0.204 | 2 | .5944 | +0.403 | 3 | .5954 | +0.825 | 3 | .6230 | +0.648 | 3 |
| 6121.5402 | +0.217 | 5 | .5412 | +0.436 | 5 | .5421 | +0.834 | 5 | .5937 | +0.639 | 3 |

TABLE III. (Continued)

| Yellow | | | Green | | | Blue | | | Ultraviolet | | |
|---|---|---|---|---|---|---|---|---|---|---|---|
| JD Epoch | $\Delta m$ | $n$ | Epoch | $\Delta m$ | $n$ | Epoch | $\Delta m$ | $n$ | Epoch | $\Delta m$ | $n$ |
| 6122.5956 | +0.229 | 3 | .5966 | +0.438 | 3 | .5975 | +0.842 | 3 | .6278 | +0.613 | 3 |
| 6123.5360 | +0.225 | 3 | .5369 | +0.439 | 3 | .5379 | +0.833 | 3 | .5657 | +0.635 | 3 |
| 6124.5507 | +0.237 | 5 | .5516 | +0.454 | 5 | .5525 | +0.848 | 5 | .5835 | +0.643 | 5 |
| 6125.5484 | +0.229 | 3 | .5485 | +0.446 | 3 | .5449 | +0.844 | 3 | .5753 | +0.649 | 1 |
| 6126.5339 | +0.242 | 6 | .5348 | +0.441 | 6 | .5357 | +0.846 | 6 | .5729 | +0.589 | 6 |
| 6131.5188 | +0.245 | 3 | .5159 | +0.437 | 5 | .5168 | +0.798 | 4 | .5631 | +0.573 | 5 |
| 6132.5502 | +0.219 | 5 | .5415 | +0.440 | 5 | .5423 | +0.786 | 6 | .5923 | +0.577 | 4 |
| 6134.5171 | +0.228 | 2 | .5180 | +0.420 | 2 | .5189 | +0.771 | 2 | .6201 | +0.490 | 2 |
| 6140.5583 | +0.190 | 8 | .5670 | +0.405 | 6 | .5520 | +0.665 | 6 | .5233 | +0.313 | 5 |
| 6149.4981 | +0.195 | 4 | .5294 | +0.412 | 5 | .5218 | +0.781 | 4 | .5144 | +0.586 | 3 |
| 6152.5718 | +0.192 | 4 | .5727 | +0.392 | 4 | .5667 | +0.772 | 2 | .5728 | +0.474 | 3 |
| 6153.5442 | +0.192 | 6 | .5451 | +0.392 | 6 | .5460 | +0.747 | 6 | .4948 | +0.483 | 5 |
| 6154.5506 | +0.218 | 5 | .5506 | +0.407 | 6 | .5451 | +0.776 | 5 | .4871 | +0.500 | 7 |
| 6155.5389 | +0.189 | 7 | .5398 | +0.385 | 7 | .5407 | +0.773 | 7 | .4848 | +0.478 | 5 |
| 6158.5014 | +0.175 | 1 | .5023 | +0.385 | 1 | .5032 | +0.700 | 1 | .4781 | +0.370 | 4 |
| 6160. | | | | | | | | | .4925 | +0.329 | 1 |
| 6163.5251 | +0.166 | 3 | .5259 | +0.385 | 3 | .5267 | +0.627 | 3 | .4783 | +0.234 | 6 |
| 6164. | | | | | | | | | .4635 | +0.156 | 3 |
| 6167.5063 | +0.290 | 4 | .5072 | +0.399 | 4 | .5082 | +0.576 | 4 | .4695 | +0.054 | 4 |
| 6168.5530 | +0.170 | 1 | .5599 | +0.392 | 2 | .5608 | +0.631 | 2 | .5434 | +0.167 | 1 |
| 6169.5507 | +0.174 | 4 | .5511 | +0.397 | 4 | .5471 | +0.688 | 3 | .5045 | +0.171 | 5 |
| 6172.5207 | +0.188 | 7 | .5208 | +0.405 | 7 | .5217 | +0.707 | 7 | .4675 | +0.271 | 4 |
| 2436174.5211 | +0.194 | 8 | .5186 | +0.401 | 8 | .5231 | +0.684 | 7 | .4685 | +0.248 | 4 |
| 6175.5170 | +0.171 | 6 | .5209 | +0.400 | 7 | .5185 | +0.677 | 6 | .4715 | +0.243 | 5 |
| 6178.5353 | +0.195 | 3 | .5272 | +0.410 | 3 | .5371 | +0.687 | 3 | .4564 | (+0.314) | (1) |
| 6185.5149 | +0.189 | 2 | .5111 | +0.363 | 1 | .5166 | +0.610 | 2 | .4926 | +0.046 | 3 |
| 6188.4954 | +0.154 | 2 | .4963 | +0.360 | 2 | .4972 | (+0.587) | (2) | .4675 | +0.021 | 4 |
| 6190. | | | | | | | | | .5060 | −0.035 | 4 |
| 6194. | | | | | | | | | .4604 | −0.122 | 2 |
| 6195.4875 | +0.141 | 2 | .4884 | +0.314 | 2 | .4893 | +0.514 | 2 | .4683 | −0.140 | 2 |
| 6200.4791 | +0.127 | 1 | .4800 | +0.296 | 1 | .4809 | +0.537 | 1 | .4628 | −0.104 | 3 |
| 6202.4709 | +0.127 | 1 | .4718 | +0.293 | 1 | .4727 | +0.481 | 1 | .4700 | −0.224 | 1 |
| 6205. | | | | | | | | | .4627 | −0.323 | 2 |
| 6207.4719 | +0.150 | 1 | .4731 | +0.261 | 1 | .4771 | +0.384 | 2 | .4657 | −0.390 | 2 |
| 6208.4734 | +0.075 | 1 | .4743 | +0.262 | 1 | .4755 | +0.346 | 1 | .4674 | −0.428 | 2 |
| 6209.4704 | +0.071 | 1 | .4713 | +0.192 | 1 | .4722 | +0.305 | 1 | .4692 | −0.569 | 1 |
| 6210.4696 | +0.046 | 1 | .4705 | +0.202 | 1 | .4714 | +0.252 | 1 | .4687 | −0.613 | 1 |
| 6212.4677 | +0.052 | 1 | | | | | | | .4668 | −0.662 | 1 |
| 6370.7980 | −0.123 | 3 | .7988 | −0.016 | 3 | .7996 | +0.043 | 3 | .7972 | −1.251 | 3 |
| 6371.7936 | −0.128 | 2 | .8005 | −0.017 | 3 | .8013 | +0.053 | 3 | .8032 | (−1.189) | 1 |
| 6372.7831 | −0.120 | 2 | .7743 | −0.017 | 1 | .7906 | +0.060 | 3 | .7823 | −1.234 | 2 |
| 6382.7583 | −0.162 | 5 | .7592 | −0.037 | 5 | .7600 | −0.030 | 5 | .7954 | −1.368 | 6 |
| 6387.7558 | −0.129 | 2 | .7425 | −0.034 | 3 | .7473 | +0.032 | 4 | | | |
| 6394.7368 | −0.112 | 6 | .7380 | +0.024 | 7 | .7388 | +0.123 | 7 | .7938 | −1.027 | 7 |
| 6401.7345 | −0.127 | 3 | .7276 | −0.002 | 4 | .7361 | +0.112 | 3 | .7693 | −1.142 | 4 |
| 6414.6491 | −0.052 | 1 | | | | | | | | | |
| 6420.7227 | −0.129 | 5 | .7099 | −0.053 | 3 | .7203 | +0.036 | 4 | .7690 | −1.207 | 5 |
| 6424.6978 | −0.119 | 4 | .6986 | −0.012 | 4 | .7004 | +0.046 | 4 | .7304 | −1.193 | 3 |
| 6425.6925 | −0.133 | 5 | .6885 | −0.015 | 4 | .6893 | −0.011 | 4 | .7254 | −1.320 | 3 |
| 6430.6766 | −0.078 | 6 | .6854 | +0.011 | 3 | .6678 | +0.064 | 3 | .7144 | −1.163 | 3 |
| 6433.6856 | −0.040 | 3 | .6824 | +0.045 | 7 | .6778 | +0.079 | 3 | .7168 | −1.145 | 4 |
| 6434.6520 | −0.042 | 2 | .6437 | +0.042 | 3 | .6520 | +0.071 | 3 | .6701 | −1.156 | 1 |
| 6435.6884 | −0.041 | 6 | .6902 | +0.056 | 7 | .6913 | +0.083 | 6 | .7300 | −1.140 | 2 |
| 6438.7441 | −0.049 | 5 | .6904 | +0.073 | 4 | .7271 | +0.104 | 4 | .7106 | (−1.133) | 1 |
| 6445.6231 | −0.002 | 5 | .6187 | +0.111 | 6 | .6215 | +0.120 | 7 | .6637 | −1.150 | 5 |
| 6455.6542 | +0.032 | 2 | .6527 | +0.177 | 3 | .6527 | +0.181 | 3 | .6777 | −1.156 | 2 |
| 6457.6148 | +0.076 | 4 | .6170 | +0.179 | 7 | .6135 | +0.171 | 5 | .6570 | −1.178 | 7 |
| 6459.6556 | +0.059 | 4 | .6504 | +0.177 | 4 | .6514 | +0.158 | 5 | .6870 | −1.189 | 1 |
| 6469.5900 | +0.074 | 4 | .5682 | +0.174 | 4 | .5680 | +0.079 | 5 | .6171 | −1.354 | 3 |
| 6470.5712 | +0.095 | 3 | .5835 | +0.169 | 3 | .5837 | +0.097 | 3 | .6028 | −1.328 | 3 |
| 6475.5589 | +0.110 | 5 | .5813 | +0.184 | 4 | .5813 | +0.120 | 4 | .6034 | −1.304 | 5 |
| 6476. | | | | | | | | | .5900 | −1.238 | 10 |

TABLE III. (Continued)

| Yellow | | | Green | | | Blue | | | Ultraviolet | | |
|---|---|---|---|---|---|---|---|---|---|---|---|
| JD Epoch | $\Delta m$ | $n$ | Epoch | $\Delta m$ | $n$ | Epoch | $\Delta m$ | $n$ | Epoch | $\Delta m$ | $n$ |
| 6482.6220 | +0.110 | 5 | .6005 | +0.186 | 4 | .6028 | +0.139 | 3 | .5819 | −1.201 | 4 |
| 6489.6283 | +0.045* | 7 | .6036 | +0.169 | 3 | .6038 | +0.146 | 3 | .5849 | −1.205 | 3 |
| | *Flare | | | | | | | | | | |
| 2436493.5054 | +0.031 | 3 | | | | | | | .5568 | −1.183 | 2 |
| 6497.4855 | −0.037 | 3 | .5004 | +0.103 | 3 | .5007 | +0.086 | 3 | .5222 | −1.311 | 6 |
| 6507.5331 | −0.045 | 1 | | | | .5323 | +0.071 | 1 | .5339 | −1.201 | 1 |
| 6508.5083 | −0.047 | 2 | .5467 | +0.058 | 1 | .5091 | +0.075 | 2 | .6225 | −1.218 | 5 |
| 6514.5364 | −0.095 | 2 | .5348 | +0.028 | 2 | .5356 | +0.038 | 2 | .5492 | −1.310 | 2 |

lengths. The sky was monitored as often as necessary. The integration time was $60\times10^{-5}$ days. On almost every night the check star was observed in order to check the constancy of the comparison star. Data for the stars are given in Table II. The observed normal points in the sense VV Cephei minus comparison star, corrected for relative extinction, are given in Table III. The epoch is heliocentric from Greenwich mean noon and $n$ indicates the number of observations making up each normal point. These are plotted as dots in Figs. 6, 7, and 8. The check star minus comparison star is shown for each wavelength.

In order to extend the observing season during egress, observations were made by Binnendijk on the 28-inch reflector on eight nights at the same time observations were being made on the siderostat. Five additional nights were then obtained. These observations, reduced to the system of the Pierce photometer, are given in Table IV, and are plotted in Figs. 6, 7, and 8 as crosses.

In addition to the foregoing observations, G. Larsson-Leander (1957, 1959) has observed the system extensively in blue and yellow light. His observations are not restricted by the seasons due to his location (60°$N$).

During eclipse the light of the M star varies rather smoothly. The long slope at JD 2435760 is similiar to one at JD 2436100 and occurs again at JD 2436450. The average time between these slopes is 345 days. This is so close to the 349-day value between visual peaks on McLaughlin's light curve that they no doubt represent the same phenomenon. The 345-day cycle is made up of two waves, one of small amplitude ($S$ wave) followed by one of large amplitude ($L$ wave). The $S$ wave plus $L$ wave may be represented as the resultant sum of a sine and cosine function, but there is not sufficient coverage in time to confirm this.

A curious and abrupt pulselike phenomenon occurred at JD's 2435729, 2436141, 2436166, and 2436469. These are interesting because they have larger amplitudes in the shorter wavelengths whereas the waves already referred to have larger amplitudes in the longer wavelengths. Table V lists the amplitudes in magnitudes of the various variations. In the table the depth of eclipse $d$ in the various wavelengths is included and plotted in Fig. 12. The wavelengths have been rounded off, the amplitudes of the wave were interpolated from Larsson-Leander's material, and the epoch is the central date of the phenomenon. The $L$ wave appears to increase linearly with wavelength. The amplitudes of the pulses increase with decreasing wavelength just as the depth of eclipse does. Because of this, it is tempting to associate these with the B star. However, A. Deutsch could not find any trace of the B star on a spectrogram taken on JD 2436142 and Wright (1958) places the system only a week past third contact on JD 2436187. These pulses may be due to either a shell about the B star or perhaps a fluorescence in the atmosphere of the M star due to a brief increase in radiation from the B star. The depth of eclipse was

TABLE IV. Photometric normal points (28-inch reflector).

| Yellow | | | Blue | | | Ultraviolet | | |
|---|---|---|---|---|---|---|---|---|
| JD Epoch | $\Delta m$ | $n$ | Epoch | $\Delta m$ | $n$ | Epoch | $\Delta m$ | $n$ |
| 2436185.5494 | +0.162 | 2 | .5502 | +0.625 | 2 | .5495 | +0.062 | 2 |
| 6188.5197 | +0.153 | 1 | .4780 | +0.604 | 1 | .4701 | +0.003 | 3 |
| 6194.5247 | +0.138 | 3 | .4922 | +0.520 | 3 | .4753 | −0.143 | 3 |
| 6197.5326 | +0.137 | 2 | .5054 | +0.525 | 2 | .4957 | −0.116 | 2 |
| 6200.5158 | +0.143 | 2 | .4863 | +0.512 | 2 | .4762 | −0.133 | 2 |
| 6202.5087 | +0.131 | 4 | .4837 | +0.475 | 2 | .4978 | −0.238 | 2 |
| 6207.5820 | +0.087 | 2 | .6077 | +0.373 | 2 | | | |
| 6208.5274 | +0.085 | 1 | .5150 | +0.387 | 1 | .5079 | −0.433 | 1 |
| 6209.4953 | +0.066 | 2 | .4833 | +0.303 | 2 | .4700 | −0.571 | 3 |
| 6213.5420 | +0.075 | 1 | .5670 | +0.323 | 1 | .5767 | −0.630 | 1 |
| 6215.5145 | +0.055 | 2 | .4914 | +0.313 | 2 | .4737 | −0.584 | 3 |
| 6223. | | | .5107 | +0.240 | 4 | .4955 | −0.723 | 4 |
| 6227.4932 | +0.038 | 1 | .4947 | +0.276 | 1 | .5100 | −0.723 | 1 |

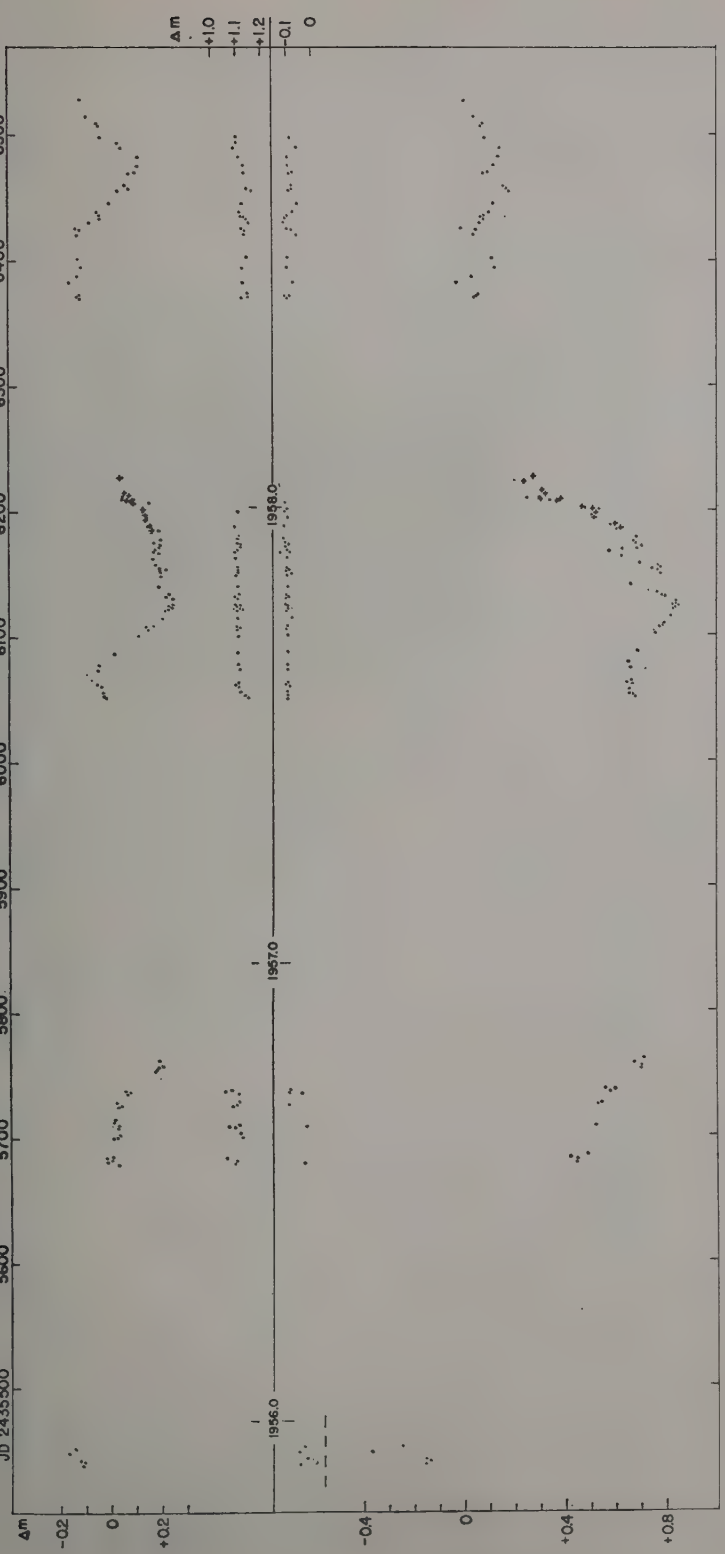


FIG. 6. Yellow (top) and blue (bottom) photometry by the author in the sense variable minus comparison star. Check star is shown across the middle of the figure. The 28-inch observations are indicated by crosses.

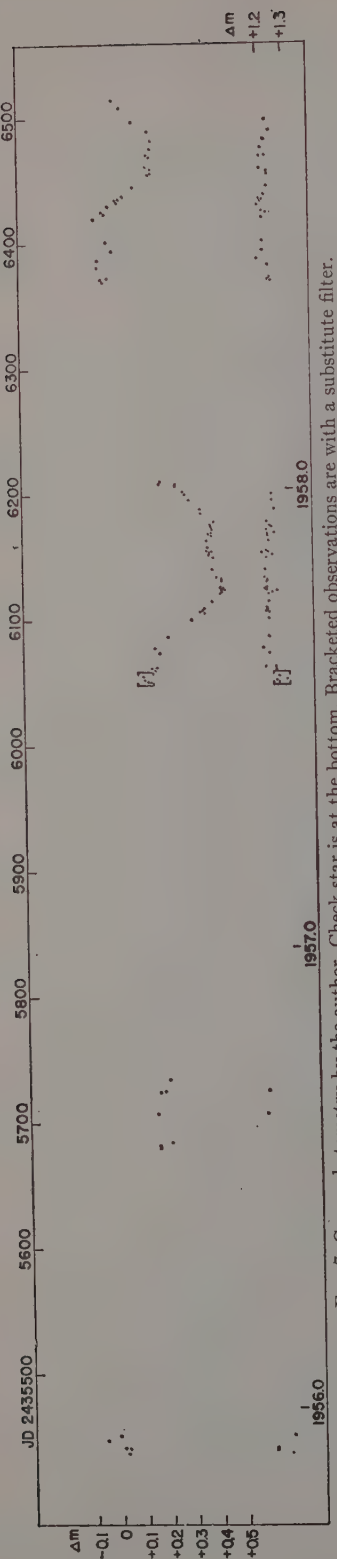


FIG. 7. Green photometry by the author. Check star is at the bottom. Bracketed observations are with a substitute filter.




FIG. 8. Ultraviolet photometry by the author. Check star is at the bottom. The 28-inch observations are indicated by crosses.

TABLE V. Amplitudes.

| Color | | $S$ | $L$ | $P_1$ | $P_2$ | $P_3$ | $d$ |
|---|---|---|---|---|---|---|---|
| Yellow | 5300 | (0m18) | 0m30 | 0m04 | 0m05 | 0m00 | 0m20 |
| Green | 4900 | ... | 0.25 | 0.04 | 0.05 | 0.01 | 0.28 |
| Blue | 4300 | (0.12) | 0.20 | 0.14 | 0.15 | 0.11 | 0.64 |
| Ultraviolet | 3800 | ... | 0.15 | 0.23 | 0.28 | 0.20 | 1.76 |

determined by a rectification procedure which will be explained.

On JD 2436489 a rather sudden change in the yellow light occurred during a 36-minute interval. The light became brighter by 0m.03+ and subsided during this time. This is shown in Fig. 9 where the ordinate is in instrumental intensity units. A rapid change such as this must be quite local in origin, but it is impossible to say which star is involved. Observations in the other three wavelengths are lacking because telescope time on that night was limited and the observations in the other wavelengths were already complete. The flare is real as can be seen from the constancy of the sky and comparison star. Abrupt changes of 0m.1 or more have been reported to occur in a short period to time, but this is the only evidence for such changes found during this investigation.

## SOLUTION

To find a solution, Larsson-Leander's light curves were used because they are continuous. A straightforward solution is impossible, due to the intrinsic variations. Following a suggestion by J. E. Merrill, the light curve was rectified by subtracting the $S$ and $L$ waves, making allowance for the descending slope of the long-term wave $M'$. The rectified light curves were then converted into intensities and folded back upon the egress branch and a $\psi$ solution was made following the method of Russell and Merrill (1951). The resulting solution in blue is shown in Fig. 10. The elements obtained are

| | Blue | | Yellow |
|---|---|---|---|
| $x$ | 0.6 | Assumed | 1.0 |
| $k$ | 0.13 | | 0.05 |
| $\theta_e$ | 14°.81 | | 14°.35 |
| $\theta_i$ | 11°.24 | | 12°.87 |
| $i$ | 92°(88) | | 91°(89) |
| $r_g$ | 0.23 | | 0.24 |
| $r_s$ | 0.03 | | 0.01 |
| 1st contact | 2435639 | | 2435678 |
| 2nd contact | 5717 | | 5708 |
| Mid-eclipse | 5947 | | 5947 |
| 3rd contact | 6177 | | 6240 |
| 4th contact | 6251 | | 6270 |

These solutions would have reasonable validity provided the assumptions about the constancy of the M star's intrinsic variations hold and provided the B star is not variable. It is obvious from a comparison between the times of the contacts in the blue and yellow given in the foregoing that something is wrong. Treating the branches separately it is possible to fit ingress very well with a small value, $k=0.1$, and egress with a somewhat larger value, $k=0.3$. This would suggest that the B star changed its effective size drastically during the eclipse, and from the shape of the egress branch that it changed in brightness also. However, this is rather startling and we may look for another explanation.

An alternate and consistent solution may be derived from Larsson-Leander's color curve shown in Fig. 11. Assuming that the B star's color does not change drastically as its light varies then any abrupt change in the color of the system will be due to eclipse. The color changes sharply more positive between JD 2435655 and 2435680, and sharply less positive between JD 2436180 and 2436210. The slopes are identical but of opposite sign. Rounding of the color curve before and after these dates can be caused by a shell about the B star. The asymmetry in the bottom of the eclipse coincides with the M star's $L$ wave and may indicate an abnormal brightening in the longer wavelengths.

It is easily seen on inspection of the light curves that third contact in the ultraviolet light occurred long before third contact in the other colors. This adds support to the notion that the shell causes the rounding off of the color curve. If this is so we can estimate the times of contact for the B star and its shell. We find

| | B Star | Shell |
|---|---|---|
| 1st contact | 2435656 | 2435626 |
| 2nd contact | 5683 | 5713 |
| Mid-eclipse | 5931 | 5931 |
| 3rd contact | 6179 | 6149 |
| 4th contact | 6206 | 6236 |

Assuming $i=90°$, we have for the B star

$$(D-d)/(D+d)=r_s/r_g=k=0.05,$$

and for the shell (subscript, $r$=ring, or in this case =shell),

$$r_r/r_g=k=0.17.$$

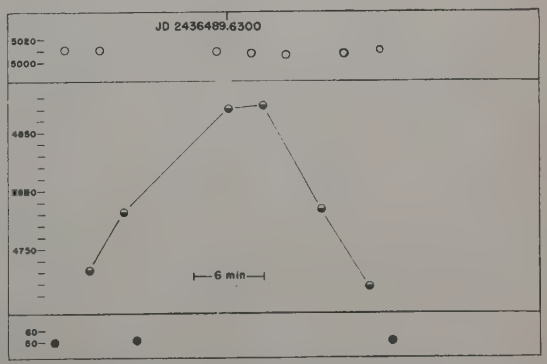


FIG. 9. Flare of VV Cephei in instrumental intensity units. Open circles are comparison star readings, half-filled circles are VV Cephei readings, and filled circles are sky plus dark current readings.

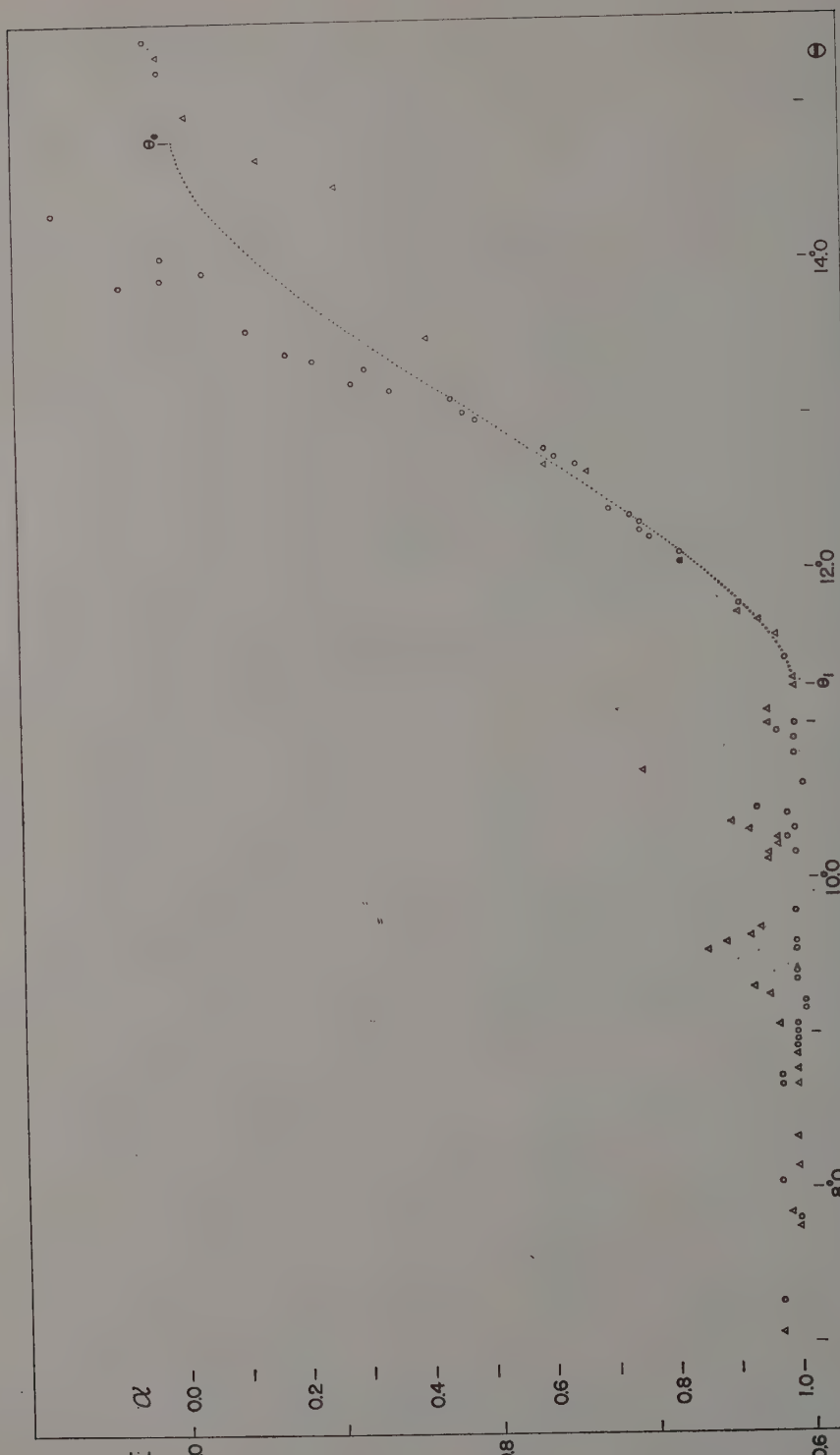


FIG. 10. Rectified blue light curve. Open circles are from ingress; triangles are from egress. The dotted curve is the best $\psi$ solution.

t then follows that the ratio of the size of the shell to hat of the B star is three. McKellar, Wright, and Francis (1957) have estimated the size of the shell at ngress to be twice the size of the B star.

The time of mid-eclipse given by the color curve grees within a day with the time of mid-eclipse given by Gaposchkin's (1937) elements.

## DISCUSSION

The apparent visual magnitude of the M star (obtained from the light at mid-eclipse) is approximately $5^{m}.25$. For a parallax of $+0''.005$ and an absorption of $+0^{m}.10$ (Risley 1943) the absolute visual magnitude of the M star is $-1.36$. If the parallax were $0''.004$ the absolute magnitude would be $-1.84$. In any case, this disagrees with the absolute visual magnitude associated with the classification M2+Ia —Iab assigned to the M star by Keenan and Wright (1957).

The absolute visual magnitude of the B star follows from the depth of eclipse and the relation

$$L_B/L_M = 0.17/0.83 = 2.512^{(-1.36-M_B)};$$

hence $M_B = +0.36$. For a parallax of $0''.004$, we get $M_B = -0.12$. Thus the B star in any case is an underluminous shell star. Assuming a bolometric correction of 2.2 magnitudes, the radius of the M star can be estimated by means of Stefan's law. The M star's bolometric magnitude is about $-4$, which leads to a radius of 200 $R_\odot$, or 300 $R_\odot$ when Goedicke's value for the temperature is used. Based on the circular model, this would indicate that the radius of the orbit is about 6 a.u., but it has already been shown that $a_1$ is of the order of 10 a.u. For the circular model at external contact and $i = 90°$,

$$r_0 = \sin\theta_e/(1+k),$$

$r_0$ being in terms of unit radius of the orbit $a$. However, if the orbit is eccentric the relation for $r_0$ becomes

$$r_0 = \frac{\sin\theta_e}{1+k} \cdot \frac{a(1-e^2)}{1-e\cos\nu},$$

where $a$ is the semi-major axis of the relative orbit and $\nu$ is the true anomaly at the time of eclipse.

In the case of the astrometric orbit it can be shown that $r_0 \sim 0.29a$. If the mass ratio is 0.8, then $r_0 \sim 1200$ $R_\odot$. In the case of the spectroscopic orbit we find $r_0 \sim 0.12a$ or $r_0 \sim 580$ $R_\odot$. This latter radius corresponds to an effective temperature of approximately 1800° according to Stefan's law when a bolometric magnitude of $-4$ is used. The astrometric case under the same conditions requires an effective temperature of 1200°.

There is thus a contradiction between the astrometric and the spectroscopic information at two points. (1) the effective temperature is too low; (2) the absolute

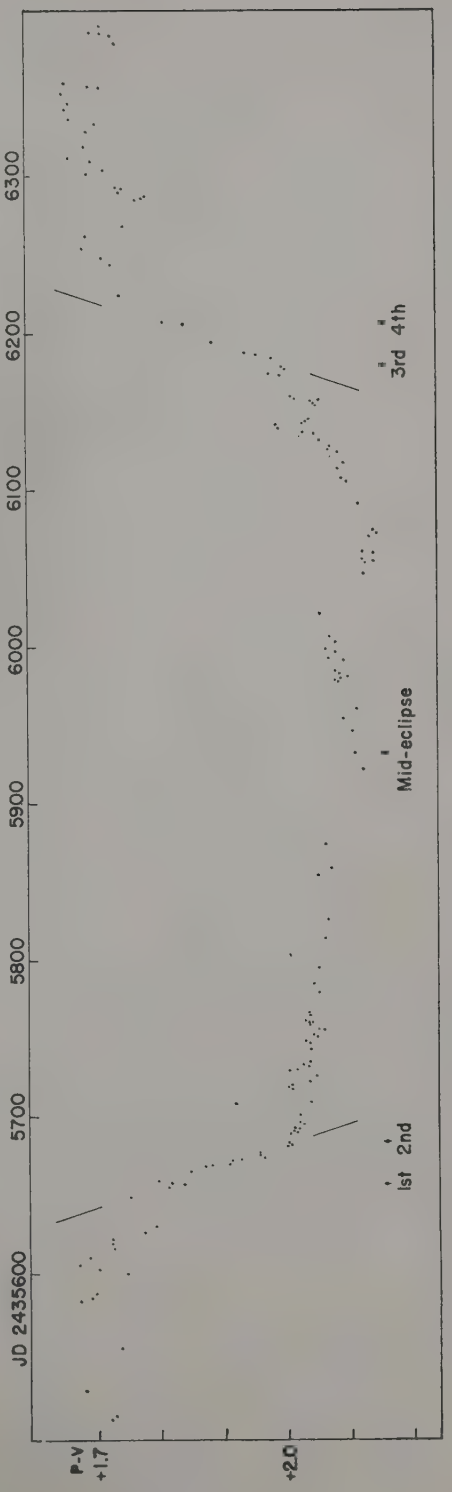


FIG. 11. Color curve from Larsson-Leander's observations. Times of contact are given below the curve. Slopes for the body eclipse are indicated.

magnitudes disagree. If the temperatures are to be brought into agreement without changing the parallax very drastically, then the radius of the M star must be decreased. In order to decrease the size of the M star and still satisfy the eclipsing data the mass ratio must increase. This is not at all impossible. For example, if the mass ratio were unity the M star would have a radius of 500 $R_\odot$, an effective temperature of about 2100°, and each star would have a mass of 10 $M_\odot$. The mass ratio may well be more nearly 2 than 1.

The question of the absolute magnitude might perhaps be explained by an argument due to M. Schwarzschild. The M component of VV Cephei is known to be a magnetic variable (Babcock 1958) with a field strength varying between approximately +600 to −600 gauss. The ratio of the magnetic energy density $E_m$ to the thermal energy density $E_t$ may be written as

$$\frac{E_m}{E_t}=\frac{\mu A|H|^2}{8\pi\rho kT},$$

where $\rho$ is the density, $k$ the gas constant, $T$ the temperature, $\mu$ the molecular weight, $A$ the unit atomic weight, and $|H|$ the absolute value of the field strength in gauss. At the surface of the sun the magnetic field is so small (a few gauss perhaps) that the ratio cited plays no role. However, in a sunspot where the magnetic field is large (a few thousand gauss) the ratio is nearly unity and the magnetic energy density can no longer be ignored. For VV Cephei $\rho\sim10^{-8}$, $T\sim3000°$, $|H|\sim600$, and $\mu=\frac{1}{2}$ or 1. If $\mu=\frac{1}{2}$, the value of the ratio is approximately 3. If $\mu=1$ and $T$ is decreased slightly, then the ratio is slightly greater than 10. Thus the effects of the magnetic field cannot be ignored when discussing the spectrum or spectral classification of this star. The effect would be one of lifting the atmosphere and thereby sharpening the absorption lines without appreciably increasing the size of the star.

In the previous analysis the spectroscopic value for periastron passage has been used. The latest data still prefer 1942 and though this differs considerably from the value preferred by the astrometric material the disagreement might be found in the first four years of the astrometric series. During these years there is an abnormally large scatter in the values of $\xi$ when compared with the later years. This situation will be improved as the orbit is covered for the second time.

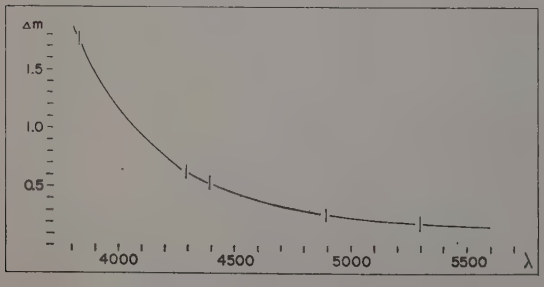


FIG. 12. Depth of eclipse.

The absolute magnitude of the M star and its size depend strongly on the parallax which depends upon the linear value of $\alpha$ given by the spectroscopy and the angular value of $\alpha$ given by the astrometry, which is in turn affected by the light of the B star. Within limits these values will not change except possibly toward a slightly larger value of the parallax. The real unknown in the solution is the mass ratio, which must always be assumed. If a reasonable estimate of the mass ratio can be made the dimensions become more rigidly defined. This estimate can be made using a beam interferometer.

On the assumption of a mass ratio of unity the maximum separation between the two stars will occur around 1972 and will be on the order of 0".08. Such a measurement would require a beam of the order of two meters and should be made around 4200 A, where the two sources are equally bright. A larger angular separation would indicate that the B star is the less massive of the two stars, where as a smaller or unmeasurable separation would indicate that the B star is the more massive.

The geometry of the next eclipse can be determined more readily if the intrinsic variations of the stars are better known. The M star certainly possesses two variations, one with a 13.7-year period and the other of slightly less than a year. The latter of these may be the resultant of two minor variations; this can be simply tested by seeing if the $L$ wave remains linear with the wavelength or not. Little is known of the B star's variations except that they appear to be quite erratic. If this is the case the accuracy of the solution will always be limited. Photoelectric observations now in progress in the ultraviolet light, where the light of the B star dominates, should show whether the variations of the B star's light is periodic or not. At the same time observations in the near infrared follow the M star's variations essentially free of the B star's light.

Because the diameter of the M star is rather large, an analysis of the spectroscopy around periastron passage (1942 and 1962) will be of considerable interest. Even if the M star were as small as 300 $R_\odot$, its boundary would be rather close to the Lagrangian inner-contact surface at periastron passage and border upon an unstable condition. Wood (1957) has considered the question of instability for eclipsing binaries based upon the well-known cases of period changes and erratic light-curve behavior. In the case of VV Cephei it is doubtful whether a change in period can be detected in the next few centuries. Also, the light curve is so erratic that it is difficult to associate general instability with it. P. Merrill has stated that the shell about the B star is constantly collapsing upon the B

star. This material must come from the M star's atmosphere, which indicates that an unstable condition must be present. The collapsing shell may be the cause of the light variations associated with the B star. Recent spectroscopic observations at Lowell Observatory confirm that this is not a "normal" shell star. The Paschen-$\gamma$ line seems to be present at 10940 A, but the *He* line at 10830 A is not. In P Cyg, for example, both lines are present, the *He* line being the stronger. The Paschen-$\gamma$ identification is very weak due to the fact that the M-star's continuum is very strong there.

ACKNOWLEDGMENTS

Special thanks are due F. B. Wood and P. van de Kamp for their encouragement and help throughout this study. I should also like to thank G. Larsson-Leander, D. B. McLaughlin, and L. Binnendijk for the use of their observational material and many useful suggestions. Thanks are due J. E. Merrill and M. Schwarzschild for valuable discussions of the solutions and also to the staff members of the Sproul and the Flower and Cook Observatories for their constant help and interest. A final note of thanks is due Mrs. M. L. Binnendijk who measured the majority of the astrometric plates for me, to W. Blitzstein who kept the photometer in perfect working order during the crucial observing period, and to Alvin Sweet for his help with the drawings.

This paper has been abstracted from a dissertation submitted to the faculty of the University of Pennsylvania in partial fulfillment of the requirements for a degree of Doctor of Philosophy.

REFERENCES

Babcock, H. W. 1958, *Astrophys. J.*, Suppl. Ser. III **30**, 201.
Binnendijk, L. 1943, *Bull. Astron. Inst. Neth.* **10**, 9.
Blitzstein, W. 1958, *Present and Future of the Telescope of Moderate Size*, edited by F. B. Wood (University of Pennsylvania Press, Philadelphia).
Gaposchkin, S. 1937, *Harvard Circ.* 421.
Goedicke, V. 1938, *Publ. Univ. Michigan* **8**, 1.
Keenan, P. and Wright, J. 1957, *Publs. Astron. Soc. Pacific* **69**, 457.
Larsson-Leander, G. 1957, *Arkiv Astron.* **2**, 12, 135.
——. 1959, *ibid.* 27, 301.
Lippincott, S. 1957, *Astron. J.* **62**, 55.
McKellar, A., Wright, K., and Francis, J. 1957, *Publs. Astron. Soc. Pacific* **69**, 442.
Risley, A. 1943, *Astrophys. J.* **76**, 156.
Russell, H. and Merrill, J. 1950–54, *Princeton Contrib.* 23–26.
Smart, W. 1949, *Text-Book on Spherical Astronomy* (Cambridge University Press, New York).
van de Kamp, P. 1942, *Astron. J.* **49**, 149.
——. 1947, *ibid.* **52**, 185.
——. 1951, *Pop. Astron.* **59**.
Vyssotsky, A. and Williams E. 1958, *Publ. Leander-McCormick Obs.* **10**, 36.
Wood, F. 1957, *I.A.U. Symp.*, No. 3.
Wright, K. O. 1958, *Epsilon Aur and VV Cep Observations*, Bull. 10, (F. B. Wood, Coordinator, University of Pennsylvania, Philadelphia).

# A List of Relatively Cool Stars in the Vicinity of the North Galactic Pole

A. R. Upgren, Jr.
*Warner and Swasey Observatory, Case Institute of Technology, Cleveland, Ohio*
(Received August 16, 1960)

In the course of a more extensive investigation of late-type stars in the vicinity of the north galactic pole, a number of relatively cool stars have been found. The list of M and carbon stars prepared for the present discussion contains the magnitude and spectral class for each star and is probably complete to a photographic magnitude of 13.0 in an area of about 400 square degrees. A limited statistical study indicates that the ratio of dwarfs to giant stars to this limiting magnitude in the area covered, is about one to three. Nineteen dwarf M stars were found. The space density of these dwarfs was found to be about 39 stars per 1000 cubic parsecs as against 36.3 per 1000 cubic parsecs for the known stars within five parsecs of the sun.

## INTRODUCTION

A CATALOGUE is given which contains the spectral class, luminosity class, and magnitude of 80 late-type stars of photographic magnitude 13.0 and brighter in a region of about 400 square degrees surrounding the north pole of the galaxy. The region extends from $11^h30^m$ to $13^h$ in right ascension and from $+25°$ to $+50°$ in declination, and is described by Slettebak and Stock (1959).

The catalogue includes 75 M-type stars, five carbon stars and no S stars. Since the entire region was surveyed uniformly, this list may be considered to be complete to an approximately uniform limiting magnitude. An identification chart showing all of the stars in the catalogue is soon to be published in a more extensive survey of late-type stars in this region. For the time being the coordinates given in Table I should be sufficient for identification.

## DATA

The spectrographic plates used for this survey were taken with the 80 cm–120 cm Hamburg Schmidt telescope and the 4° objective prism, and have been described by Slettebak and Stock (1959). A portion of the region was also photographed with IIa-O and 103a-O plates of exposure times 3 minutes and 24 minutes, respectively, taken with the Case Schmidt telescope and the new ultraviolet transmitting objective prism, which gives a dispersion of 580 A/mm at $H\gamma$, a dispersion almost identical to that of the Hamburg equipment.

## THE CATALOGUE

The stars which have been classified in this investigation are listed in Table I. The first three columns give a catalogue number, and the BD and HD numbers for the stars common to those catalogues. All of the stars in Table I which are also in the AGK2 catalogue have 1950 positions as given in that catalogue. The remaining BD stars have positions obtained by applying precession to the 1855 positions. All remaining stars have coordinates estimated from their positions on the plates and are probably accurate to about three minutes of arc.

The photographic magnitudes listed in Table I, column 6, were taken from the AGK2 catalogue when available except for two stars (No. 65 and 70), which have a known blue magnitude in the *UBV* system as given by Stock and Wehlau (1956). All remaining magnitudes are indicated by a colon and were determined by flyspanking charts of the *Lick Atlas*. Photoelectric sequences from the list of Stock and Wehlau were used wherever possible. Otherwise, sequences were taken from the AGK2 catalogue.

## REMARKS

Each plate was examined for stars of spectral class G5 or later, and all stars selected were classified twice on the Yerkes system. The two independent classifications were averaged. The stars which were classified as M stars were reclassified by direct comparison of the spectral images with those of standard stars of the Yerkes system of classification on plates taken with the Case Schmidt telescope.

Two luminosity criteria were used to separate the M stars into giants and dwarfs. These are the intensity of the λ4227 line of neutral calcium and the intensity of the continuum between this line and the G band relative to the continuum on the short-wave side of the λ4227 line, criteria 1 and 2 of Nassau and Keenan (1946). The internal consistency between the two independent classifications using these criteria was very high.

Nine stars, all classified here as dwarfs, are found in the lists of M dwarfs of Vyssotsky *et al.* (1943, 1946, 1952, and 1956) and two of these are also in the *Proper Motion Catalogue* of Luyten (1955). In addition, eight known variables and two additional stars listed as giants by Adams *et al.* (1935) are classified as giants or emission-line stars except for two of the variables which are carbon stars. The spectral classes given in column 8 are those of the reference listed in the same column.

Nineteen of the 75 M stars in Table I are classified as dwarf stars, and all of the other 56 are assumed to

TABLE I. Late-type stars at the NGP.

| No. | BD | HD | $\alpha$ (1950) | $\delta$ (1950) | $m_{ptg}$ | Sp | Remarks |
|---|---|---|---|---|---|---|---|
| 1 | | | $11^h34^m9$ | 48°59′ | 12.3: | M2 III | |
| 2 | | | 35.2 | 47 14 | 11.8: | M4 III | |
| 3 | 42°2233 | 101366 | 37.4 | 42 18 | 8.8 | M0 III | |
| 4 | | 101605 | 38.7 | 38 47 | var. | M5:e | RU UMa |
| 5 | 45 1955 | 101585 | 39.0 | 44 28 | 9.0 | M0 III | Adams gM3 |
| 6 | 36 2216 | 102159 | 43.0 | 36 10 | 8.6 | M5 III | TV UMa |
| 7 | 33 2151 | | 43.4 | 33 13 | 11.5 | M6 III | |
| 8 | 44 2126 | | 44.6 | 43 45 | 10.0 | M6 III | |
| 9 | 43 2149 | | 44.6 | 42 39 | 10.4 | M4 III | |
| 10 | 49 2086 | | 45.6 | 48 48 | 9.8 | M2 III | |
| 11 | 36 2219 | | 48.4 | 35 32 | 11.2 | M1 V | Vyssotsky No. 135 M2 |
| 12 | | | 51.6 | 41 02 | 12.3: | M3 III | |
| 13 | | | 51.8 | 45 51 | 12.9: | M3 III | |
| 14 | 37 2228 | | 52.0 | 37 25 | 11.5 | M7 | |
| 15 | 29 2228 | | 52.3 | 29 02 | 11.6 | M0 V | Vyssotsky No. 136 M0 |
| 16 | 37 2230 | 103500 | 52.7 | 37 02 | 7.6 | M0 III | |
| 17 | 45 1977 | 103796 | 54.7 | 45 17 | 10.3 | M2 III | |
| 18 | | | 55.8 | 38 06 | 12.6: | M2 III | |
| 19 | 40 2491 | | 59.7 | 39 50 | 11.1 | M5 III | |
| 20 | 30 2217 | 104710 | 12 01.0 | 29 57 | 9.0 | M2 III | Adams gM5 |
| 21 | 29 2261 | | 07.9 | 28 36 | 10.8: | M1 III | |
| 22 | | | 08.6 | 41 19 | 11.9 | M2 V | Vyssotsky No. 636 M0 |
| 23 | | | 09.4 | 49 59 | 12.7: | M4 III | |
| 24 | | | 09.6 | 40 14 | 13.0: | M1 V | |
| 25 | | | 09.6 | 45 17 | 12.7: | M5 III | |
| 26 | | | 10.1 | 39 57 | 12.9: | M2 V | |
| 27 | 35 2325 | | 10.8 | 35 12 | 11.6 | M1 III | |
| 28 | | | 10.9 | 31 58 | 13.0: | M0 V: | |
| 29 | 27 2104 | | 11.1 | 27 25 | 11.2 | M2 III | |
| 30 | 49 2126 | | 12.9 | 49 01 | 11.8 | M2 V | Vyssotsky No. 640 M0 |
| 31 | 44 2175 | | 13.2 | 44 12 | 10.8 | M2 III | |
| 32 | 29 2271 | | 13.3 | 29 05 | 10.8 | M3 III | |
| 33 | 42 2287 | | 13.7 | 42 11 | 9.9 | M0 III | |
| 34 | 28 2097 | 106814 | 14.4 | 28 01 | 9.7 | M2 III | |
| 35 | | | 15.8 | 46 53 | 12.7: | M3 V | |
| 36 | 29 2279 | | 17.1 | 28 40 | 12.1 | M2 V | Vyssotsky No. 644 M2=LFT 896 |
| 37 | 42 2296 | | 19.4 | 42 25 | 10.6 | M0 V | Vyssotsky No. 649 M0=LFT 898 |
| 38 | 28 2110 | | 20.1 | 27 53 | 12.3 | M3 V | Vyssotsky No. 134 M0p |
| 39 | 50 1915 | | 20.4 | 50 19 | 10.5 | M2 III | |
| 40 | | | 20.7 | 44 35 | 12.8: | M5 III | |
| 41 | | | 21.3 | 28 12 | 12.8 | M3 V | Vyssotsky No. 654 M0 |
| 42 | 41 2292 | 107905 | 21.4 | 41 00 | 9.7 | M1 III | |
| 43 | 46 1784 | | 22.5 | 45 52 | 10.6 | M5 III | |
| 44 | 47 1958 | | 22.7 | 46 59 | 11.4: | M6 III | |
| 45 | | | 23.2 | 38 02 | 12.6: | M2 V | |
| 46 | | | 24.7 | 37 38 | 12.5: | M2 V | |
| 47 | | | 25.4 | 45 09 | 12.3: | M3 III | |
| 48 | 30 2279 | | 26.1 | 29 52 | 10.3 | M0 III | |
| 49 | 42 2310 | | 26.4 | 42 22 | 11.8: | M2 III | |
| 50 | 42 2312 | | 27.2 | 42 16 | 11.4 | M1 III | |
| 51 | | | 28.0 | 31 47 | 11.4: | M8 | T CVn |
| 52 | 44 2199 | | 29.6 | 43 46 | 10.6 | M6 III | |
| 53 | 46 1792 | | 29.8 | 45 46 | 9.8 | M1 III | |
| 54 | | | 32.2 | 36 29 | 13.0: | R : | |
| 55 | | | 32.8 | 34 35 | 12.3: | M2 III | |
| 56 | | | 33.7 | 42 00 | 12.7: | M2:V | |
| 57 | 27 2152 | | 34.4 | 27 21 | 12.1 | M7 | |
| 58 | 33 2256 | | 34.9 | 32 53 | 11.9: | M8 | |
| 59 | | | 36.8 | 24 54 | 12.7: | M2 III | |
| 60 | 38 2355 | | 39.2 | 37 30 | 11.9: | M4 III | |
| 61 | | | 40.1 | 31 22 | 12.7: | R | |
| 62 | | | 40.1 | 43 19 | 12.6: | M2:V | |
| 63 | 42 2334 | 110687 | 41.2 | 41 32 | 9.4 | M3 III | |
| 64 | 46 1817 | 110914 | 42.8 | 45 43 | 8.1 | N | Y CVn |
| 65 | 27 2167 | 110964 | 43.2 | 27 24 | 10.7 | M4 III | Stock and Wehlau No. 22 M3.5 |
| 66 | 48 2055 | 111129 | 44.3 | 47 39 | 9.4 | M2 III | |
| 67 | | 111223 | 45.6 | 38 39 | var. | M7e | U CVn |
| 68 | | | 48.9 | 40 38 | 12.4: | M4 V | |
| 69 | 47 1998 | 112082 | 51.0 | 46 56 | 8.8 | M3 III | |
| 70 | 29 2336 | 112172 | 51.9 | 28 43 | 10.7 | M3 III | Stock and Wehlau No. 157 M4 |
| 71 | 47 2003 | 112264 | 52.7 | 47 28 | 7.1 | M5 III | TU CVn |
| 72 | 36 2321 | | 53.8 | 35 37 | 10.8 | M2 III | |

TABLE I. (Continued)

| No. | BD | HD | $\alpha$ (1950) | $\delta$ (1950) | $m_{ptg}$ | Sp | Remarks |
|---|---|---|---|---|---|---|---|
| 73 | | | $12^h54^m1$ | 43°45′ | 12.5: | R | |
| 74 | 43°2283 | | 54.5 | 43 19 | 12.1 | M4 III | |
| 75 | 36 2322 | | 55.7 | 35 30 | 11.9 | M0 V | Vyssotsky No. 298 M0 |
| 76 | | | 56.9 | 40 50 | 12.5: | M0:V: | |
| 77 | 45 2076 | | 57.0 | 44 50 | 12.0: | M3 III | |
| 78 | 38 2389 | 112869 | 57.0 | 38 05 | 10.8 | R | TT CVn |
| 79 | 44 2243 | | 58.0 | 44 10 | 11.9: | M5 III | TW CVn |
| 80 | | | 58.9 | 45 55 | 12.0: | M5 III | |

be giants, since the few for which no luminosity class is given in Table I are all either known variable stars or have a spectral class of M7 or later, probably too late a class for a dwarf star. No supergiants were detected although it is difficult to separate such stars from giants at the spectral dispersion employed here.

Four of the five carbon stars were found to be of spectral type R and one of type N. Three of the four R stars appear to be previously unknown. All three are very faint, hence they lie at a considerable distance from the galactic plane. If the value −0.4 given by Sanford (1944) is taken for the absolute visual magnitude for these stars, and +3.0, a mean of nine carbon stars listed by Johnson (1955), for the *B-V* color, the distances from the galactic plane are about 1000 parsecs for stars No. 54, 61, and 73.

## STATISTICAL DISCUSSION

The statistical results of this section are provisional in nature as they are based on magnitudes of limited accuracy. However, care has been taken to check for scale and internal systematic errors.

Shown in Fig. 1 are cumulative Wolf diagrams for the giants and for the dwarfs listed in Table I. The abscissa for Fig. 1 gives the photographic magnitude, and the ordinate the number of stars brighter than that magnitude. The solid and open dots represent the total numbers of giants and dwarfs, respectively, to the indicated limiting apparent photographic magnitude, and have been plotted for each half-magnitude increment. The theoretical values of the cumulative Wolf diagram are shown by the curved lines in Fig. 1. These curves have been computed on the assumption of a uniform space density of both giants and dwarfs and no space absorption. The curves have been fitted arbitrarily to the observed points at magnitude 7.5 for the giants, and 11.0 for the dwarfs, since these are the brightest limiting half-magnitudes which include at least one star.

Only in the case of the dwarfs does the curve continue to show a good fit up to a photographic magnitude of 13.0, the limit for this survey. This close agreement suggests that the limiting magnitude of 13 for this investigation is approximately correct. The space density of the giants according to Fig. 1 appears to decrease sharply for magnitudes fainter than 9.0, indicating a drop in the number of giants with increasing distance from the galactic plane. Those giant stars fainter than magnitude 9.0 belong primarily to the galactic halo. Although no definite mean absolute magnitude can be assigned to these stars, a rough estimate of −0.4, the value given by Keenan and Morgan (1951) for the mean visual absolute magnitude, and a color index of +1.6 (Allen 1955) yield a distance of about 400 parsecs, a reasonable value for the beginning of a transition between the edge of the disk and the start of the galactic halo. There is no appreciable difference in the concentration toward the galactic plane between the early and the late M-giant stars. Thus, although many of the late M-giants may be intrinsic variables with magnitudes of questionable value, their inclusion in this statistical discussion does not appreciably alter the results.

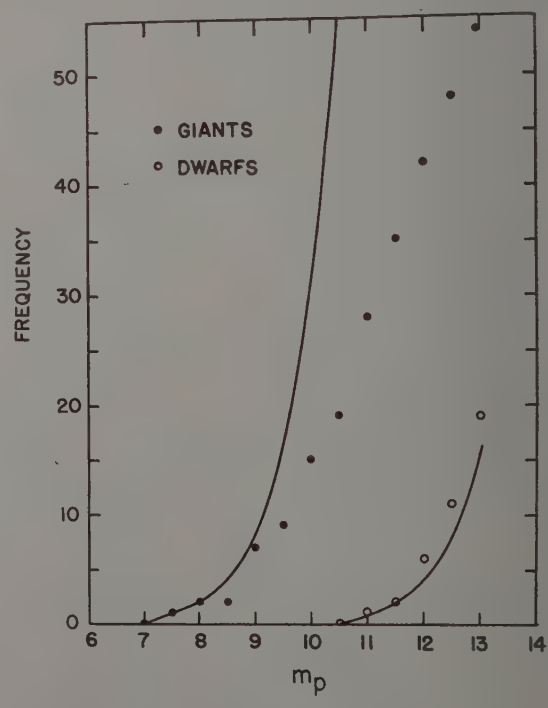


FIG. 1. Cumulative Wolf diagrams for giants and dwarfs.

An estimate of the space density of the 19 M-dwarf stars shows a value in general agreement with that of the solar neighborhood. According to Gliese (1957) there are 19 single stars or double systems within five parsecs of the sun which have spectral classes of M0 to M4. If a mean absolute visual magnitude of +9.8 and a mean color index of +1.4 are assumed for the 19 dwarf stars listed in Table I [the values are those for M2V stars as given by Allen (1955)] then the resulting modulus for the limiting distance for dwarf stars in this investigation is 1.8, and the corresponding limiting distance is 23 parsecs.

The volumes are 524 and 487 cubic parsecs, respectively, for the space within five parsecs of the sun and the volume covered in this survey. The density of M dwarfs based on these figures is 36.3 and 39.0 M-dwarfs per 1000 cubic parsecs, respectively (for the two volumes). The agreement between these figures indicates that the number of dwarfs found in this search is about as expected.

ACKNOWLEDGMENTS

I wish to thank Dr. J. J. Nassau and Dr. C. B. Stephenson for their many helpful suggestions concerning problems related to this investigation and Dr. J. Stock for arranging the loan of the plates from the Hamburg Observatory.

REFERENCES

Adams, W. S., Joy, A. H., Humason, M. L., and Brayton, A. M. 1935, *Astrophys. J.* **81**, 187.

Allen, C. W. 1955, *Astrophysical Quantities* (Athlone Press, London, England), pp. 177, 183.

Gliese, W. 1957, *Mitteilungen Serie A*, Nr. 8, Astronomisches Rechen-Institut in Heidelberg.

Johnson, H. L. 1955, *Ann. d'Astrophys.* **18**, 292.

Keenan, P. C. and Morgan, W. W. 1951, *Astrophysics*, edited by J. A. Hynek (McGraw-Hill Book Company, New York), p. 23.

Luyten, W. J. 1955, *A Catalogue of 1849 Stars with Proper Motions Exceeding 0".5 Annually* (The Lund Press, Minneapolis, Minnesota).

Nassau, J. J. and Keenan, P. C. 1946, *Astrophys. J.* **104**, 458.

Sanford, R. F. 1944, *Astrophys. J.* **99**, 145.

Slettebak, A. and Stock, J. 1959, *A Finding List of Stars of Spectral Type F2 and Earlier in a North Galactic Pole Region*, Hamburger Sternwarte.

Stock, J. and Wehlau, W. 1956, *Astron. J.* **61**, 80.

Vyssotsky, A. N. 1943, *Astrophys. J.* **97**, 381.

——. 1956, *Astron. J.* **61**, 201.

Vyssotsky, A. N., Janssen, E. M., Miller, W. J., and Walther, M. E. 1946, *Astrophys. J.* **104**, 234.

Vyssotsky, A. N. and Mateer, B. A. 1952, *Astrophys. J.* **116**, 117.

# FURTHER REPORTS OF OBSERVATORIES

**Lockheed Solar Observatory,** Lockheed Aircraft Corporation, Burbank, California.

A study of the solar atmosphere by means of high-speed $H_\alpha$ cinematography was initiated by the Lockheed Aircraft Corporation, California Division, in the fall of 1958. This report encompasses the 18-month period commencing with inception of routine observations January 1, 1959, closing June 30, 1960.

*Personnel.* The Solar Physics Project has been under the directorship of G. E. Moreton, previously Principal Investigator, Convair Radio Astronomy Project. H. E. Ramsey, formerly Sacramento Peak Observatory Chief Observer, joined the project September 1959. In addition, the research group consists of J. W. Harvey, N. W. Christie, and G. F. Anderson. G. A. Carroll is in charge of instrumentation design and construction.

Some recent visitors have been Drs. R. Grant Athay, J. W. Warwick, Richard Hansen, and Norman Macdonald, of the High Altitude Observatory; Dr. James W. Dungey, Atomic Weapons Research Establishment, England; Professor Robert Leighton, California Institute of Technology; Dr. Eugene N. Parker, University of Chicago; Dr. I. G. Poppoff, Stanford Research Institute; and Professor John R. Winckler, University of Minnesota.

*Facility.* The observing site is located at an elevation of 1500 feet, in the Hollywood Hills, Los Angeles. The well-known atmospheric inversion, resulting in local "smog," has proved beneficial: inhibited convective air flow apparently contributes to prolonged periods of good seeing. Long periods of cloud-free sky allow excellent observational continuity: in spite of equipment-down time during the initial weeks, observations have been conducted 85% of the days in this reporting interval. The facility consists of a heliograph incorporating a three-inch $f/33$ objective lens, secondary reimaging optics, Hallé 0.5 A bandpass $H_\alpha$ birefringent filter, and Acme pin-registration camera. The system is photoelectrically guided, and mounted on the original Climax coronagraph loaned by HAO for this work, and modified to serve as a heliograph by Lockheed. The 18-mm solar image is photographed each 10 sec on 200-foot lengths of Eastman 4-E 35-mm film. A clock is imaged adjacent to the sun; photometric standards are impressed on each roll.

*Observing Program.* Six frame per minute cinematographic observations are conducted daily from about 1600 hr UT to sunset. The 35-mm negatives are scanned daily with an automatic film reader, and occurrences of flares and associated phenomena reported in accordance with IGY–IGC procedures. Daily flare reports are made by telegraph to the Boulder World Data Center; other World Data Ce ters receive tabulated data monthly. Concomitant v ual observations are conducted daily in the aft noons and continuously on weekends; occurrences major flares are reported by telephone to the Belvoir World Warning Agency; such observatio have resulted in five world-wide geophysical aler During summer 1959 a continuous visual patrol sulted in successful rocket firings from Pt. Argue by the Naval Research Laboratory team measuri flare-enhanced x rays.

In order to handle the flare data as routinely possible, extensive measurements for each flare a recorded on IBM punch cards and data compilati is accomplished by IBM tabulation. Monthly fla patrol results appear regularly in those publicatio concerned with solar data.

Beginning January 1960 cinematography was a complished with the filter band pass displaced a proximately 0.5 A to the blue side of $H_\alpha$. Futu observational research will be conducted with thr sequentially programed exposures each 10 sec at and at wavelengths displaced to the blue and red.

Since May 1960 the IGY–IGC activities ha received partial support from the National Scien Foundation.

*Research Summary.* An immediate consequence the high time-resolution cinematography, good se ing, clear sky, and modern data-processing tec niques has been the detection of a large numb of small-scale short-duration chromospheric even During the 2932 observing hours, a total of 40 flares have been detected and recorded on pun cards; 94% of these events are subflares. The month flare frequency averaged about 1.6 flares per hou Of the flares recorded by Doppler-shifted radiati in 1960, 50% have an associated surge or filame activation.

Studies of the influence of flares on filaments Moreton have resulted in detection of seven even where dark filaments were unambiguously activat by flares separated by distances up to $1R_\odot$. The fi ments undergo "abrupt" activation; initial opac changes can be determined to $\pm 10$ sec. The respon ble flares appear to have a distinct "explosive" pha suggestive of hydrodynamic effects independent other observed phenomena. If a disturbance leav the flare at the explosive phase and travels the sho est route to the filaments, then the inferred veloci of propagation for the disurbances is $\sim 1000$ km/s The velocity suggests close association with hi velocity disturbances assumed to cause type-II rad emission and associated with geomagnetic storms.

Further investigation of this new class of even

gan January 1960 by operating the heliograph at $_{\alpha}$—0.5 A, enhancing Doppler-shifted radiation from aments and moving features. This has resulted in nfirmation of inferred 1000 km/sec disturbances om flares: three events have been photographed here *direct* measurement of faint propagating disrbances confirm the velocities obtained from subquent filament activation.

This report interval culminated with a singularly gnificant observation: on June 25, 1960 an extenve disturbance was photographed propagating from flare at ~2500 km/sec. The disturbance was visie over 400 000 km from the flare.

H. E. Ramsey has been analyzing film records, udying loop prominences seen in absorption on the sk, and the occurrences and properties of preflare ament activations. J. W. Harvey has developed a notographic technique which may make possible asy and accurate measurement of high-velocity flare xpansions. N. W. Christie has investigated dataandling techniques and is collaborating with Harvey n statistical analysis of subflares, surges, and radio oise.

A discussion of flare-activated filaments has been ompleted by R. Grant Athay, of HAO, and Moreon, and has been submitted for publication. A study as been completed by Moreton in collaboration with ugene Greenstadt, of Space Technology Laboraories, relating Satellite Pioneer V magnetometer ata to solar activity; the results are being readied or publication.

G. E. Moreton, *in charge*

**National Aeronautics and Space Administration, Washington 25, D. C.**

OBSERVATIONAL PROGRAM

Vanguard III and Pioneer V were launched within his period. The Lyman-alpha detectors on Vanguard III saturated in the Van Allen Belt but the micrometeorite experiment confirmed the results from Explorer I within a factor of 2. From these observations he dust density in space near the earth is estimated o be approximately $10^{-20}$ g/cm$^3$.

Pioneer V contained experiments for measuring he interplanetary magnetic field and ion densities in nterplanetary space. An intense solar storm occurred n April 1, during the active life of this probe. It vas found that the magnetic field disturbance followng a solar flare is not localized in the earth's magetic field as had previously been assumed. Some f the interesting results are

(1) An interplanetary magnetic field exists with steady magnitude of slightly more than one gamma. This field fluctuates in intensity up to ten gammas during periods of solar flare activity.

(2) The planar angle of the interplanetary magnetic field forms a large angle with the plane of the ecliptic, perhaps as much as 90 deg.

(3) The exospheric ring current about 2500 miles in diameter and at a distance of about 40 000 miles from the earth causes a westward moving current estimated at five million amperes.

(4) The geophysical magnetic field extends at times 65 000 miles from the earth.

(5) The sudden decrease in galactic cosmic rays associated with large solar flares does not depend on the presence of the earth's magnetic field.

Goddard Space Flight Center launched three night-sky rockets in the spring of 1960 for stellar and nebular photometry in the ultraviolet. The results have not yet been reduced but the flights were successful and the program will be continued. Development of detectors for the ultraviolet has been undertaken and will be continued and expanded during the coming year.

A program for the scientific study of the moon, planets, and interplanetary space by means of space probes was formulated and instrumentation development has been started for the early flights in this program. The first lunar flights in this program will carry a vidicon camera and gamma-ray spectrometer on the spacecraft and a single-axis seismometer and decelerometer on a capsule to be impacted on the moon. The first planetary probe will contain an ultraviolet spectrograph and radiometer. All flights will carry an interplanetary package consisting of radiation experiments in various energy ranges and a magnetometer.

Instrumentation is partially complete for a satellite to study the sun in the wavelength region below 2000 A. Experiments for the Orbiting Solar Observatory Satellite will be furnished by Ames Research Center, Goddard Space Flight Center, University of California, University of Colorado, University of Minnesota, and the University of Rochester.

The George C. Marshall Space Flight Center was preparing a satellite to observe 100 Mev gamma radiation from space. The Massachusetts Institute of Technology is responsible for the scientific instrumentation and the Marshall Space Flight Center for the satellite structure, power supplies, telemetry system, and auxilliary instrumentation.

The Marshall Space Flight Center is studying the motions of a satellite about its center of mass due to interactions with the space environment and is analyzing the observed motions of Explorers IV and V. They are also studying the applicability of image intensifier and image orthicon techniques. Negotiations are underway for a test using minor planets to evaluate these techniques.

The Ames Research Center carried out an extensive study of a satellite to be used for astronomical observations with a telescope up to 36 inches in di-

ameter. Practical problems associated with control, guidance, and data transmission of such a satellite were studied, particularly under the direction of R. M. Crane. Removal of the primary component of the earth's gravitational field may permit particularly delicate control of the instruments. Among disturbing factors remaining are

(1) The gradient of the earth's gravitational field.
(2) Solar radiation pressure.
(3) Interaction with the earth's magnetic field.
(4) Aberration of light.

THEORETICAL AND LABORATORY STUDIES

*Jet Propulsion Laboratory.* Y. Hiroshige and F. Yagi worked on the theory of the interaction between a dipole magnetic field and a conducting fluid issuing from the center of the dipole field. This has obvious application to the sun. H. Lass studied dynamical problems associated with a satellite of the moon. He concluded that little knowledge of the moon's internal structure would be gained from one. He also formulated for a steady-state universe a special relativity cosmology which satisfies all observations. T. Kreiter studied lunar crater distribution extensively. R. Carr has been investigating the use of seismological techniques for determining the structure of the moon, particularly viewed as a layered medium consisting of concentric spherical shells. C. Barth and A. Hildebrandt measured interaction processes between atoms, molecules, ions, and electrons that occur in the upper atmosphere of the planets. Electron paramagnetic resonance spectrometry and optical spectroscopy were used.

*The Ames Research Center.* The Ames Research Center has long specialized in studies of high-speed dynamic phenomena. Under the direction of H. Julian Allen, studies of the interaction of meteors with the earth's atmosphere were made. Comparison of the results with several well-recorded meteor falls indicated that the phenomenon of deceleration and ablation of material in iron meteorites can be accounted for.

*Goddard Space Flight Center.* Under the direction of the Goddard Space Flight Center some minitrack stations were used to track the stronger radio stars (Cygnus and Cassiopeia) and the sun. The stations used are near the same longitude and 108-Mc radio bursts could thus be recorded simultaneously at several locations. Combining these observations nearly eliminates atmospheric effects and positions can be obtained which are accurate to two minutes of arc. Those solar bursts which can be observed with the minitrack systems are time-correlated with solar *H*-alpha flares. S. Huang studied the possibility of habitable planets in other solar systems and predicted regions in which a fourth body can be stable in the earth-moon or similar systems. He also started computations of stellar models by a perturbation technique. B. Donn showed that ion clusters of the type hypothesized by V. I. Krassovsky cannot occur in interstellar space. In addition, he applied various theoretical and observational results from other fields to the origin and properties of interstellar grains and studied properties of an icy-conglomerate comet nucleus.

In the Theoretical Division of the Goddard Space Flight Center, J. O'Keefe, Ann Eckels Bailie, and K. Squires completed their analysis of the Vanguard orbit for the determination of the earth's gravitational field. P. Musen developed the theory for lunisolar effects on an artificial satellite and more recently, the theory of radiation pressure effects from the sun. The effect on the Vanguard orbit was found to be measurable; that on Echo is part of the present Echo observational program. As a result of B. Stromgren's visit, a project of astrophysical calculations in the field of stellar interiors was initiated. This involved much of the junior staff. C. Hayashi and R. Cameron studied the evolution of giant stars with special reference to the double cluster h and $\chi$ Persei.

R. Jastrow and W. Cameron in conjunction with Professor Urey of the University of California initiated an investigation of the early stages of formation of the planetary bodies. G. J. F. MacDonald continued his study of resonances in the earth resulting from major earthquakes. G. J. F. MacDonald, R. Jastrow, and P. Musen have been redeveloping the lunar theory to improve the values of the moments of inertia of the moon. J. O'Keefe and P. Lowman investigated tektites. G. J. F. MacDonald is studying free oscillations in the earth's atmosphere as a guide to large-scale effects produced by thermal sources. I. Harris and R. Jastrow in collaboration with J. Chamberlain of Yerkes Observatory have been calculating the thermal equilibrium of the upper atmosphere and the effect of temporal variation in solar radiation.

NANCY G. ROMAN, *Chief,*
*Astronomy and Astrophysics*

## ABSTRACT

**The Luminosity Functions of Galactic Star Clusters.*** SIDNEY VAN DEN BERGH AND DAVID SHER, *David Dunlap Observatory*.—The luminosity functions of 20 galactic clusters down to $m_{pg} \approx 20$ have been determined by means of star counts on 170 plates obtained with the Palomar 48-inch Schmidt. It is found that striking differences exist between the main-sequence luminosity functions of individual clusters. Also it appears that the faint ends of the luminosity functions of galactic clusters differ systematically from the van Rhijn-Luyten luminosity function for field stars in the vicinity of the sun in the sense that (with one exception) all the clusters which were investigated had luminosity functions which either decrease or remain constant below $M_{pg} = +5$. The differences between individual clusters and the differences between the luminosity functions of clusters on the one hand and field stars on the other show that the luminosity function of star creation is not unique. This result is taken to indicate that the luminosity function with which stars are created probably depends on the physical conditions prevailing in the region of star formation.

* This abstract of a paper presented at the 106th Meeting of the American Astronomical Society was omitted, through an editorial oversight, from the abstracts of the meeting published in the November 1960 No. 1284 issue of the *Astronomical Journal*.

## NOTICE

### Graduate Laboratory Development Program

THE National Science Foundation announces that March 1, 1961 is the next closing date for receipt of proposals in the Graduate Laboratory Development Program. Proposals received after March 1 will be reviewed following the next closing date, September 1, 1961. This program requires at least 50% participation by the institution with funds derived from non-Federal sources.

Purpose of the grants is to aid institutions of higher education in modernizing, renovating, or expanding graduate-level basic research laboratories used by staff members and graduate students. Only those departments having an on-going graduate training program leading to the doctoral degree in science at the time of proposal submission are eligible at present.

Proposals, as well as requests for additional information, should be addressed to: Office of Institutional Programs, National Science Foundation, Washington 25, D. C.

## ERRATUM

*Astron. J.* **65**, 354.

Left column, line −8: for 900 read 800.
Left column, line −5: for IV read III-IV.
Right column: delete last 11 lines; substitute "The maximum in the space velocity frequency distribution for the thirty weak *CN* stars occurs at approximately 50 km/sec, with only 20% of the velocities exceeding 65 km/sec."

# Author Index to Volume 65

(A) indicates Abstracts, (N) indicates Notices. It will be noted that there are no references to "see someone else" in the Author Index. Although it has meant a little duplication, there have been included under each author all articles in which he was author or co-author. All articles in which the author has participated are arranged in the chronological order of publication. A bibliography with author names arranged as in the original article is obtained by insertion of the author's name in the indicated (——) space under each indexed name.

# Subject Index to Volume 65

Numerals in boldface type refer to volume numbers. (A) indicates abstract. (S) indicates symposium.